Review Article

Tanglong Zhu* and Zhen Wang*

Advances in processing and ablation properties of carbon fiber reinforced ultra-high temperature ceramic composites

https://doi.org/10.1515/rams-2024-0029 received October 26, 2023; accepted May 13, 2024

Abstract: With the continuous development of hypersonic vehicles, higher demands are being placed on all aspects of the performance of thermal protection materials. Carbon fiber reinforced ultra-high temperature ceramics composites (C_f/UHTCMC) have an extremely bright prospect as thermal structures and anti-ablation components of hypersonic vehicles and rockets, by reason of their superior thermal shock, oxidation and ablation properties, high fracture toughness, and damage tolerance. However, due to the complicated fabrication process and harsh service environment of C_f/UHTCMC, there are still some pivotal scientific issues that need to be clarified on structural evolution and performance mechanisms. The aim of this work is to review the latest research progress in processing methods, matrix modification, oxidation ablation mechanism, structure, and property regulation as well as elevated temperature mechanical properties of C_f/UHTCMC, summary, and prospect of the future research trend of C_f/UHTCMC, to provide reference for further promoting the improvement and development of C_f/UHTCMC.

Keywords: C_f/UHTCMC, material fabrication, matrix modification, ablation behaviors, elevated temperature mechanical properties

1 Introduction

Since the middle of the twentieth century, aerospace technology has developed rapidly around the world, and the competition in the international aerospace field has become increasingly fierce. Among them, the hypersonic vehicle is a collective term for missiles, trans-atmospheric vehicles, hypersonic aircraft and other equipment that travel at speeds in excess of Mach 5 [1–3]. Its technical characteristics such as large lift-drag ratio, high mobility and reliability, fast flight speed, strong real-time strike capability, strong penetration and counter-defense capabilities, impel it to become the strategic development direction of future dual-use military and civilian aircraft, which is of great significance in promoting the development and implementation of low-cost reusable civil space launch vehicles [4–7].

Advanced thermal protection system is one of the pivotal technologies for the development of hypersonic vehicle. The hypersonic vehicle generates violent friction with the air during flight, which makes its sharp leading edge, leading edge of wing, and other components expose to extremely harsh service environments, resulting in a sharp increase in pressure and temperature [8-11]. When the flight speed reaches Mach 10, the stationary point temperature of the nose cone and sharp leading edge can reach 2,500°C. During re-entry process, the flight speed is greater than Mach 24, while the nose cone and leading edge of the wing will be subject to a harsh thermal environment with higher instantaneous ultra-high temperature and high heat flux density. Due to the high temperature corrosive gases containing metal ions above 2,000°C produced by solid propellant combustion, the hot end of the engine requires to simultaneously withstand a sequence of extreme environmental tests, such as high heat flux density, high thermal load, high temperature/stress gradient, high-pressure airflow, high-energy particle erosion, and high-temperature oxidation and erosion [12-14]. Therefore, in order to maintain the intact aerodynamic shape of the vehicle and protect the power system from burning, while

^{*} Corresponding author: Tanglong Zhu, Engineering & Technology Center for Aerospace Materials, Wuzhen Laboratory, Jiaxing 314500, China, e-mail: ztl_8198@163.com

^{*} Corresponding author: Zhen Wang, Engineering & Technology Center for Aerospace Materials, Wuzhen Laboratory, Jiaxing 314500, China; Zhejiang Hangyin Advanced Materials Tech Co., Ltd, Jiaxing 314500, China, e-mail: wangz@wuzhenlab.com

taking into account the weight reduction, the desired thermal protection material should possess low density, high strength and toughness, thermal shock resistance, oxidation and ablation resistance, mechanical erosion resistance [15–17], *etc*.

Ultra-high temperature structural materials are a new subfield with superior high temperature mechanical properties and oxidation ablation resistance that offer applications in aircraft sharp leading edges, engine combustion chambers, and nozzles [18,19]. Ultra-high temperature ceramics (UHTCs) are generally considered to be carbides (ZrC, HfC, TaC), nitrides (ZrN, HfN), and borides (ZrB₂, HfB₂, TiB₂) of refractory transition metals of elements table IV_B and V_B group of periodic table [20-22], which have the ability to maintain chemical stability in non-inert atmosphere above 2,000°C. Many efforts have been done to investigate the fracture, structure, toughness, electrical resistivity, thermal conductivity, thermal expansion, oxidation behaviors, and ablation properties of UHTCs [23-25]. The results have indicated that the UHTCs are severely restricted as thermal protection system for aerospace application because of their inherent brittleness and poor damage tolerance. Thus, main focus of recent study is to introduce toughening phases into UHTCs to enhance the fracture toughness, thermal shock, and reliability.

The carbon fiber reinforced ultra-high temperature ceramic composites (C_f/UHTCMC) are composed of elevated temperature resistant carbon fiber as reinforcement and UHTC as matrix, which combines the high-temperature resistance and ablation resistance of the ceramic matrix with the low density, and high toughness and strength brought by carbon fibers [26-28]. Carbon fibers are extensively utilized for the reinforcement of UHTC composites due to their excellent high temperature performance and no significant loss of strength within 2,000°C under inert atmosphere [29–32]. Through the design of the interphase, the carbon fiber and the matrix have a moderate bond, the interphase can effectively transfer the load and enhance the strength. Moreover, by means of the fiber/interphase debonding, fiber pull-out, bridging, crack deflection, and other toughening mechanisms during the fracture failure to achieve effective energy dissipation, thereby enhancing the toughness and thermal shock resistance [33-35]. In terms of high temperature oxidation and ablation resistance, the oxide melt produced by the oxidation of UHTC can effectively cover the surface of the composite, heal the pores and cracks, prevent oxygen from diffusing into the composite, thus protecting the matrix and fibers inside the composite, endowing the composite with superior high temperature oxidation and ablation resistance up to 3,000°C, and still boasting a high strength retention after ablation [36–40]. As mentioned above, C_f /UHTCMC are typically considered to be the main focus of research in thermal protection system.

This review will cover the latest research progress and future development directions in $C_f/UHTCMC$ over the last decade, with the greatest emphasis on continuous carbon fiber reinforced UHTC composites since these are expected to provide the best toughening effect. The interphase structure, matrix composition, preform configuration, fabrication technique, mechanical properties, oxidation, and ablation properties of $C_f/UHTCMC$ were presented.

2 Material fabrication

C_f/UHTCMC are composed of UHTC matrix, continuous fiber fabric, or chopped fibers, as well as the interphase between fiber and matrix. The preparation process directly determines the fiber strength retention, distribution uniformity, matrix density, pore distribution, microstructure, fracture strength, toughness, oxidation and ablation properties, *etc.* Currently, the preparation methods of C_f/UHTCMC primarily include: precursor infiltration and pyrolysis (PIP) [41–43], slurry infiltration (SI) [44–46], reactive melt infiltration (RMI) [47–49], chemical vapor infiltration (CVI) [50–52], hot pressing (HP) [53–55], pressureless sintering [56,57], *in-situ* reaction [58–60], and others.

2.1 PIP

PIP is a universal process to introduce UHTCs precursor into fiber preforms under vacuum or external pressure, and then pyrolyze at elevated temperature to yield UHTCs matrices, an overview of which is depicted in Figure 1. In general, the PIP process requires several infiltration and pyrolysis cycles to fabricate a denser composite due to

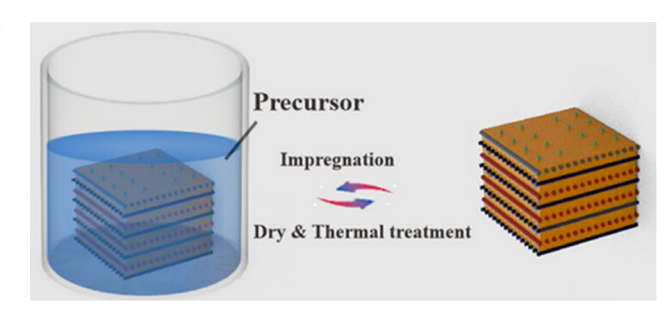


Figure 1: Brief illustration of C_f/UHTCMC prepared by PIP process [61].

mass loss and volume shrinkage caused by precursors curing and pyrolysis.

Improvements of PIP process are to achieve a higher composite density while reducing the number of impregnation-pyrolysis cycles. Consequently, the precursor synthesis, ceramic yield, ceramic transformation mechanism, rheological properties, and wettability of the precursor are critical. Presently, many examples with respect to precursors for ZrC, HfC, SiC, ZrB₂, and HfB₂ ceramics have been reported. Jiang *et al.* [62] developed a facile and promising aqueous solution-derived precursor approach for the synthesis of HfC nanoparticles by using hafnium tetrachloride and sucrose as raw materials. In Yao *et al.*'s report [63], pitch resin was added directly to the mixture of

organic polymeric precursor of zirconium carbide (PZC) and polycarbosilane (PCS) to provide an additional carbon source, limiting the reaction of ZrO₂ intermediates with pyrocarbon (PyC) and carbon fibers during the carbothermal reduction process. When the PZC/PCS/resin mass ratio was 20:1:5 and the number of PIP process was ten, the fracture strength of the C/C–SiC–ZrC composites was 247.4 MPa, which was 52.2% higher than that of the composites without resin. Jiao *et al.* [64] produced 3D C/C–HfC–SiC composites from a combination of polyhafniumcarboxane and PCS. Cai *et al.* [65] reported a facile and scalable polymeric precursor approach for fabricating HfC–SiC ceramic nanocomposites, and the ceramic transformation process is presented in Figure 2. Zhao *et al.* [66] decomposed the mixed solution

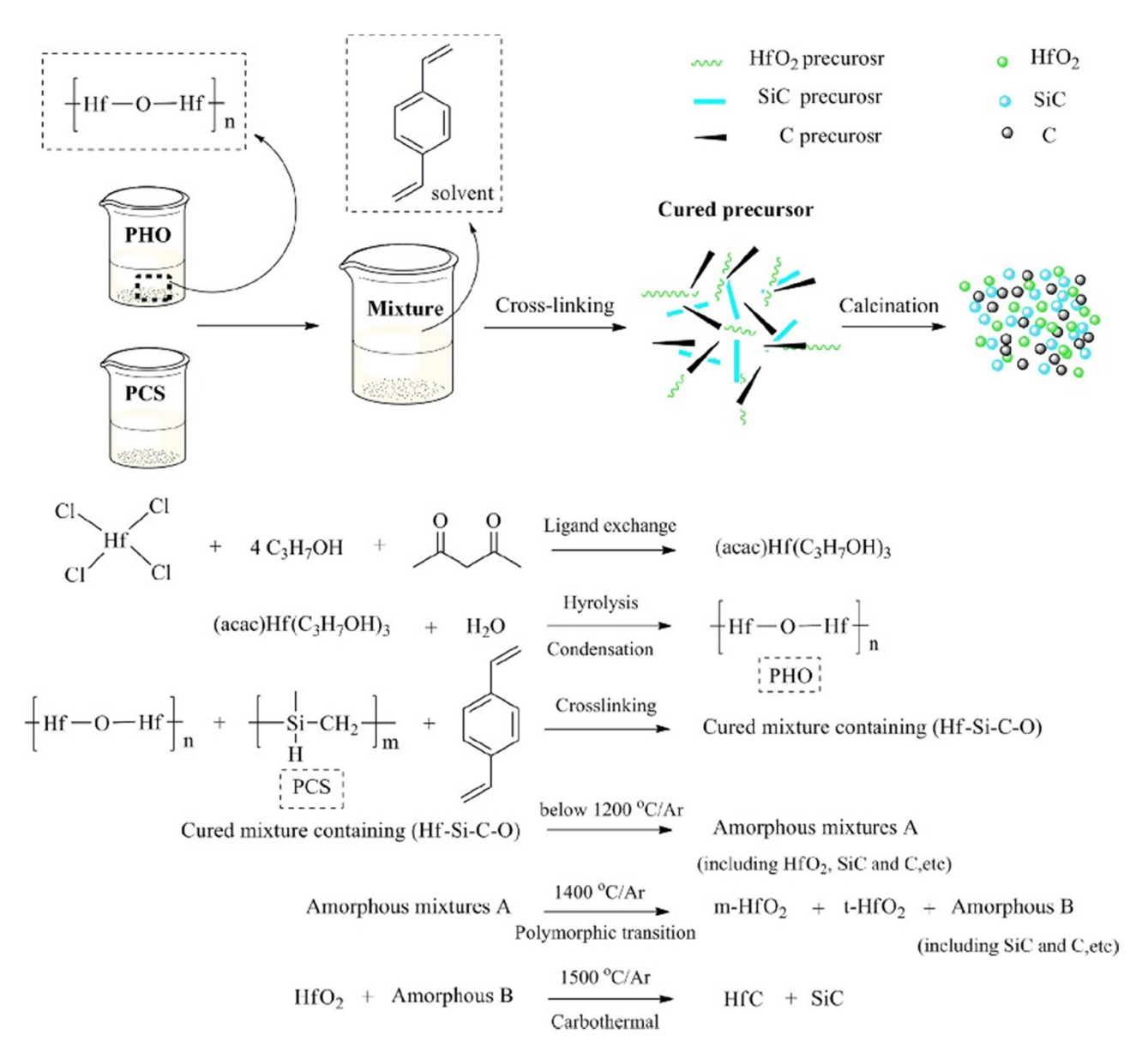


Figure 2: Ceramic transformation mechanism of HfC-SiC ceramic nanocomposites [65].

of ZrB₂ precursor (ceramic yield was about 30 wt%) and PCS (ceramic yield was about 55 wt%) for 2 h at 1,400-1,600°C to obtain C/SiC-ZrB₂ composites. High entropy ceramic phases can be generated from some precursors, which may be ideal choice for more extreme service environment applications [67]. Cai et al. [68] prepared $C_f/(Ti_{0.2}Zr_{0.2}Hf_{0.2}Nb_{0.2}Ta_{0.2})C-SiC$ composites with excellent mechanical and ablation resistance properties by successively impregnating (Ti_{0.2}Zr_{0.2}Hf_{0.2}Nb_{0.2} Ta_{0.2})C precursor and PCS (Figure 3), the flexural strength and fracture toughness were 322 MPa and 8.24 MPa·m^{1/2}, respectively. Accordingly, the ablation behavior and mechanism of $C_f/(Ti_{0.2}Zr_{0.2}Hf_{0.2}Nb_{0.2}Ta_{0.2})C$ –SiC were revealed [69]. Ziegler et al. [70] also found that the composites became embrittled as PIP cycles increased due to residual stresses at the matrix/ fiber interphase caused by volume shrinkage during pyrolysis. Heat treatment of precursors to remove the more volatile oligomeric precursors can increase the ceramic yields [71]. King et al. [72] enhanced the ceramic yield of the commercially available PCS (SMP-10) from 77 to 83% via heat treatment of the precursor before curing, while improving the rheological properties of the precursor.

PIP method has the following advantages: (1) lower the temperature required for precursor pyrolysis, less the mechanical and thermal damage to fiber/matrix interphase; (2) simpler equipment, allowing for near net shape; (3) the composition, structure, and properties of matrix can

be controlled by designing the molecular structure of the precursor; and (4) the design of the fiber preform allows the preparation of composites with complex geometry. However, the following problems still exist: (1) long densification cycles, high porosity, difficulty in achieving complete density, and many obturators in the matrix [73] and (2) UHTC precursors are difficult to synthesis, costly, and unstable. All these issues restrict the development of PIP process in the fabrication of $C_{\rm f}/UHTCMC$.

2.2 SI

The SI method is the most typical technique in which the ceramic powders are uniformly dispersed in a solvent to form a suspension slurry, which is introduced into the fiber fabrics and then made into $C_f/UHTCMC$ after drying, high temperature sintering, and other densification processes, the fabrication process is shown in Figure 4.

Vacuum and pressure-assisted impregnation are typically applied to introduce the UHTC slurry into the fiber preform. Chen *et al.* [75] utilized pressure impregnation to infiltrate TaC slurry into the interior of the fiber preform, repeated impregnation-drying followed by the introduction of the SiC matrix using the CVI process, and finally obtained C/SiC-TaC composites. Paul *et al.* [45] and

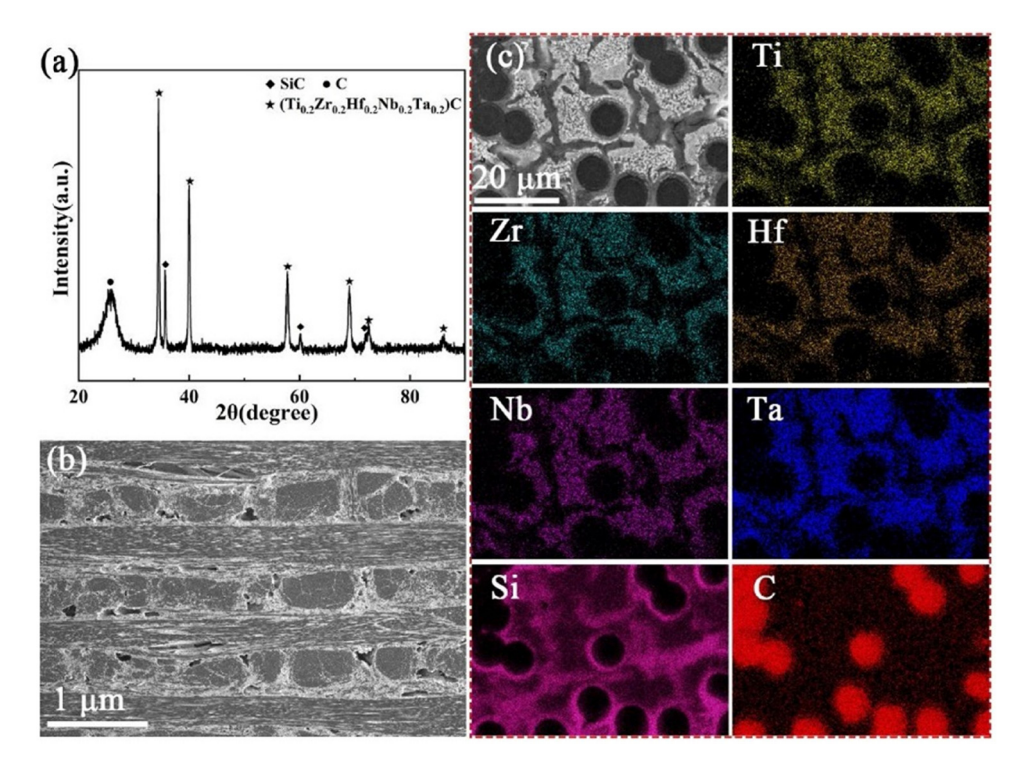


Figure 3: (a) XRD pattern, (b) SEM images, and (c) EDS analysis of the C_f/(Ti_{0.2}Zr_{0.2}Hf_{0.2}Nb_{0.2}Ta_{0.2})C-SiC composites [68].

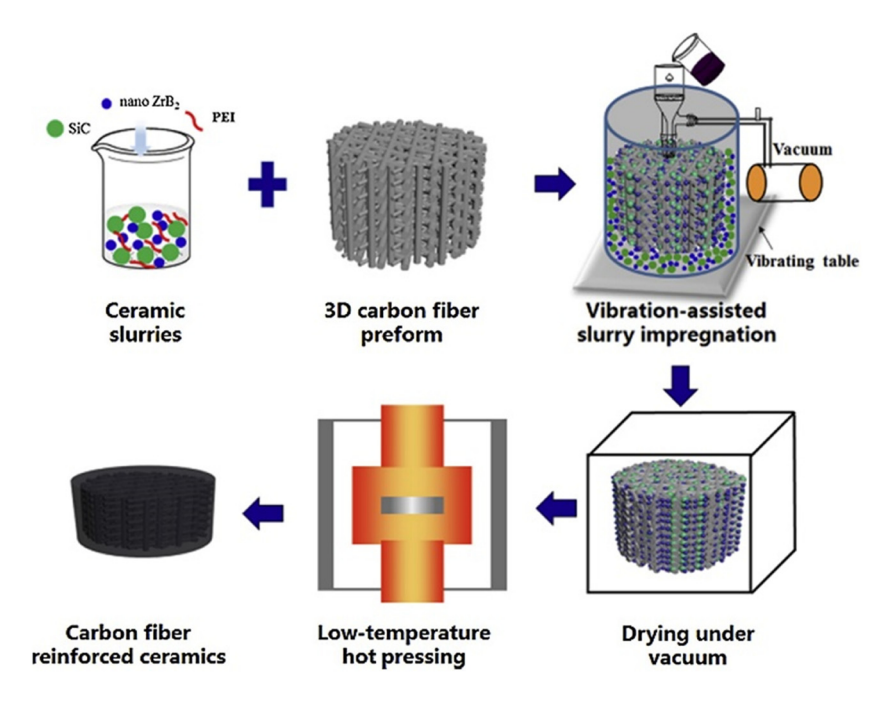


Figure 4: Process flow of C_f/UHTCMC prepared by SI method [74].

Tang et al. [46] fabricated a series of C_f/UHTCMC by vacuum slurry impregnation and evaluated their ablation properties. However, the ceramic powders tended to concentrate on the exterior of the preform, resulting in a limited depth of penetration. In order to solve the problem that the traditional vacuum slurry impregnation is difficult to fill the internal pores of the fiber preform, Baker [76,77] developed the slurry injection technique. The principle is based on vacuum slurry impregnation supplemented by the injection process, the ceramic slurry is directly injected into the pore space within the fiber fabrics, and the fluidity of ceramic slurry is used to achieve the filling of the slurry within and between the fiber bundles. Baker utilized this technology to fabricate C/HfC composites with high density, homogeneous ceramic phase distribution, high shear strength and excellent oxidation ablation resistance. In Tammana et al.'s [78] study, C_f/C-ZrC-SiC composites were prepared using a combined injection and vacuum infiltration of slurries technique followed by pyrolysis of the phenolic resin used as a bonding agent. Although the density is only 60% of theoretical, it was a relatively lowcost strategy. Zhang et al. [74,79] introduced the ceramic phase into the three-dimensional fiber weave via vibrationassisted slurry impregnation and produced C_f/ZrB₂-SiC composites with a relative density of 93.4 % and a flexural strength of 254 ± 22 MPa after heat treatment at 1,500°C for 2h under 30 MPa. The fracture toughness of 6.72 \pm 0.21 MPa·m^{1/2} and the fracture work of 2,270 J·m⁻² were improved by 14.8 and 36%, respectively compared to the

 C_f /ZrB₂–SiC composites prepared by the conventional slurry method due to the vibration assisted more uniform distribution of the ceramic phases.

Multiple authors have coated the slurry of UHTC powders onto fiber cloth, which was stacked, pressed, dried, and sintered to produce C_f/UHTCMC. In Chen et al.'s work [80], C_f/ZrB₂-SiC composites with 2D carbon fiber cloth as reinforcement were prepared through the combined processing of SI and HP. In addition, the influence of different stacking orientation and the matrix layer thickness on the thermal stress, fibers degradation, and cracks during HP was studied by finite element simulation. The result revealed that thermal stress distribution of composites was in good agreement with the cracks formation and fibers broken in the composites. Meanwhile, the thermal stress distribution in the composites was closely related to the matrix layer thickness and the relative position of fiber bundles. Thus, optimizing the stacking direction of carbon fiber cloth and matrix layer thickness is an effective method to reduce thermal stress and alleviate fiber degradation and cracking in the composites. Zoli et al. [81] utilized the hand lay-up to infiltrate SiC-ZrB₂ slurry into the fiber preform and prepared C/SiC-ZrB2 composites using HP and spark plasma sintering (SPS) for different sample sizes, respectively, breaking through the system scaling technique from laboratory scale samples to industrial grade components, as shown in Figure 5.

The SI method is characterized by simple process, short preparation cycle, low cost, controllable matrix

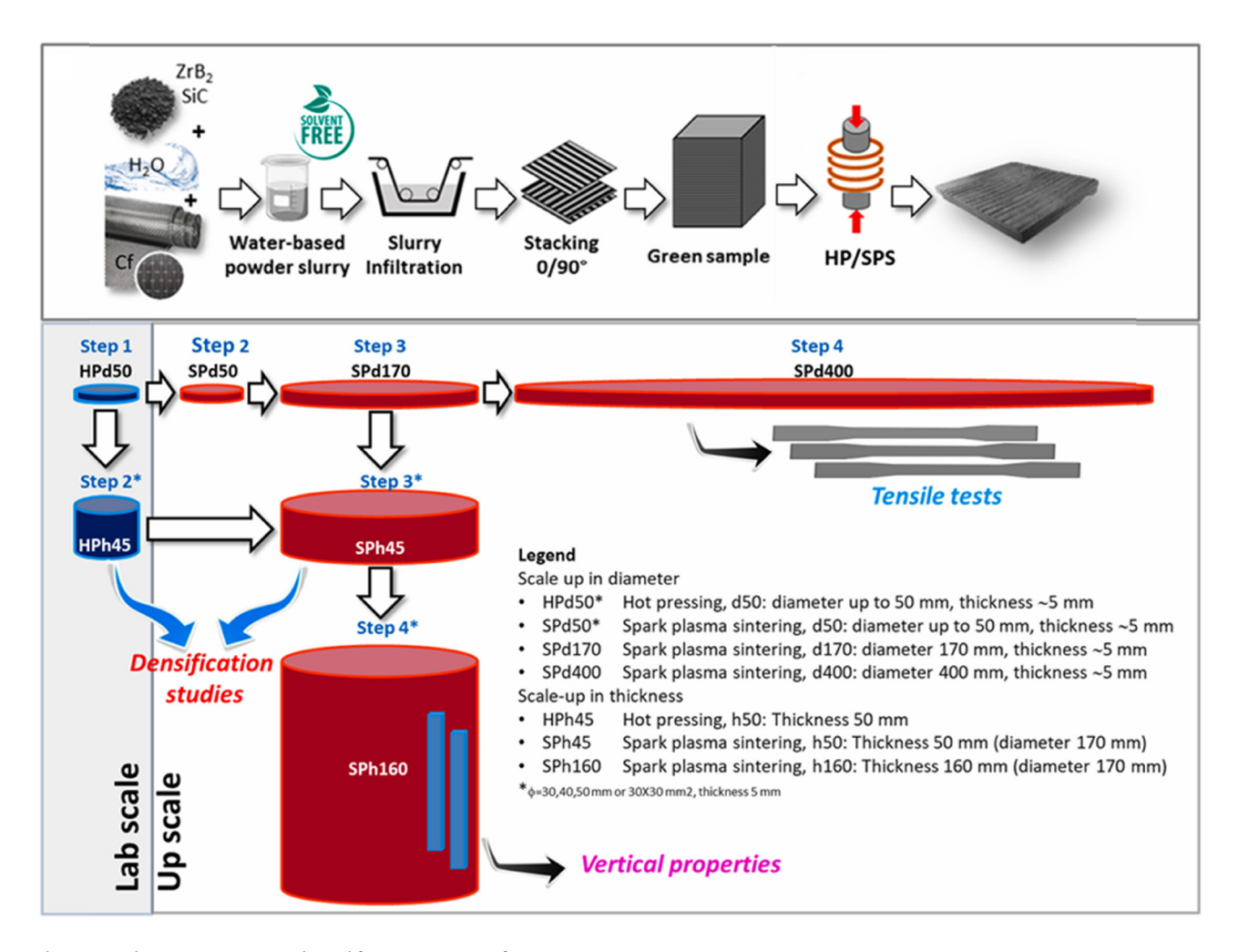


Figure 5: Fabrication process and amplification strategy of C/SiC-ZrB₂ composites [81].

component and content as well as few defects. However, the poor permeation effect on fiber preforms with a volume fraction of 20% or more results in low densification and non-uniform distribution of the UHTC phase.

2.3 RMI

The basic principle of RMI is that the molten metal or alloy penetrates the porous preform driven by capillary force and reacts *in situ* with the carbon/boron matrix of the preform to form ceramic phase, resulting in ceramic matrix composites (CMCs), as shown in Figure 6. Chen *et al.* [82] prepared C/ZrC composites *via* RMI using C/C preforms with different PyC contents and studied the effects of PyC content on microstructure, mechanical, and ablation properties. The mechanism of ZrC formation during the preparation of C/ZrC composites by RMI was investigated in depth by Zou *et al.* [83]. During the holding and initial cooling stages of the RMI, small ZrC particles nucleated

heterogeneously and grew coalesced to form larger islandshaped ZrC particles. The growth of ZrC was diffusion-controlled and determined by the diffusivity of carbon through the growing ZrC product layer around the carbon source. Wang et al. [84-86] fabricated C/C-ZrC, C/C-ZrC-SiC and C/SiC-HfC composites from Zr, Si_{0.87}Zr_{0.13}, and HfSi₂, respectively, and systematically investigated their mechanical and ablation resistance properties. Zeng et al. [87,88] prepared C/ C-TiC-ZrC and C/C-SiC-TiC-ZrC composites by RMI using Zr-Ti alloy and Zr-Ti-Si hybrid powder, respectively. Chen et al. [89,90] selected ZrSi2 alloy to penetrate into porous C/C-B₄C preform to manufacture C/SiC-ZrC-ZrB₂ composites, which exhibited excellent oxidation ablation resistance under 2,100°C per 300 s plasma ablation conditions. The typical morphology of Zr aggregation (spore-shaped) and SiC residuals were observed at the (PyC-SiC)2 interphase, as shown in Figure 7. The characterization results of the interphase revealed that the main reason for the interphase degradation was due to the reaction of PyC with Zr, while SiC layer of the interphase may melt under

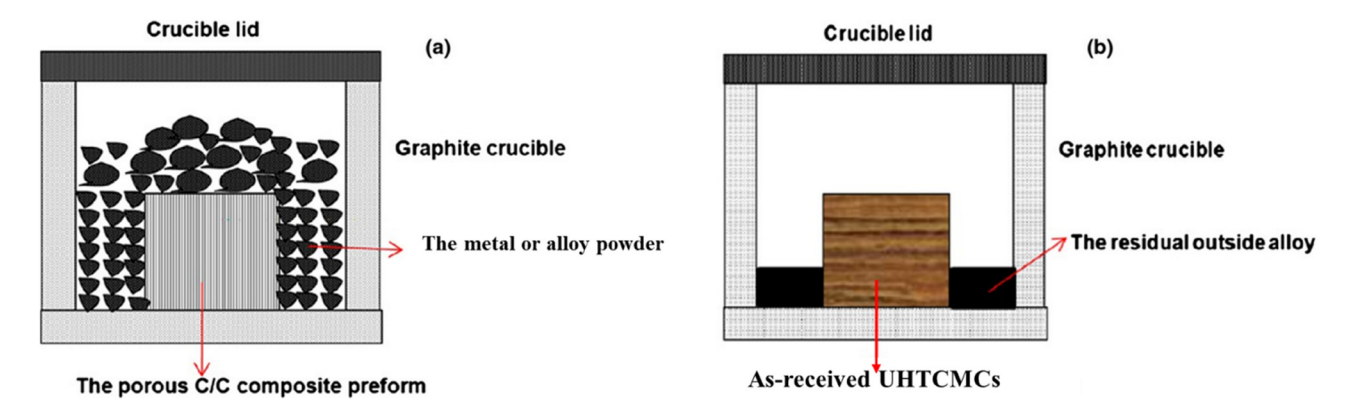


Figure 6: Schematic of RMI process for C_f/UHTCMC (a) before RMI and (b) after RMI [93].

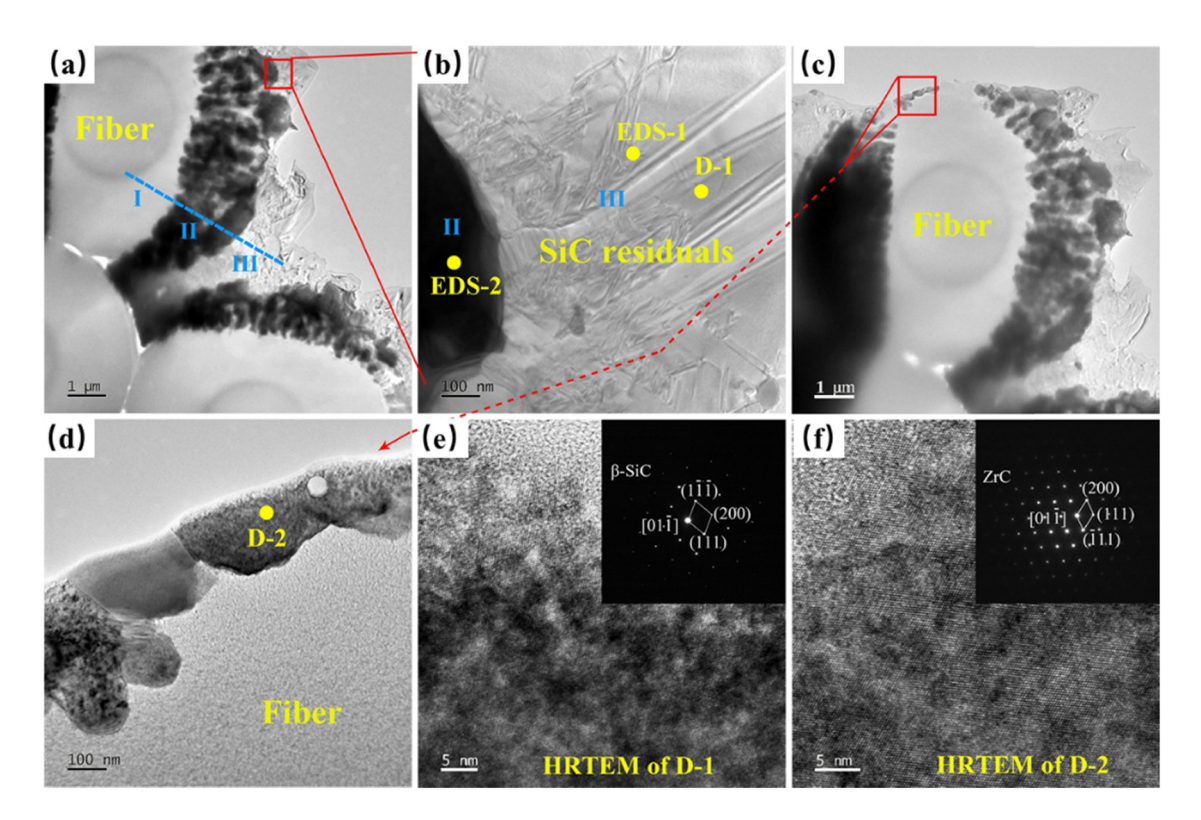


Figure 7: TEM images of the damaged (PyC-SiC)₂ interphase: (a)-(d) TEM bright-field images and (e) and (f) high resolution images from D-1 marked in (b) and D-2 marked in (d) [91].

the huge released heat from the in situ reactions according to the thermodynamic and heat conduction calculations [91]. Guo et al. [92] first reported the rapid preparation of dense carbon fiber reinforced (TiZrHfNbTa)C high-entropy ceramic composites by RMI, which exhibited superior flexural strength (612.6 MPa) and low ablation rates. Presently, RMI has become one of the main processes for the preparation of C_f/UHTCMC. This process has the merits of short cycle time, low cost, high density, high matrix bonding strength and is suitable for the preparation of large-size components with complex shapes. However, due to the higher reaction temperature, the elevated temperature metal or alloy melt is extremely susceptible to corrode the fiber and interphase, resulting in a severe impact on the mechanical properties. Moreover, due to the reactive infiltration kinetics control, the metal or alloy melt is not easily consumed, and the large size residual metal is prone to appear, which seriously deteriorates the mechanical properties and stabilization at elevated temperature.

The RMI process is one of the most commercially promising technologies for the large-scale, low-cost preparation of C_f/UHTCMC. Therefore, to overcome the shortcomings of the process, such as fiber degradation and residual metal, is a pivotal concern for many scholars. In response to the drawbacks of the RMI process, relevant researchers have carried out a great deal of improvement research work in recent years, mainly focusing on two aspects: one is to adjust the composition of reactive melt, and the other is to optimize the pore and matrix structure of the fiber preform. Vinci [94] and Kütemeyer [95] fabricated C_f/UHTCMC composites with lower fiber degradation by infiltrating Zr₂Cu alloys into C_f/ZrB₂–B and C_f/ZrB₂–B–C porous preforms at 1,200°C, respectively. The viscosity of the elevated temperature melt and the wettability with the substrate will influence the penetration process. Xu et al. [96,97] developed a molten salt assisted RMI process by using K_2MeF_6 (Me = Zr, Ti) molten salt mixed with Si and Zr-Si powders to reduce the viscosity of the melt and improve the wettability of the melt with the carbon in the matrix, which allowed Zr and Si to dissolve in the molten salt and infiltrate into preform together at temperature below 1,400°C, and react with pyrolytic carbon matrix

to produce carbides, as shown in Figure 8. As mentioned above, the means of adjusting the composition of reactive melt can reduce the fiber etching and residual metal in the preparation process, so as to enhance the comprehensive properties of the resulting composite, but decreasing the proportion of UHTCs matrix. Thus, only the adjustment and improvement of melt composition cannot fundamentally overcome the shortcomings of RMI process.

Numerous studies have shown that pore structure is the hinge to RMI process, pore size and distribution determine the infiltration behavior of the melt, which in turn affects the phase composition and distribution. Chen *et al.* [98] fabricated C/B₄C–C preforms with different pore structures by slurry impregnation and sol–gel, respectively, and comparatively investigated the effect of pore structure on the melt infiltration process of ZrSi₂ and the properties of the resulting C/ZrC–ZrB₂–SiC composites. The result showed that the pore size distribution of C/B₄C–C preform prepared by sol–gel was more uniform, and the pore closure time during the melt infiltration process was longer, resulting in a more uniform distribution of the matrix phase and better mechanical properties of the composite. Compared to large and dense carbon/boron substrates, micron or

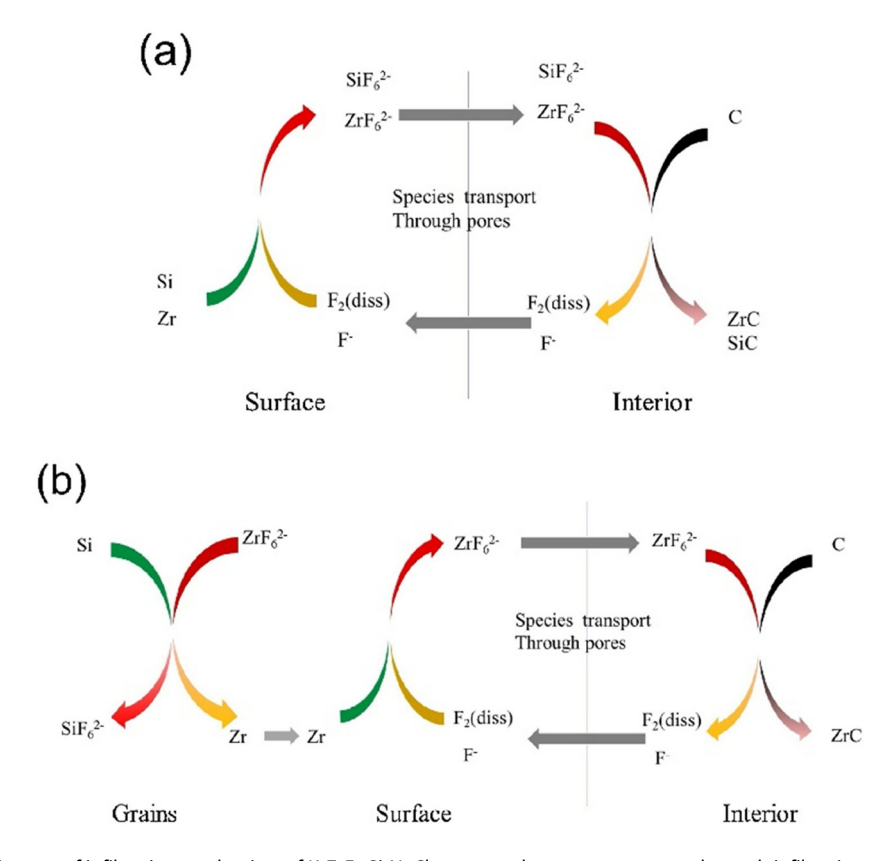


Figure 8: Schematic diagram of infiltration mechanism of K_2ZrF_6 -Si-NaCl system at low-temperature molten salt infiltration stage: (a) dissolution of Zr and Si particles in salt and (b) complete loop of molten salt reactions [96].

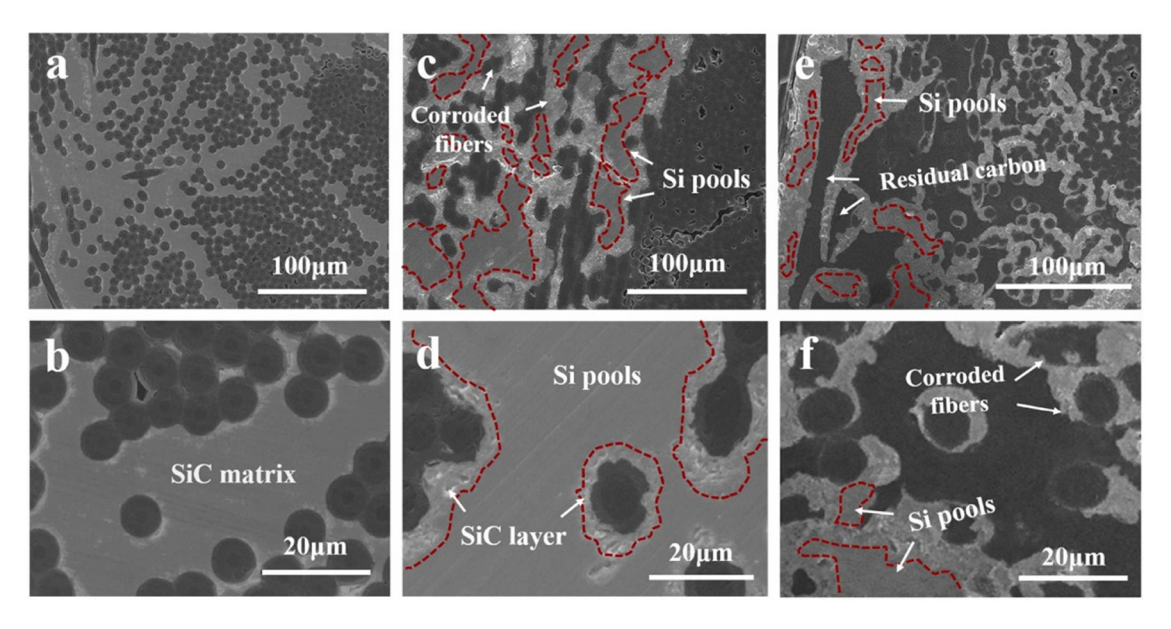


Figure 9: SEM images of C/SiC composites prepared with (a) and (b) C/NC; (c) and (d) C/PyC, and (e) and (f) C/ReC [102].

submicron porous substrates have the advantages of larger specific surface area, smaller skeletal particles and higher reactivity [99]. The introduction of porous substrates instead of large dense substrates can facilitate the full reaction of the preform substrate with melt to some extent. Zhao et al. [100-102] utilized carbon fiber reinforced nanoporous carbon matrix (C/NC) preforms which consisted of overlapping nanoparticles and abundant nanopores to obtain highperformance C/SiC composites after silicification. The effect of C/NC on the composition and microstructure of C/SiC composites was explored by comparing C/C preforms with conventional PvC and resin carbon (ReC) matrices, Figure 9. The nanoporous carbon matrix basically achieved complete ceramic transformation, and the prepared C/SiC composites had higher densification, low carbon fiber damage, almost no unreacted carbon, and residual silicon in the matrix, with the highest flexural strength (218.1 MPa). Nevertheless, the ReC and PyC matrices had lower ceramic transformation, the corresponding C/SiC composites have lower densification and a large amount of unreacted carbon, residual silicon, and etched carbon fibers, which exhibited lower flexural strength of 170.5 and 128.0 MPa, respectively. In summary, the ideal porous carbon/boron matrix should possess smaller pore size and skeleton particles, moderate porosity, and atomic orderliness.

2.4 CVI

The CVI process involves the decomposition of the reaction gas at elevated temperature into radicals which nucleate

and grow on the surface of the preform to form a continuous matrix [103], as shown in Figure 10. This process is diffusely used for the preparation of C/C and C/SiC composites owing to the good continuity of the matrix prepared, the high degree of crystallization, and excellent mechanical and ablation properties. In addition to growing C and SiC matrices, the CVI process can also be utilized to fabricate UHTC matrices in $C_f/UHTCMC$. For example, HfC and ZrB_2 can be prepared according to Eqs. (1) and (2).

$$HfCl_4 + CH_4 + H_2 \stackrel{Ar}{\rightarrow} HfC + 4HCl + H_2,$$
 (1)

$$ZrCl_4 + 2BCl_3 + H_2 \xrightarrow{Ar} ZrB_2 + HCl.$$
 (2)

Sayir [105] prepared C/HfC, C/TaC, and C/HfC-TaC composites by CVI process, but the composites had low density

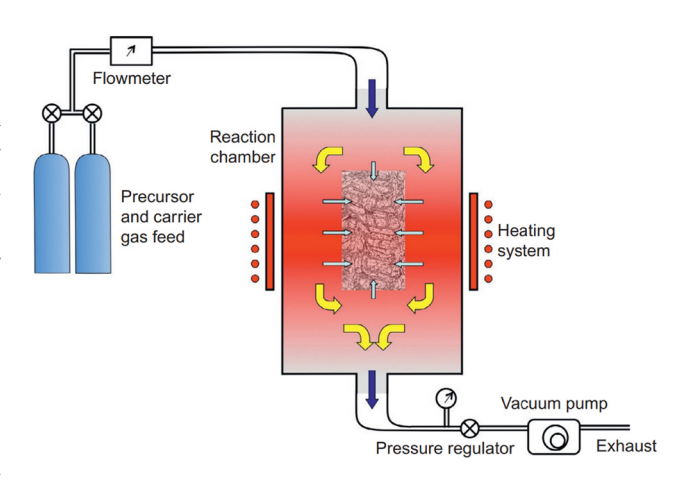


Figure 10: Schematic description of CVI process [104].

and poor mechanical properties. Chen *et al.* [106] applied CVI to deposit TaC on carbon fibers using $TaCl_5$ –Ar– C_3H_6 – H_2 source, but there was also inability to densify. This is because the infiltration of isothermal CVI tends to occur near the outer surface of the preform, where the gas concentration and temperature are highest, resulting in the crusting phenomenon [107]. Electromagnetic-coupling CVI (E-CVI) applied electromagnetic field and thermal gradient into carbon fiber preform, thus partially overcoming the limitations of slow deposition rate and shallow penetration depth. Hu *et al.* [108] designed and fabricated sandwich-

structured C/C-SiC composite with a processing cycle of only 20 h using two-step E-CVI process, and investigated the related deposition mechanism [109], as shown in Figure 11.

The CVI method, which deposited ceramic matrices with high melting point at lower temperature, is suitable for fabricating CMCs with complex geometric structures. The lower pressure and temperature of CVI process results in less mechanical and thermal damage to the fibers and allows the composition and properties of the composite to be regulated by designing the process conditions. The main

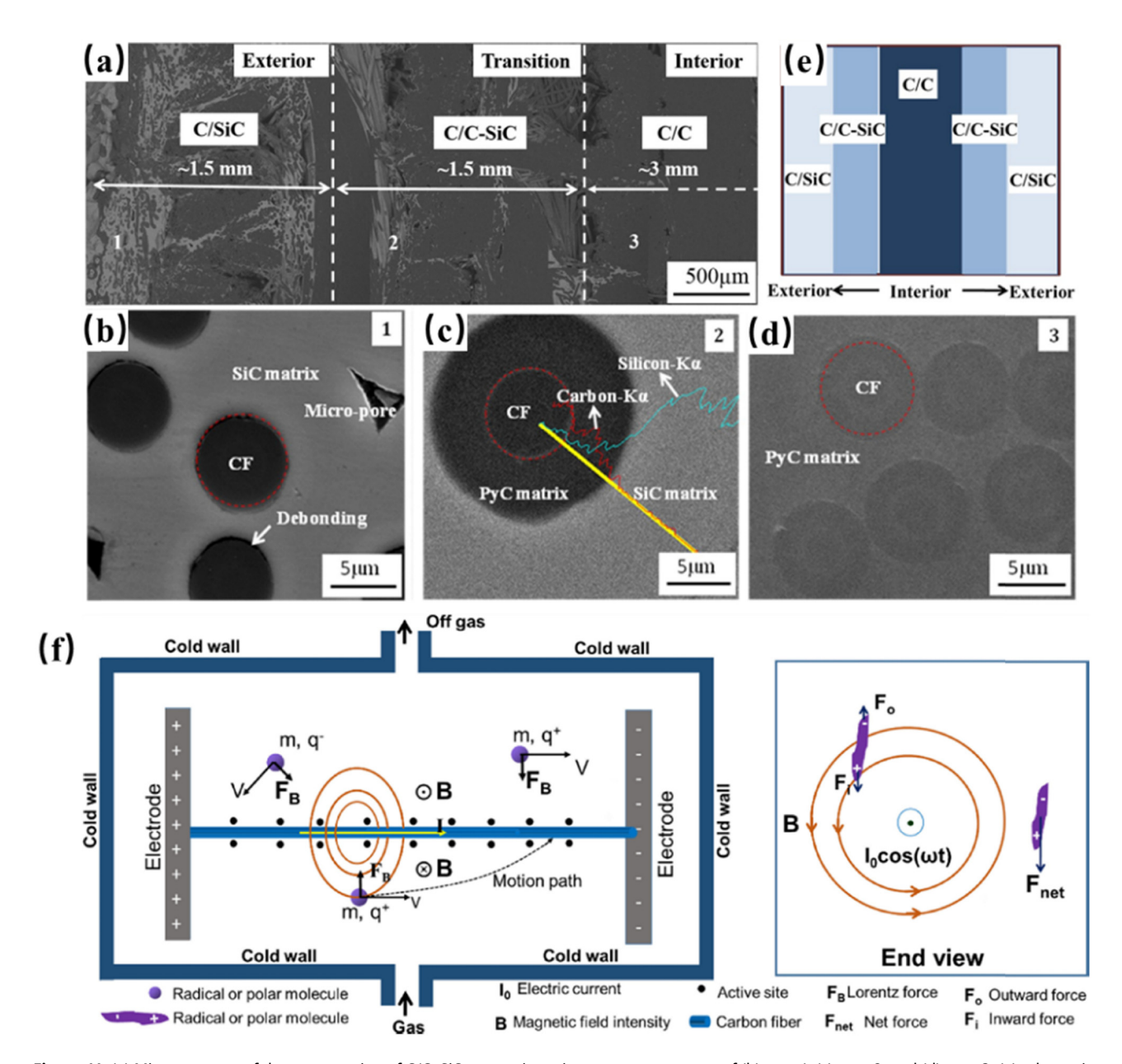


Figure 11: (a) Microstructure of the cross-section of C/C–SiC composite, microstructures pattern of (b) area 1, (c) area 2, and (d) area 3; (e) schematic diagram of the composite and (f) schematic of the E-CVI process [108,109].

disadvantages of the CVI method are slow reaction rate, long preparation cycle, high-energy consumption, and high cost. Moreover, this method suffers from shallow penetration depth and different proportion of gas phase raw materials in the preparation of UHTC phases for large components, leading to inconsistent matrix composition at various locations in the product. As a result, there is rather limited literature on the preparation of UHTC phases directly from CVI method. Currently, the CVI method is commonly utilized for density composites prepared by other methods, fabricating UHTC interphase, or UHTC coating.

2.5 Others

The main preparation methods of C_f/UHTCMC, such as PIP, SI, RMI, and CVI, have been discussed previously, each with their advantages and disadvantages. Several other methods have also been studied, including chemical liquid vapor deposition (CLVD) [110-112], in situ reaction [113-115], sol-gel [116-118], powder pre-infiltration (PPI) [119,120], HP, pressureless sintering, additive manufacturing (AM), etc. Each method has unique advantages in terms of controlling microstructure, performance, and cost. However, these methods have not yet been extensively used in C_f/UHTCMC. The few available reports that cover these techniques are briefly described below.

He et al. [121] fabricated C/C-ZrC-SiC composites via CLVD process using carbon fiber preforms with different densities and investigated the effect of preform density on the microstructure and ablation behavior of the composite. Shen et al. [122] prepared C/C-ZrC composites via an in situ synthesis by carbothermal reduction reaction of ZrO2 and carbon in which ZrO₂ was completely converted to ZrC. With zirconium oxychloride octahydrate, tetraethoxysilane, and phenolic resin as raw materials for gel precursor, Zeng et al. [123] introduced ZrC-SiC matrix into the porous C/C composites by impregnation of gel precursor under negative pressure, followed by heat-treatment process for carbonization and carbothermal reaction. The PPI process involves pre-dispersing UHTC powders into carbon fiber preforms during fabric preparation. Tang et al. [124] combined this technique with a rapid CVI densification process to manufacture C/ZrB₂-SiC composites. HP is typically used for the preparation of short carbon fiber reinforced UHTC composites, which can achieve a high theoretical density (>90%) [125]. However, carbon fibers are accessible to degradation during the HP process, resulting in the reduction of mechanical properties [126], and it is difficult to produce complex geometries. Cheng et al. [127] fabricated C/ZrC-SiC composites with PyC interphase by HP using ZrC,

SiC powders, and short carbon fibers. Kannan et al. [54] reported a joint of reactive hot pressing (RHP) and PIP to prepare C_f/SiC-ZrB₂-Ta_xC_v composites using C_f cloth, PCS, ZrB₂ and Ta powders at 4 MPa and 1,200°C. Zoli et al. [128] demonstrated that it is possible to replicate the microstructure and mechanical properties of continuous fiber reinforced ZrB2-SiC composites densified by HP, using the SPS technique. The micromorphology of the specimens reinforced pitch-based carbon fibers sintered by SPS at 1,850°C and 40 MPa is shown in Figure 12. Pitch-based carbon fibers remained intact even without coatings due to their graphitic structure [129]; however, the lack of coatings resulted in a stronger fiber/matrix interphase which restricted the fiber pull-out. Pressureless sintering is one of the simplest sintering techniques, suitable for components with different geometries, with low preparation cost and can be exploited for large-scale commercial production. Zhou et al. [57] successfully manufactured PyC-C_{sf}/ZrB₂-SiC-ZrC composites through cold isostatic molding and pressureless sintering using B₄C as sintering additive, and analyzed the effect of B₄C on the sintering and ablation mechanism for PyC-C_{sf}/ZrB₂-SiC-ZrC composites.

AM technologies offer novel approaches for fabricating C_f/UHTCMC and their constructions. According to the different technological routes, AM technologies can be classified as stereolithography [130], digital light processing [131], selective laser sintering [131], extrusion free forming [132], binder jetting [133], direct ink writing (DIW) [134], and hybrid AM [135]. It is worth noting that after AM forming, conventional matrix densification processes such as CVI, PIP, RMI, HP, and other sintering techniques are typically required to obtain C_f/UHTCMC components. The fabrication of CMCs using AM techniques has attracted a great deal of interest [136,137] and many efforts have been undertaken in C/SiC [138–143]; however, there has not been significant success in C_f/UHTCMC. Figure 13 presents the preparation process and mechanical properties of continuous carbon fiber reinforced ZrB2-SiC composites via DIW and low temperature HP sintering. It was found that the flexural strength, fracture toughness, and the work of fracture were 388.3 MPa, $10.04 \,\mathrm{MPa \cdot m^{1/2}}$ and $2,380 \,\mathrm{J \cdot m^{-2}}$, respectively, when the thickness of the carbon interphase was about 110 nm [144]. In addition, a novel processing route that combined with DIW and RMI was developed to prepare short carbon fiber reinforced ZrB₂-SiC composites [145]. AM technologies have the advantages of small batch rapid prototyping, complex geometry, lower cost, customizable composition and performance, biomimetic structure design, etc., which offers an important avenue for manufacturing C_f/UHTCMC. Nonetheless, the AM technologies in terms of C_f/UHTCMC are still in

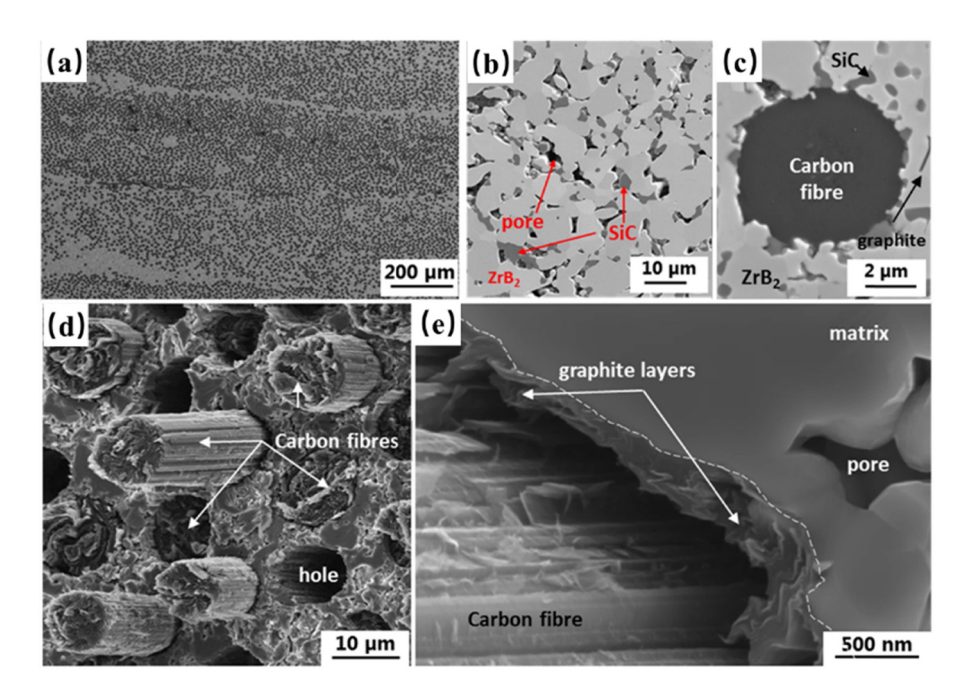


Figure 12: SEM images of the specimens reinforced pitch-based carbon fibers: (a) cross section; (b) detail of the matrix, the light phases are ZrB₂, grey phases are SiC, and dark areas are pores; (c) single fiber section; (d) fracture surface; and (e) detail of fiber/matrix interphase [128].

the initial stage, and numerous problems and challenges remain, limiting its development. First, some critical defects may be introduced during the AM and densification process, which greatly restrict the mechanical properties, reliability, and repeatability of the resulting composites, including but not limited to residual pore, cracks, stronger or weaker interfacial bonding, and matrices and fibers inhomogeneity. Second, developing a new AM technology and equipment that combines this with continuous carbon fiber reinforcement is one of the biggest challenges currently faced.

3 Ablation behaviors of C_f/UHTCMC

For the extreme service environment of hypersonic vehicle, the long-term resistance to oxidation, ablation, and corrosion are significant parameters of $C_f/UHTCMC$. The oxidation and ablation mechanism of $C_f/UHTCMC$ is the formation of a compact oxide layer with moderate viscosity and low saturated vapor pressure on the surface [146], which is protective to ingress of oxygen and mechanical denudation. Moderate viscosity means that the oxide layer is able to heal the pores and cracks on the surface of the material, while with the ability to resist mechanical scouring [147]. The low saturated vapor pressure can slow down the volatilization loss of the oxide layer, thus effectively hindering the spread of oxidation into the interior of material [148].

Single-phase C_f/UHTCMC (C/ZrC, C/HfC, C/TaC, etc.) form refractory metal oxides with high melting points on the surface after oxidation, which generally exist in the form of oxide particles, making it difficult to form compact oxide layers, thus singlecomponent C_f/UHTCMC have poor oxidation resistance [149]. The researchers introduced boron and silicon elements into C_f/UHTCMC to enable the composite to form oxides (B₂O₃, SiO₂) that are more layer-forming at low and medium temperatures when exposed to the oxygen-containing atmosphere, forming low eutectic oxides with ZrO₂/HfO₂ or filling cracks and pores between particles [150–152]. While ZrO₂/ HfO₂ skeleton also decreases the volatile consumption of the oxide layer, leading to slow inward diffusion of oxygen. Therefore, multi-phase UHTCs can make the oxides protective layer more stable and self-healing at elevated temperature, significantly enhancing the oxidation and ablation performances. Commonly available methods for testing ablation properties involve high-velocity oxy flame (HVOF), scram jet, arc jet, oxyacetylene torch (OAT), and laser ablation [153]. Among these assays, HVOF and OAT are relatively fast and inexpensive initial screening techniques. Scram jet and arc jet are closest to the hostile environments of real aerospace applications, but are extra expensive to test and not widely available. In addition to the physical and chemical properties of C_f/UHTCMC, the ablation properties are also related to heat flux, gas flow rate, combustion gas chemistry, and distance and angle between the flame and the sample. Table 1 summarizes the thermal ablative methods used for testing

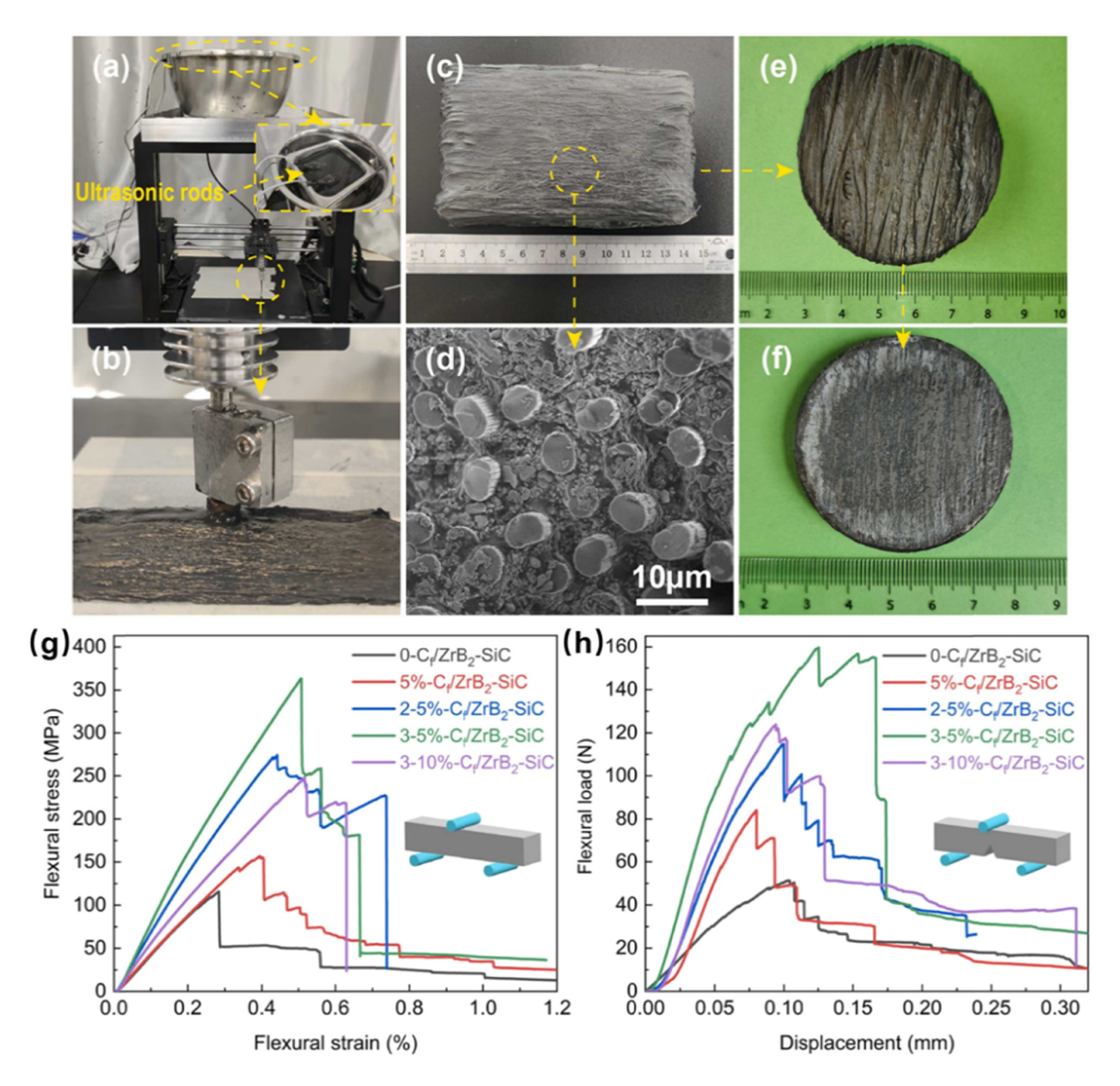


Figure 13: (a) and (b) Optical image of the C_f/ZrB₂-SiC composite fabricated by DIW; (c) Macroscopic morphology, and (d) microstructure of the C_f/ZrB₂-SiC green body; Physical photographs of (e) heat-treated sample and (f) final sintered C_f/ZrB₂-SiC composite. Flexural stress (load)-strain (displacement) curves of (g) three-point bending bars and (h) single-edge notched beam specimens for C_t/ZrB₂-SiC composites [144].

C_f/UHTCMC and their ablation behavior. It should be noted that the investigations in connection with UHTCs coating are not involved in this work.

Based on the results summarized in Table 1, the ablation resistance of multiphase C_f/UHTCMC is basically outstanding. The borides oxidize rapidly to generate B₂O₃ at approximately 600°C, form a glassy B₂O₃ phase on the surface below 1,000°C, providing oxidation protection for the underlying substrate [164,165]. Above 1,000°C, however, this protection mechanism fails due to the evaporation of B₂O₃. The addition of SiC can significantly enhance the oxidation resistance of C_f/UHTCMC by generating silicate glasses at moderate temperature of 1,200–1,650°C [166]. Nevertheless, at higher temperatures, oxidation mechanism of SiC changes from "passive oxidation" to "active oxidation," producing gaseous SiO rather than molten SiO₂ [167]. The oxidation behavior of ZrC-SiC and HfC-SiC has also been reported in the literature, with the formation of Zr (Hf)O₂-SiO₂ solid solution fluid oxide layers and Zr(Hf)O₂ solid skeleton as a barrier to oxygen diffusion at

Table 1: Ablation resistance properties of various C_f/UHTCMC reported in the literature

Material	Detailed fabrication process	Density (g·cm ⁻³)	Open porosity (%)	Ablation method	Temperature (°C) Time (s)		Heat flux (MW·m ⁻²)	Linear ablation rate (µm·s ⁻¹)	Mass ablation rate	Ref.
C/ZrC	3D fiber reinforcement infiltrated with ZrC precursor, curing, pyrolysis at 1,200°C, after 16 cycles, heat treatment at 1,600°C	1	1	ОАТ	2,297	300	4.187	4	6 mg·s ⁻¹	[154]
C/C-HfC	2D needled carbon fiber felts initially treated by CVI of PyC, infiltration of HfC precursors, heat treatment at 1,500–1,600°CC	2.01	ı	Plasma flame	2,300	240	I	5.31 ± 0.02	0.55 ± 0.02 mg·s ⁻¹ ·cm ⁻²	[155]
C/(C-SiC) _{CVI} -(ZrC-SiC) _{PIP}	PyC–SiC volume ratio of 0.12 deposited in preform by CVI, infiltration of PZC–PCS (4:1) precursors and further treatment at 1.500°C	2.30 ± 0.05	18.1 ± 1.5	OAT	2,100	009	ı	0.94	0.13 mg·s ⁻¹ ·cm ⁻²	[156]
C/C-HfB ₂ -SiC	2.5D needled carbon fiber preform treated by CVI of PyC, further infiltrated by HfB ₂ slurry to obtain C/C-HfB ₂ preform; PIP of PCS within preform to form dense C/C-HfB ₂ -SiC	4.07	7.58	ОАТ	2,500	120	3.86	0.415	0.5 mg·s ⁻¹	[157]
C/HfC–SiC	PyC deposited in preform by CVI, RMI of Hf–Si alloy in vacuum at 1,700–1,800°C for 1–2 h to generate C/HfC–SiC	3.42 ± 0.4	7.31 ± 0.49	ОАТ	3,000	120	4.186	-2.33 ± 0.14	0.06 ± 0.03 mg·s ⁻¹	[158]
C/C-SiC-HfC-ZrC	C/C preform infiltrated by the mixed precursors (PZC/PHC/PCS), pyrolyzed at 1.300–1.600°C	2.38	11.07	OAT	2,400	120	2.38	0.025	-0.151 mg·s ⁻¹ ·cm ⁻²	[159]
C/C-SiC-ZrC-TiC	Chopped web needled fabrics initially treated by CVI of PyC, densification at 2,000°C by RMI using Zr, Si, and Ti mixed powders as the infiltrates	3.25	5.6	OAT	2,500	09	ı	0.000	0.008 mg·s ⁻¹ ·cm ⁻²	[87]
C _r /SiC–ZrC–ZrB ₂	PyC/SiC deposited in $C_f/C-B_4C$ preform via CVI, $ZrSi_2$ melt was infiltrated into the preforms under vacuum at 1,850°C	2.47	7.4	Air plasma	2,400	09	ı	100	2.92 g·m ^{-2·} s ⁻¹	[88]

(Continued)

Table 1: Continued

Material	Detailed fabrication process	Density (g·cm ⁻³)	Open porosity (%)	Ablation method	Temperature (°C) Time (s)	Time (s)	Heat flux (MW·m ⁻²)	Linear ablation rate (µm·s ⁻¹)	Mass ablation rate	Ref.
C _r /ZrB ₂ –ZrC–SiC	3D fabrics initially treated by CVI of PyC/SiC, impregnated by ZrB ₂ –ZrC-PCS slurry, pyrolyzed at 900°C and further heat treatment at 1.500°C	2.28	13	Plasma wind tunnel	2,027	300	I	2	10 mg·s ⁻¹	[160]
C _t /ZrB ₂ –SiC–ZrC	The ZrB ₂ –PCS–Zr powder mixtures and PCS coated C _r cloth were alternatively stacked, hot pressed at 1,200°C PIP with PCS at 1,200°C	2.61	21	ОАТ	2,100	09	I	5.30	2.08 mg·s ⁻¹	[161]
C/C-ZrC-SiC-ZrB ₂	C/C-B _a C preform infiltrated by RMI of ZrSi powder at 2,100°C under Ar atmosphere	I	I	OAT	2,500	120	2.38	-1.0	0.7 mg·s ⁻¹	[40]
C _{sf} /ZrC–SiC–HfB ₂	Short carbon fiber (30 wt%)/ZrC/SiC/ HfB ₂ slurry dried and compressed. Pressureless sintering at 2,200°C	4.12	∞	ОАТ	2,810	09	ı	3.51	2.46 mg·s ⁻¹	[162]
C _f /SiC-ZrB ₂ -Ta _x C _y	Cr doth coated with PCS and ZrB2-PCS-Ta powder mixtures stacked and RHP at 1,200°C, further PIP of PCS (fran cycles)	2.82	21	ОАТ	2,000	009	ı	1.43	2.19 mg·s ⁻¹	[54]
C _f /(Ti _{0.2} Zr _{0.2} Hf _{0.2} Nb _{0.2} Ta _{0.2})C–SIC	PyC/Sic Company Co. PyC. PyC/Sic Color PyC/Sic Color PyC/Sic Color PyC/Sic PyC/Sic PyC/Sic PyColor PyColor Pycolyzed at 400°C + heat treatment at 1,700°C, further infiltrated by PCS	2.40	13.32	Air plasma torch	2,430	300	ស	2.89	2.60 mg·s ⁻¹	[68,69]
C _r /(TiZrHfNbTa)C	Needle felt C _r /C preforms infiltrated by RMI of TiZrHfNbTa high-entropy alloy	3.85 ± 0.3	1.0 ± 0.2	OAT	2,000	120	I	0.8 ± 0.1	$1.2 \pm 0.2 \mathrm{mg \cdot s}^{-1}$	[92]
C/Ti _{0.2} Zr _{0.4} Hf _{0.4} C-Ti _{0.5} Nb _{0.5} C _{0.95}	ziroy ZrC/TiC/HfC/NbC/TaC/carbon black/ pitch-based milled carbon fiber mixed, densification at 1,750°C by RMI of Zr–Ti alloy	5.69	۲5	Arc jet	1,800–1,900	300	1.2	7.1-	I	[163]

1,700–2,200°C [168–170]. Often, Zr(Hf)B₂–SiC composites possess better ablation resistance than Zr(Hf)C-SiC composites in a wider temperature range due to the synergistic effect of B₂O₃, borosilicate, SiO₂, Zr(Hf)–Si–O and Zr(Hf)O₂ skeleton [171–174]. The C/C-SiC-ZrC-TiC composites exhibited nearzero ablation behavior at 2,500°C for 60 s in an oxyacetylene flame [87]. This is attributed to the high viscosity and low volatility of the multiphase oxide layer consisting of Zr_{1-x}Ti_xO₂ dispersed in SiO₂, which resisted the ultra-high-temperature volatilization and high-speed airflow flushing. The ablation behavior of C_f/SiC–ZrB₂–Ta_xC_v under oxyacetylene flame at 2,000°C for 600 s is also reported, the pores and cracks were filled with the molten Ta_xO_y and SiO₂ [54]. Makurunje et al. [175] demonstrated the crack repair effect of a self-generating oxidation protective glass-ceramic coating arising from glassy SiO₂ as well as eutectics of TiO₂–SiO₂ and Ti₂O₅–SiO₂ when the C_f/C-SiC-TiC-TaC composites were exposed to oxidative/ablative high temperature environment. Thus, multiphase UHTCs provide an effective pathway to improve the ablation resistance of composites.

Multiple carbides typically refer to carbides containing three or more transition metal elements, which generally

still have a single-phase cubic crystal structure, while carbides of five or more elements are called high-entropy carbides (HECs) [176-178]. HECs have attracted much attention in recent years due to their high hardness, high temperature fracture strength, low thermal conductivity, high melting point, and superior oxidation resistance compared to multiphase UHTCs composites [179-181]. Zhang et al. [182] successfully developed $C_f/(Ti_{0.2}Zr_{0.2}Hf_{0.2}Nb_{0.2}Ta_{0.2})$ C-SiC composites with flexural strength and flexural modulus of 269 \pm 25 MPa and 53.3 \pm 7.9 GPa, respectively, using slurry coating and laminating combined with PIP at a low temperature of 1,200°C. However, there are few reports on the ablation resistance and mechanism of carbon fiber reinforced HEC composites because of the complexity of the composition which makes conventional exploration more difficult. In Cai's report [69], the ablation behavior and mechanism of $C_f/(Ti_{0.2}Zr_{0.2}Hf_{0.2}Nb_{0.2}Ta_{0.2})C$ -SiC composites were investigated at length, as shown in Figure 14. During the ablation process, high-entropy oxides (TiZrHfNbTa) O_x skeleton covered by highly viscous SiO₂ melt was generated at the ablation center. As the temperature decreases, (TiZrHfNbTa)O_x precipitates as a spherical oxide from the

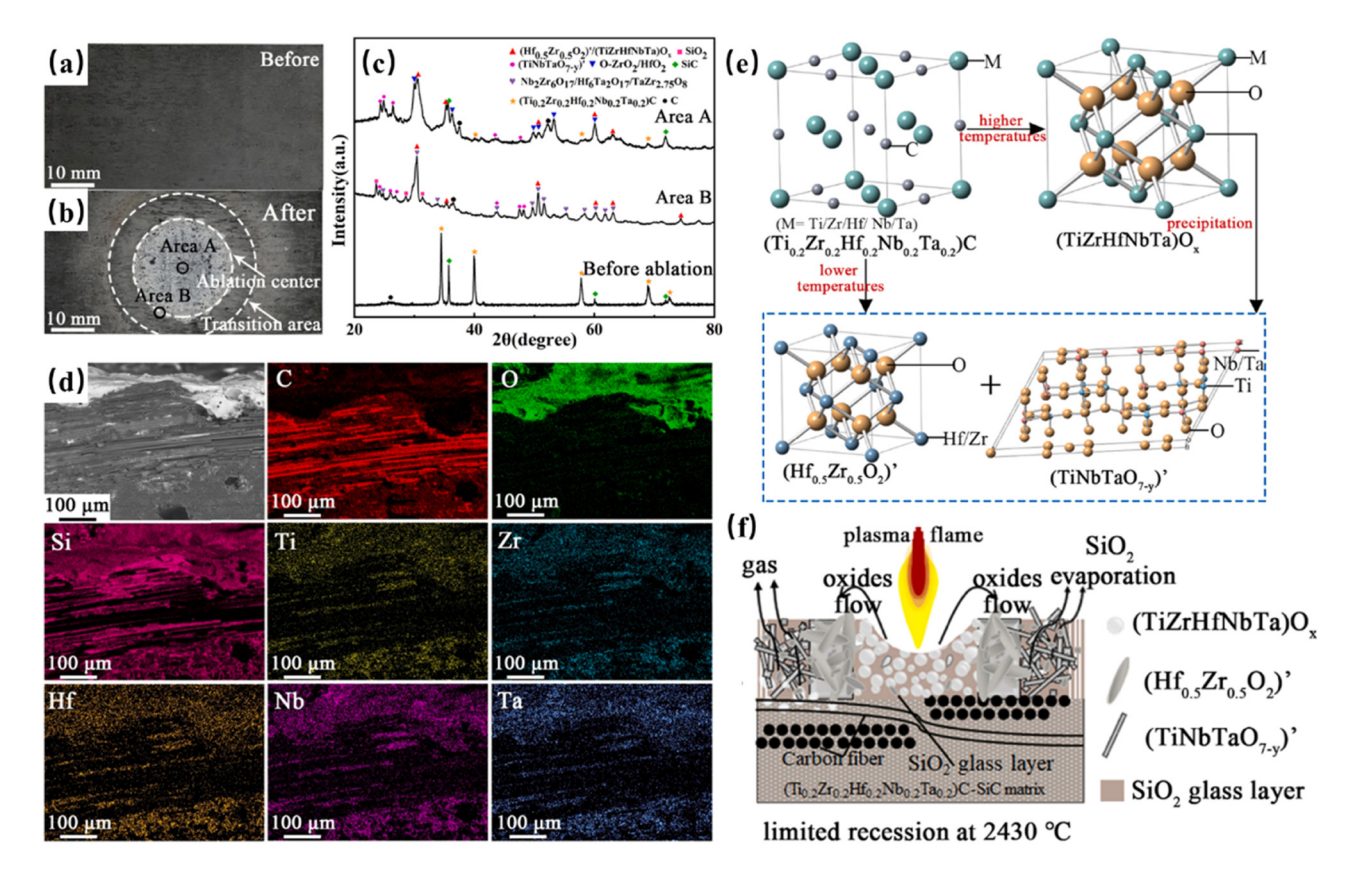


Figure 14: (a) and (b) Optical images, (c) XRD patterns, and (d) SEM image and EDS analysis of the $C_{t}/(Ti_{0.2}Zr_{0.2}Hf_{0.2}Nb_{0.2}Ta_{0.2})C$ –SiC composite before and after ablation at 5 MW·m⁻² for 300 s. (e) The phase evolution of $(Ti_{0.2}Zr_{0.2}Hf_{0.2}Nb_{0.2}Ta_{0.2})C$ during ablation and cooling. (f) Schematic diagram of ablation mechanism for $C_{t}/(Ti_{0.2}Zr_{0.2}Hf_{0.2}Nb_{0.2}Ta_{0.2})C$ –SiC composites [69].

SiO₂ melt in a gradual manner, and decomposes to form plate-like $(Hf_{0.5}ZrO_{0.5}O_2)'$ surrounded by $(TiNbTaO_{7-\nu})'$ nanocrystals. In contrast, $(Ti_0 {}_2Zr_0 {}_2Hf_0 {}_2Nb_0 {}_2Ta_0 {}_2)C$ was directly oxidized to (Hf_{0.5}ZrO_{0.5}O₂)' and (TiNbTaO_{7-v})' phases at the ablation transition area and outer area with lower temperature. Guo et al. [92] explained in detail the mechanism by which a near equimolar ratio of (TiZrHfNbTa)C HECs phase was formed by RMI in C_f/C preforms and indicated the ablation behavior of (TiZrHfNbTa)C, the oxidized products were dominantly Hf₆Ta₂O₁₇, Ti_{5.1}Ta_{4.9}O₂₀, Nb₂Zr₆O₁₇, and TaZr_{2.75}O₈ [183,184]. Arai et al. [163] successfully formed a high-entropy matrix in situ by infiltrating the Zr–Ti alloy into a composite preform containing carbon and carbide powders via RMI. The results of the arc jet ablation experiments showed the formation of a dense oxide zone consisting of composite oxides such as (Zr, Hf)O₂, Ti(Nb, Ta)₂O₇, (Zr, Hf) TiO₄, and (Nb, Ta)₂(Zr, Hf)₆O₁₇ with an average thickness of approximately 600 µm. In general, HECs present a variety of oxide morphologies during ablation influenced by entropy, temperature, and composition, resulting in a more stable oxide layer, which provides effective protection against inward oxygen diffusion and mechanical scouring of substrate materials. Carbon fiber reinforced HEC composites offer entirely new ideas and solutions for tailoring the ablation resistance of C_f/UHTCMC in the future.

The ablation properties of C_f/UHTCMC are also influenced by introduction form, particle size, content and distribution of transition metal carbide, as well as its ratio to SiC. Li *et al.* [185] selected ZrC particles/PCS xylene solution

and PZC/PCS xylene solution as impregnators to fabricate C/SiC-ZrC composites by PIP process. It is known from the results that PZC can be mixed more uniformly with PCS than ZrC particles and can generate nano-homogeneous dispersed ZrC-SiC matrices after pyrolysis, thus exhibiting better mechanical properties and ablation resistance, with linear ablation and mass ablation rates of −3.0 µm·s⁻¹ and 9.0 mg·s⁻¹, respectively, after OAT test. Jia et al. [186] prepared C/C-SiC-ZrC composites with different ZrC particle sizes (0.2, 1, and 2 µm) via the PIP process combined with additional heat treatment and evaluated their ablation properties under an oxyacetylene flame with a heat flux of 4.18 \pm 0.42 MW·m⁻² (Figure 15). The results implied that the oxide formed from small ZrC particles (0.2 µm) had a low viscosity and poor resistance to scouring, while the oxide from large ZrC particles (2 µm) was unable to seal the large gaps between ZrC particles, leading to massive ablation. Composites with ZrC particle size of approximately 1 µm exhibited the best ablation resistance, forming oxides with suitable viscosity and containing particles during ablation, which possessed better ability to resist scouring and seal cracks. The C_f/UHTCMC with different contents and distribution of UHTCs phases can be prepared by adjusting the concentration of precursors, impregnation sequence and times, as well as technological process [187-189]. He et al. [190] designed the C/C-SiC-ZrC composites with a gradient structure distribution of SiC-rich surface layer and Zr-rich center using the CLVD process, resulting in low thermal expansion coefficient and high

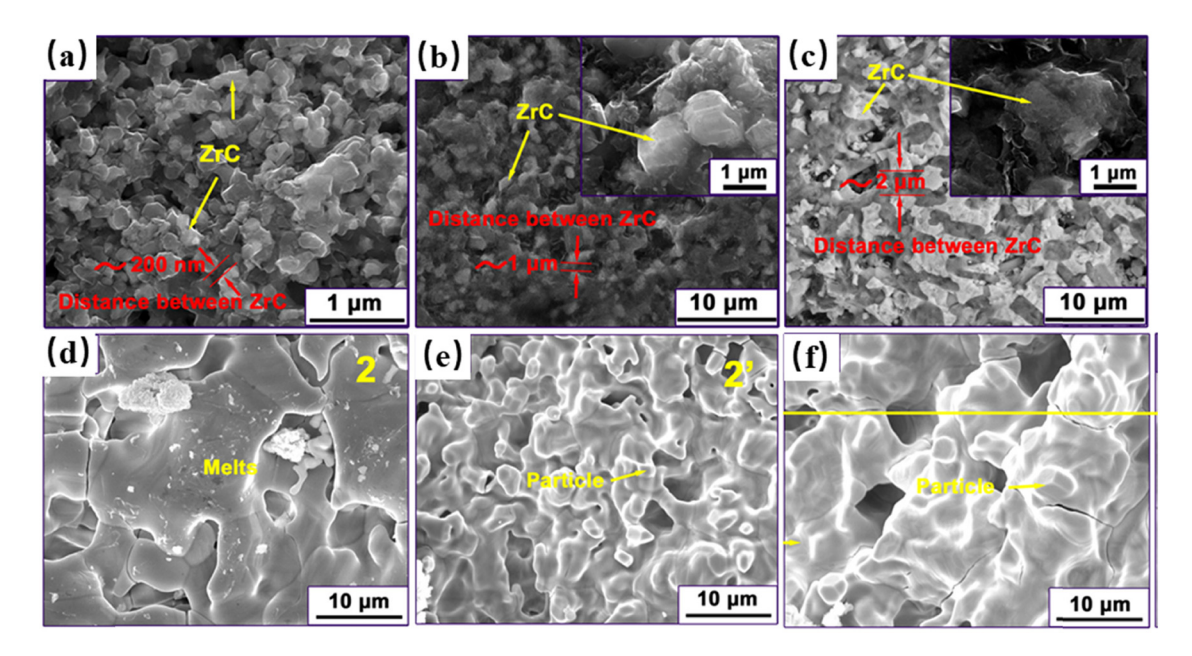


Figure 15: Cross-section microstructure of the C/C–ZrC–SiC composites with different ZrC particle sizes: (a) 200 nm, (b) 1 μ m, and (c) 2 μ m. Ablation morphology of the C/C–ZrC–SiC composites with different ZrC particle sizes: (d) 200 nm, (e) 1 μ m, and (f) 2 μ m [186].

thermal conductivity, which is of great benefit to restrict the formation and expansion of defects as well as accelerate the heat transfer, thereby reducing the O2 diffusion into the interior of the matrices and the heat accumulation, weakening the thermal erosion. The linear and mass ablation rates of the gradient composites under oxyacetylene ablation at 3,000°C and a heat flow density of 4.18 MW·m⁻² for 90 s were $1.59 \pm 0.16 \,\mu\text{m}\cdot\text{s}^{-1}$ and $1.57 \pm 0.20 \,\text{mg}\cdot\text{s}^{-1}$ respectively, a reduction of 55.9 and 67.2% compared to the uniformed distribution composites. Variations in the Zr(Hf)/Si ratio modulate the formation of glass and solid phase oxide layers, which in turn affect the oxygen diffusivities and ablation performance of C_f/UHTCMC [191–193]. Ouyang et al. [194] fabricated C/C-SiC-ZrC composites by carbothermal reaction of hydrothermal deposited oxides, and investigated the microstructure, mechanical properties, ablation behavior, and ablation mechanism of composites with different ZrC/SiC molar ratios, as shown in Figure 16. The composites with a molar ratio of ZrC/SiC ≈ 2:1 presented outstanding ablation resistance with a mass ablation rate of 0.06 mg cm⁻²· s⁻¹ and a linear ablation rate of 0.13 µm·s⁻¹ after plasma ablation at 2,300°C for 120 s. Effects of SiC/HfC ratios on the ablation properties of 3D C_f/HfC-SiC composites were also investigated systematically [195]. The C_f/HfC-SiC composite with low SiC/HfC ratio of 15.0/13.3 had the lowest weight loss of 0.245 \pm 0.012 g and erosion depth of 0.176 ± 0.008 mm.

The research works on the influence of fiber distribution, type, and orientation on the mechanical and ablation properties of $C_f/UHTCMC$ are crucial for the rational selection

of preform structures for specific components and the optimization of thermomechanical structure for specific engineering application [196-198]. Yang et al. [199] explored the effect of three typical preform structures, 3-dimensional 4-directional braided (3D4X), 3-dimensional 5-directional braided (3D5X), and 3-dimensional needle-punched integrated felt (3DZC) on the mechanical and ablation properties of C/SiC-ZrC composites. The mechanical properties of the composites with different preform structures depend on the fiber content in the load bearing direction and the matrix compactness. According to Figure 17, the composite with 3D5X preform structure possess the highest bending strength (233.29 MPa) and bending modulus (36.05 GPa) due to the highest fiber content (31.70%) in the load bearing direction and relatively low open porosity (18.96%). Meanwhile, it also has the best ablation performance, the linear ablation and mass ablation rates were 17.5 µm·s⁻¹ and 6.53 mg·s⁻¹, respectively, after 2,362°C oxyacetylene flame for 20 s. Xie et al. [197] discussed the oxyacetylene ablation behavior of different surface layer fiber structures of C/C-SiC-ZrC composites produced from 2D needled carbon fiber preforms as reinforcements. The results indicated that the ablation properties rely on the fiber orientation and the formation ability of surface protective layer. Due to the sufficient content of UHTC phase, a compactly integrated ZrO2 protective layer formed on the ablated surface of short carbon fiber web, which presented the best anti-ablation performance after oxyacetylene ablation for 90 s at 2,370°C with linear ablation and mass ablation rates of $0.82 \ \mu m \cdot s^{-1}$ and $-0.30 \ mg \cdot s^{-1}$, respectively.

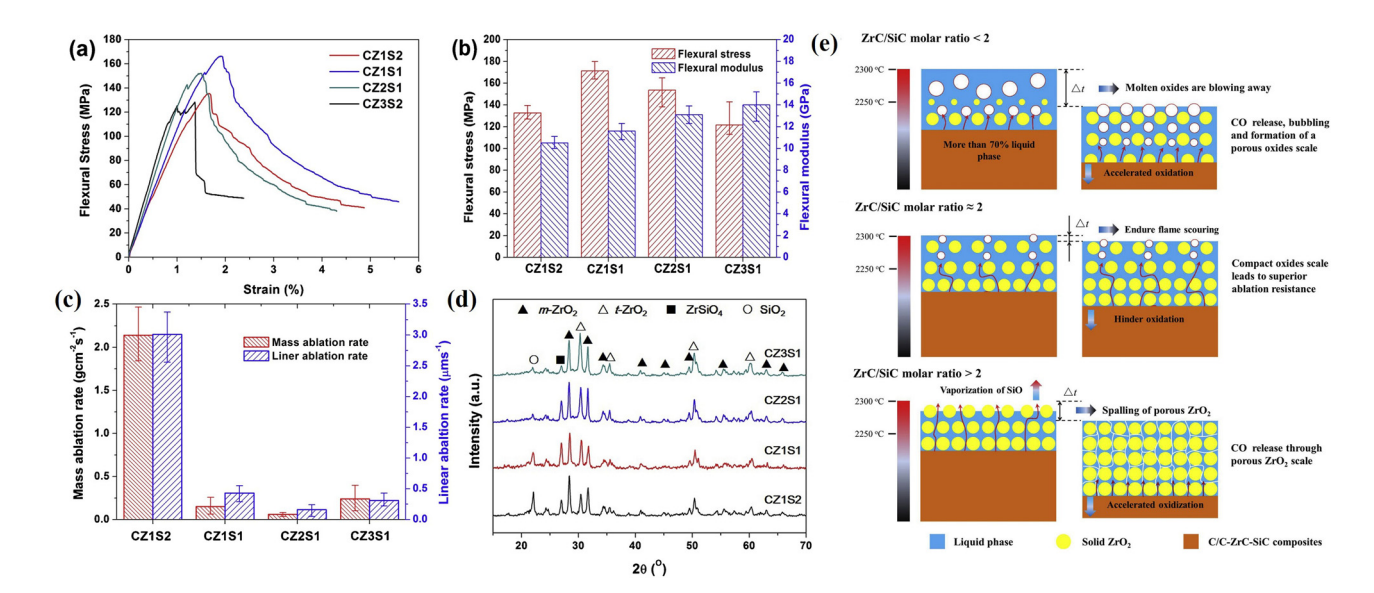


Figure 16: (a) Typical stress–strain curves, (b) flexural stress and modulus, (c) mass ablation and linear ablation rates, (d) XRD patterns after ablation, and (e) ablation mechanism of the composites with various ZrC/SiC molar ratios. (The samples with Zr/Si molar ratios of 1:2, 1:1, 2:1, and 3:1 were labeled as CZ1S2, CZ1S1, CZ2S1, and CZ3S1, respectively) [194].

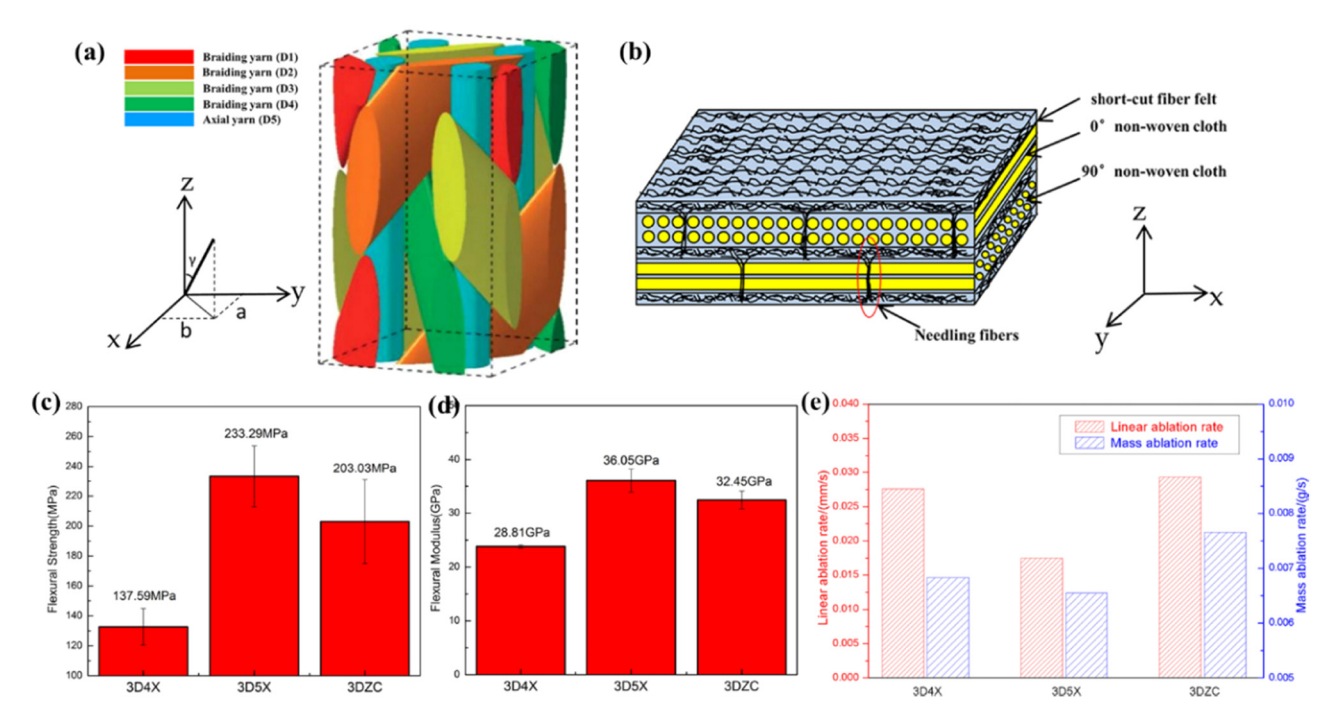


Figure 17: Schematic of different preform structures: (a) 3D4X and 3D5X; (b) 3DZC. Mechanical and ablation properties of C/SiC–ZrC composites with different preform structures: (c) bending strength; (d) bending modulus; and (e) linear ablation and mass ablation rates [199].

Nonetheless, only scattered oxide particles produced on the ablated surface of non-woven layer resulted in the poorer ablation resistance. Furthermore, the non-woven layer parallel to the flame exhibited the worst anti-ablation properties, because the fiber/matrix interphase was in preferential ablation promoting the oxidizing flame and heat transfer into inter composites and eventually accelerating the erosion. Inoue et al. [200] contrasted the oxidation resistance of short and plain-woven continuous carbon fiber reinforced ZrB2-SiC-ZrC (Csf/ZSZ and C_{pw}/ZSZ) composites fabricated by RMI process. Lateral oxidation of Cpw/ZSZ composites appeared due to its low thermal conductivity, higher fiber volume fraction and continuity of the carbon fiber. In contrast, the addition of pitch-based short carbon fiber achieves light weight and increased reliability without degradation of the oxidation behavior and thermal properties of ZrB₂-SiC-ZrC. As already discussed, the different types of preform structures have a significant effect on both the mechanical and ablation properties. Although three-dimensional braided structures have high strength and toughness, low tendency to delamination, excellent energy absorption, and outstanding fatigue properties [201], the complexity of their preparation increases as the braided direction increases, leading to long cycle time and high cost. Short carbon fiber preforms have the characteristics of low cost, automatable production, short cycle, and isotropy, but its strengthening and toughening effects are poorer [202]. Needle-punched carbon fiber preforms are the most commonly used reinforcement for C_f /UHTCMC due to their excellent designability, easy preparation, and low cost, as well as relatively high interlaminar shear strength, and can be exploited to fabricate components with various complex geometries, such as nose cones, combustion chambers, nozzle expansion segments and brake discs [203–205]. Therefore, in practice, the selection of a suitable preform structure is considered from various aspects, including the size of the component profile, service force, thermal state and operating conditions for the specific application.

Through the modulation of the above composition, structure, and fabrication process, the C_f /UHTCMC are endowed with excellent mechanical properties, and oxidation and ablation resistance. Nevertheless, the ablation rate of C_f /UHTCMC will still substantially increase at higher heat flow densities or during repeated service. Zhao *et al.* [206] investigated the cyclic ablation behavior of the C/C–ZrC–SiC– ZrB_2 composites with heat fluxes of 2.38 and 4.18 MW·m⁻² using OAT, Figure 18 shows the mass and thickness loss in the cyclic ablation of 30 s × 4 was higher than that in 60 s × 2. First of all, the medium and low temperature oxides will rapidly evaporate or undergo mechanical erosion under the conditions of ultra-high temperature or strong heat flow, resulting in the formation of porous refractory transition metal oxides on the ablation

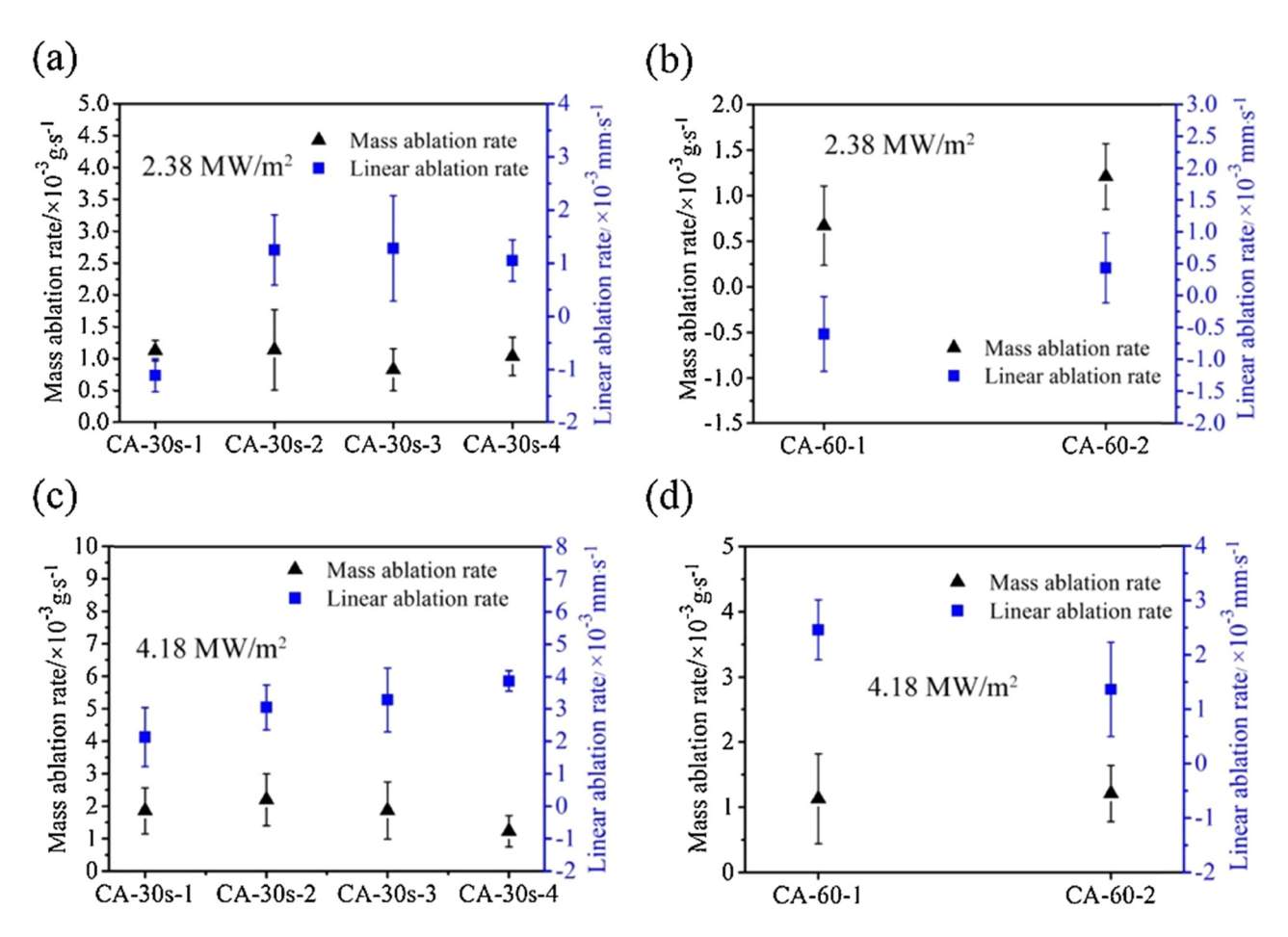


Figure 18: Ablation rates of the C/C–ZrC–SiC–ZrB₂ composites after cyclic ablation under different heat fluxes: (a) cyclic ablation of 30 s × 4 at 2.38 MW·m⁻²; (b) cyclic ablation of 60 s × 2 at 2.38 MW·m⁻²; (c) cyclic ablation of 30 s × 4 at 4.18 MW·m⁻² and (d) cyclic ablation of 60 s × 2 at 4.18 MW·m⁻² [206].

surface. The porous oxide layer cannot effectively prevent the inward diffusion of oxygen, leading to losses in fiber and hence enhance ablation rate [207–209]. Second, the refractory transition metal oxides, especially ZrO₂ generated from the oxidation of ZrC, have three crystal structures: monoclinic phase (m), tetragonal phase (t), and cubic phase (c). During the cooling from elevated temperature to room temperature, ZrO₂ undergoes a martensitic transformation from t-phase to m-phase, accompanied by a volume expansion of approximately 3.5%, which leads to the exfoliation of the oxide layer [210–212]. All of these limits the reusability of C_f/UHTCMC at higher temperatures and for longer periods.

It is known from the literature that low valance rare earth (RE) element cations (e.g., Y^{3+} , Sc^{3+} , La^{3+} , Yb^{3+} , etc.) can play a critical role in stabilizing the oxide layer and decreasing the oxygen diffusion rate [213]. In the oxidation/ablation process, Re^{3+} will replace the position of Zr^{4+} and generate oxygen vacancies, which reduces the repulsive force between oxygen-oxygen, obtains room temperature

stable t-ZrO₂ or c-ZrO₂, inhibits the phase transition from tphase to m-phase, and can reduce or eliminate the volume mutation of ZrO₂ [214]. In both of Liu et al. [215] and Zhang et al.'s [216] works, the La₂O₃ was found to effectively improve the ablation resistance of ZrB2-SiC ceramics through forming solid solution with ZrO₂ phase. The action mechanism of La in Hf-based ceramics is similar to that in Zr-based ceramics [217,218]. Moreover, the addition of RE oxides can also restrain the volatilization of the glass layer. Zhang et al. [219] investigated the effect of La₂O₃ on the oxidation behavior of SiC ceramic at 1,700°C based on firstprinciples calculations and oxidation experiments, which result in the *in situ* formation of the La₂Si₂O₇ phase with high melting point, low volatility, and low oxygen diffusion to enhance the stability of the SiO₂ glass layer. The solution energies of La³⁺ in La₂Si₂O₇ (2 0 1) and SiO₂ (0 1 1) were negative values which meant that La³⁺ could exist steadily in both structures. Since the absolute value of the solution energy for La³⁺ in SiO₂ is larger, La³⁺ was more inclined to diffuse into SiO₂. In addition, the solution energies of La³⁺ at

the interstitial site of pure SiO₂ lattice was negative, while that at substitutional was positive, which indicated that SiO₂ lattice with an interstitial La³⁺ was more stable. La³⁺ replaced some Si-O bonds and formed La-O and La-Si bonds with stronger bonds [220], which was favorable for the high temperature stability of SiO₂. A survey of influence of the RE oxides of La, Nd, Y, Sm, Yb, and Lu at 1700°C employing volatility test on the stability of SiO₂ glass, revealed that the smaller the RE³⁺ radius, the greater its solution energy in SiO₂ and the better the stability [221]. The SiO₂ glass phase has low oxygen permeability and volatility due to the presence of the high melting point Re₂Si₂O₇ phase. Of these, Lu³⁺ has the smallest ionic radius, owns the best stabilization effect. The effect of Lu₂O₃ on the oxidation resistance of SiC-ZrB₂ coating was further carried out on this basis [222]. The result indicated that ZrO₂, ZrSiO₄, and Lu₄Zr₃O₁₂ phases formed by oxidation provided effective protection for C/C composites at 1500°C up to 836 h, and the oxidation weight loss rate was 0.62 mg·cm⁻².

The viscosity of the glass phase will affect the oxygen diffusion rate in the composites, and its relationship can be expressed in the Stokes–Einstein equation [223]:

$$D = \frac{kT}{6\pi nr},\tag{3}$$

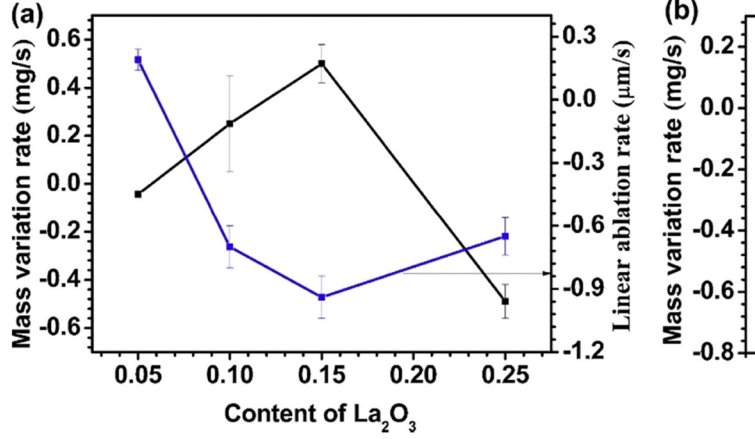
where D is the diffusion constant ($m^2 \cdot s^{-1}$), K is the Boltzmann constant ($J \cdot K^{-1}$), T is the temperature (K), η is the viscosity ($m^2 \cdot s^{-1}$), and r is the radius of the spherical particles (m). The greater the viscosity of the oxide layer, the smaller the O_2 diffusion rate.

The relationship between viscosity and oxide particles can be described by the following equation [224]:

$$\eta = a \exp\left[bV_{\rm f} + \frac{c}{T} + ds\right],\tag{4}$$

where a, b, c, and d are constants, V_f is the volume fraction of unmelted oxide particles and s is the average particle size of unmelted oxide particles. Therefore, the higher the volume fraction of oxide particles, the higher the viscosity of the oxide layer at the same temperature. Jia et al. [225] investigated the long-time ablation protection of different-La₂O₃-content (5–30 vol.%) modified ZrC coating for SiC-coated C/C composites, the linear ablation and mass ablation rates of the coating with different La₂O₃ contents are shown in Figure 19. Results displayed that ZrC coating with 15 vol.% La₂O₃ exhibited the best ablation resistance which was attributed to the formation of high-thermal-stability and low-oxygen-diffusivity oxide layer which was composed of m-ZrO2 particles and molten phases with La_{0.1}Zr_{0.9}O_{1.95} and La₂Zr₂O₇. Meanwhile, La diffused along the grain boundaries of ZrO₂ by short-circuit diffusion, refining and producing abundant nano ZrO₂ grains, which increases the viscosity of the oxide layer and decreases O2 diffusion rate.

In recent years, many efforts have been carried out to investigate the effects of different types of RE oxides on the oxidation and ablation resistance of C_f /UHTCMC, mainly including matrix modification and coating modification [226–228], the latter of which is mostly reported. Reports of the production of RE oxides as matrix composition for modified C_f /UHTCMC are fewer in number. Luo *et al.* [229] fabricated La_2O_3/Y_2O_3 -doped C/SiC–ZrC composites by RMI process in order to enhance their multiple ablation properties. Ablation results indicated that the formation of $La_2Zr_2O_7$ phase significantly improved the ablation properties of C/SiC–ZrC– La_2O_3 composites, which could withstand three



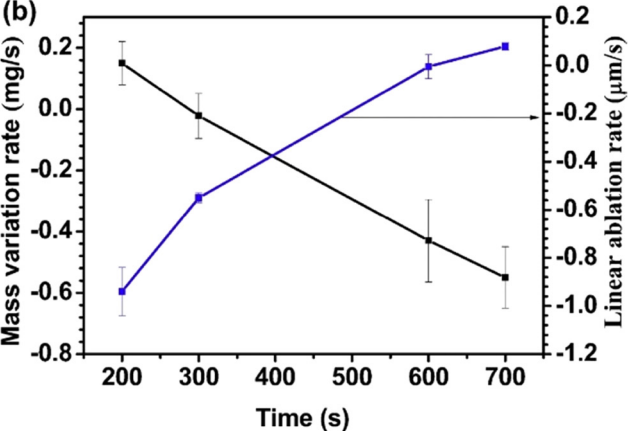


Figure 19: (a) Linear ablation and mass ablation rates of the coatings as function of La_2O_3 content and (b) linear ablation and mass ablation rates of the coating with 15 vol.% La_2O_3 as function of time [225].

times ablation under the OAT flame. While the C/SiC-ZrC-Y₂O₃ composites were severely damaged after two times of ablation, which is likely to be primarily due to the Y₂O₃ neither reacted with silica to reduce its violation nor dissolved into zirconia to suppress its phase transformation. As presented in Figure 20, XRD and SEM results supported this view. Many authors [230,231] have reported that the oxidation and ablation properties of the composites are dependent on the Y₂O₃ content. Excessive Y₂O₃ can result in either weakening the strengths of Si-O bonds and breaking the SiO₂ network structure, or causing a reduction in the resistance to high temperature oxidation. Moreover, the formation of the Y₂Si₂O₇ phase, which has a positive effect on the ablation resistance, may require a longer oxidation time or more SiO₂ [232]. Shen et al. [233] studied the effect of YC₂ on the ablation performance and behavior of C/C-ZrC composites. The generated oxides (ZrO2 and Y2O3) reacted violently with carbon and formed a great deal of pits on the carbon fibers and matrices, which provides more active sites for the thermal chemical reactions, thus accelerating the ablation. In addition, the oxygen vacancies generated by Y₂O₃-doped ZrO₂ provided access for oxygen into the internal material, which also further accelerates the ablation.

Therefore, the introduction of YC2 reduced the ablation resistance of C/C-ZrC composites. Fang et al. [234] studied the ablation properties of La₂O₃ modified C/C-SiC composites fabricated via PIP process. Experimental results show that with the transformation of La-compounds to La₂Si₂O₇ phase, the volatilization of SiO₂ was reduced, the viscosity of the oxide film was increased, and the excellent ablation resistance was obtained. Subsequently, Fang [235] prepared dense and homogeneous C/C-SiC-ZrB₂-LaB₆ composites using C_f/LaB₆ preforms by reactive sintering action of LaB₆ with Zr-precursor. The participation of ternary ceramic phase formed a dense liquid-solid oxide layer, which evolved the layer from SiO₂ to SiO₂-La₂Si₂O₇ and then to SiO₂-La₂Si₂O₇ La_{0.71}Zr_{0.29}O_{1.65}-La₂Zr₂O₇-ZrO₂ layer, significantly improving the long-time ablation resistance of the composites, as shown in Figure 21. Especially, the mass and linear ablation rates after plasma ablation for 360 s were 0.38 mg·s⁻¹ and 0.37 μm·s⁻¹, respectively. In order to solve the LaB₆ segregation problem, Fang et al. [236] developed in situ growth of LaB₆ modified C/C-SiC-ZrC composites. Doping with 22.12 wt% LaB₆, the composites exhibited the best ablation properties with the mass and linear ablation rates after plasma ablation for 120 s being 1.54 mg·s⁻¹ and 1.92 μm·s⁻¹, respectively. In

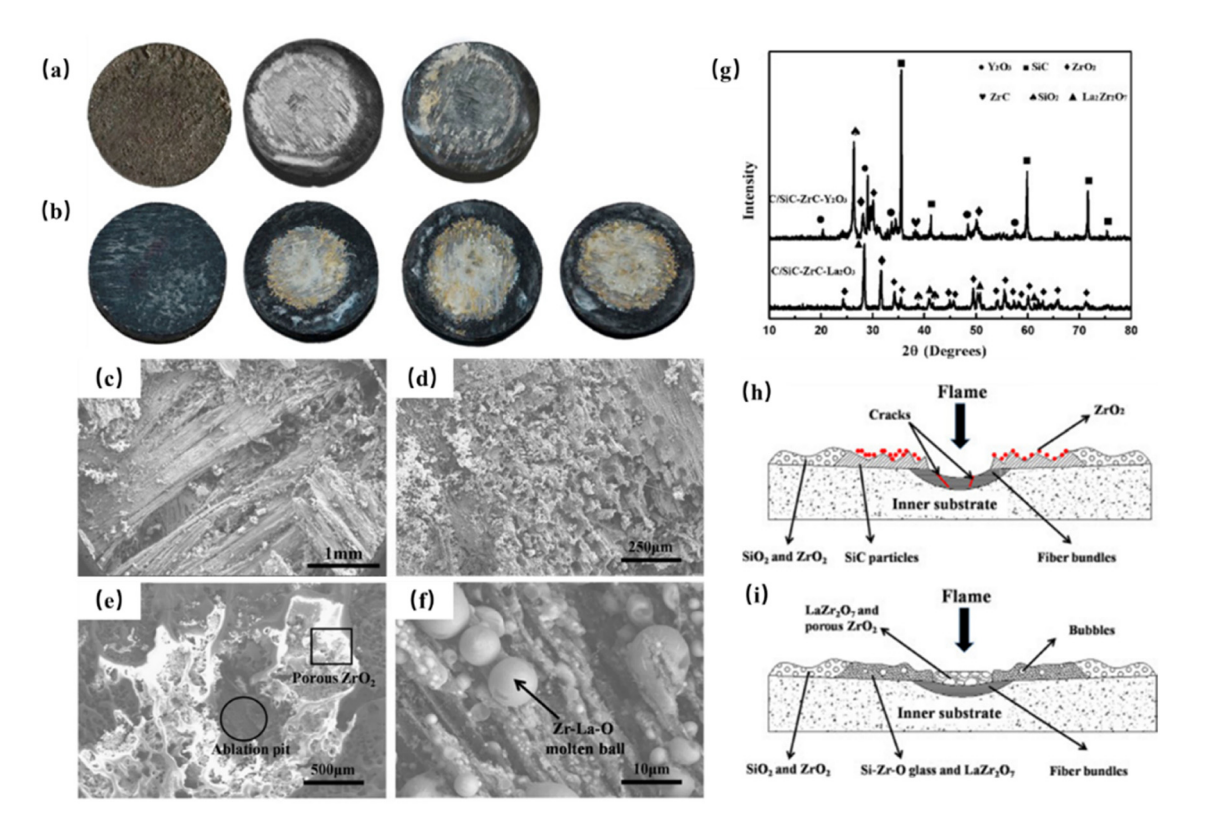


Figure 20: Macrographic images of (a) C/SiC–ZrC– Y_2O_3 and (b) C/SiC–ZrC- La_2O_3 composites before and after ablation tests; SEM images of (c) and (d) C/SiC–ZrC– Y_2O_3 and (e) and (f) C/SiC–ZrC– La_2O_3 composites after ablation tests; (g) XRD patterns of the both composites; Schematic of ablation mechanism of (h) C/SiC–ZrC– Y_2O_3 and (i) C/SiC–ZrC– La_2O_3 composites [229].

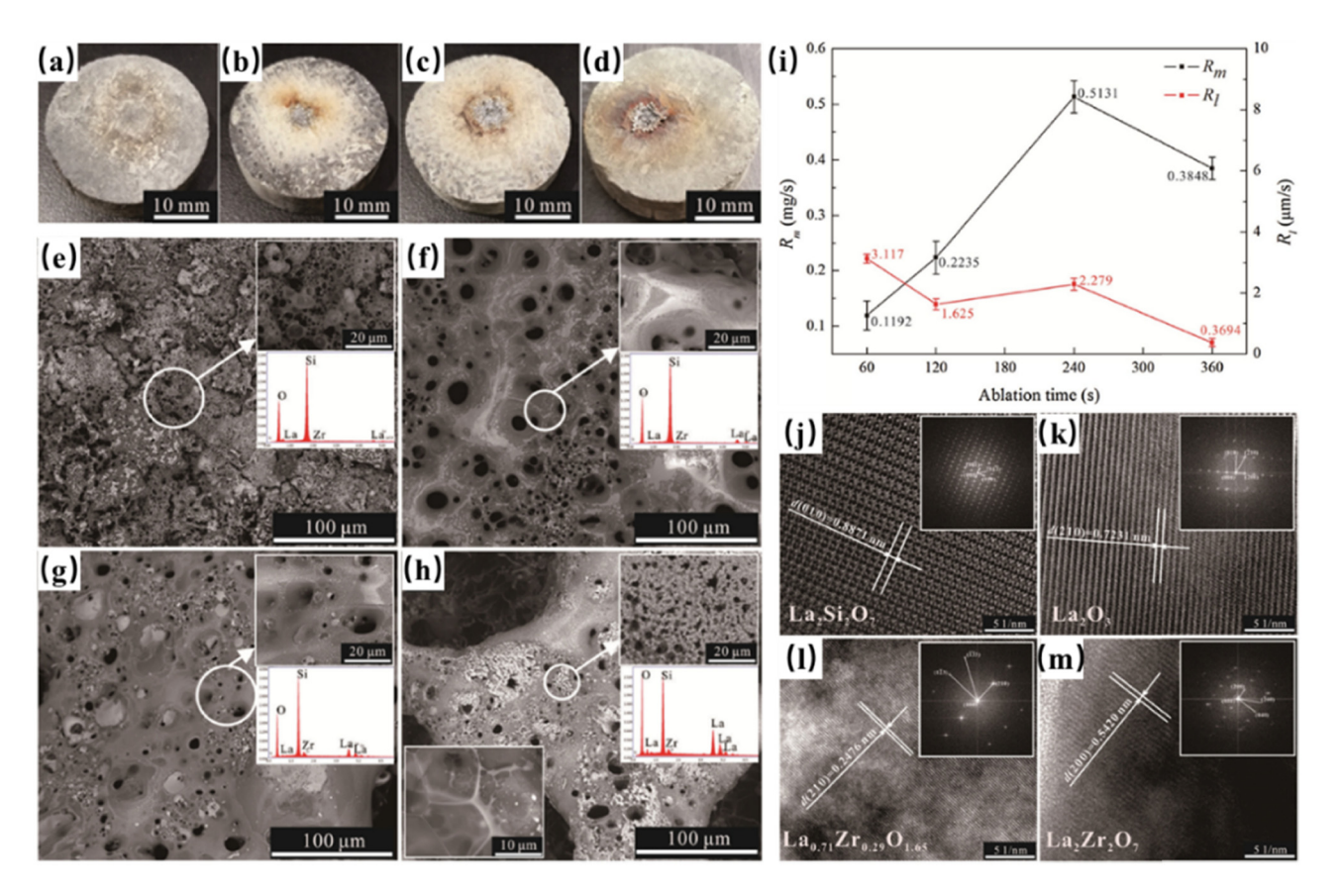


Figure 21: Optical images of C/C–SiC–ZrB₂–LaB₆ composites after ablation for (a) 60 s, (b) 120 s, (c) 240 s, and (d) 360 s; SEM images and EDS analyses of the molten glass layers after ablation for (e) 60 s, (f) 120 s, (g) 240 s, and (h) 360 s; (i) Functional curves of mass ablation and linear ablation rates to ablation time of C/C–SiC–ZrB₂–LaB₆ composites; (j)–(m) HRTEM images of the oxides after ablation for 360 s [235].

conclusion, moderate amount of Re_2O_3 is beneficial for the observed improvement in the oxidation and ablation resistance of C_f /UHTCMC by the formation of an immiscible multicomponent glass surface layer, which can lower the oxygen diffusion coefficient, increase the viscosity of the glass oxide layer, and inhibit the ZrO_2 phase transition. Currently, mainly two RE elements (La and Y) are explored for matrix modification of C_f /UHTCMC, which can be expanded to other RE elements, such as SC, Yb, *etc.* Moreover, in view of the shortcomings of modifying C_f /UHTCMC with a single RE element, two or more RE elements can be added to play a synergistic role between different elements.

Since microstructural defects such as pores and cracks are typically the prime channels for oxygen to rapidly enter the interior of materials, porosity has a momentous impact on the oxidation and ablation behaviors. Parthasarathy $et\ al.$ [237] reported the effect of porosity on the oxidation kinetics of ZrB_2 (Figure 22). Both the oxidation rate and the thickness of the oxide layer increased significantly with the increase in the porosity. So, the denser the composite, the better the oxidation resistance, as expected.

Ablation properties also have a dependency on the shape of C_f/UHTCMC components. The vast majority of ablation tests have been proceeded on plane specimens, whereas only a few researchers have studied the ablation behavior of C_f/UHTCMC with sharp shape under high heat flux [238]. Liu et al. [239] fabricated wedge-shaped C/C-SiC-ZrB₂ composites by RMI process, and investigated their ablation performance under the oxyacetylene flame with a heat flux of 2.38 MW·m⁻². Since the leading edge is subjected to higher shear force and heat flux, its ablation rate is higher than that of plane specimens, the linear ablation and mass ablation rates were 13 µm·s⁻¹ and 1.4 µg·s⁻¹, respectively. Compared to sharp leading edges, blunt edges have less heating caused by friction of the shock wave on the surface which are more compatible with the design of thermal structural components [240]. The ablation behavior of nose-shaped C/C-HfB₂-SiC composites prepared by PIP process exposed to OAT with different heat fluxes (2.38 and 4.18 MW·m⁻²) was reported by Zhang et al. [171]. During ablation in 2.38 MW·m⁻², the C/C–HfB₂–SiC composites showed better ablation performance and

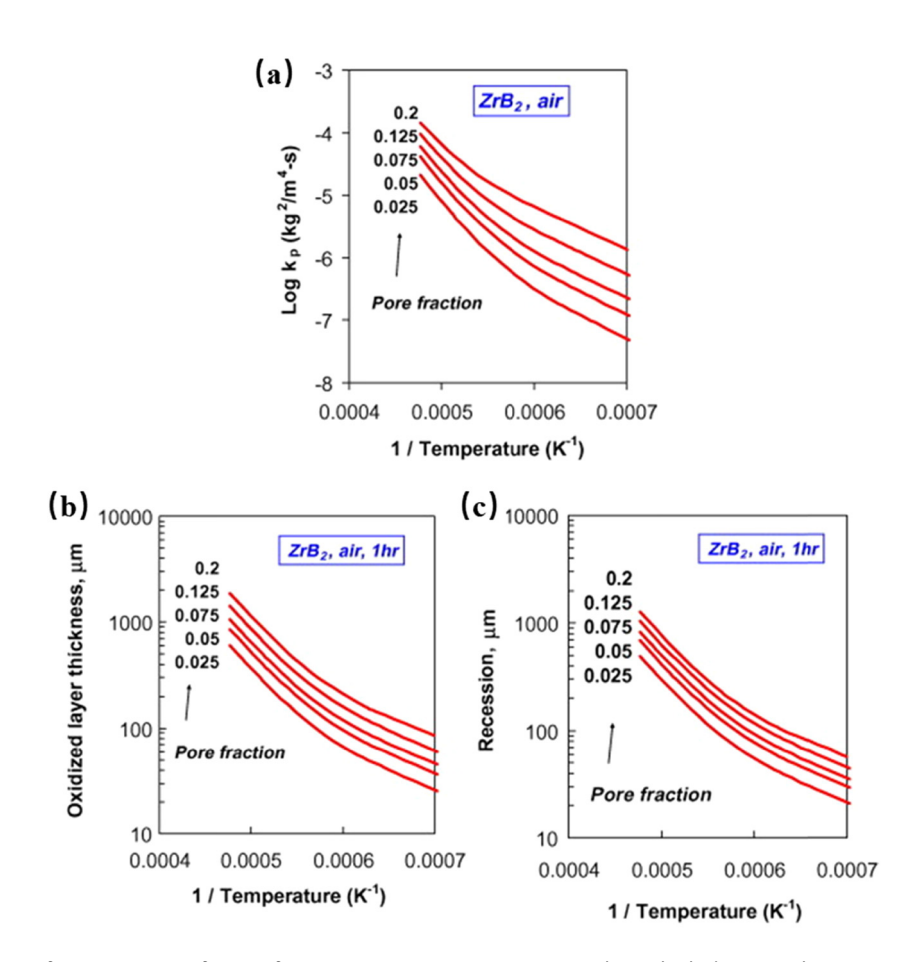


Figure 22: Effect of pore fraction on (pore fraction from 0.025 to 0.2): (a) rate constant, (b) oxide thickness, and (c) recession [237].

structural stability, mainly due to the formation of borosilicate glass, HfO2-glass, and HfO2 scale. As the heat flux increased to 4.18 MW·m⁻², the increased surface temperature and the enhanced denudation resulted in the absence of the borosilicate glass, the C/C-HfB₂-SiC composites underwent more serious ablation, with linear ablation and mass ablation rates of 22.9 $\mu m \cdot s^{-1}$ and 3.6 $\mu g \cdot s^{-1}$, respectively. In parallel, similar observations of the C/SiC-HfC composites with similar shape in plasma wind tunnel were reported also by Duan et al. [241]. Sciti et al. [242] designed a ceramic nozzle composed of a 50 vol.% carbon chopped fibers and 50 vol.% ZrB2 and tested its ablation resistance in a HVOF in conditions simulating typical exhaust engine flows, as shown in Figure 23. A fluid dynamic numerical simulation allows to predict the heat flux and temperatures in the nozzle. Although a slight oxidation occurred on the frontal side of the ceramic nozzle, it maintained original structural integrity, and there was no significant ablation of the inner throat diameter before and after the ablation test. To better simulate the real working condition, Liu et al. [243] specially designed a new ablation condition to investigate the effect of temperature gradient on the ablation

and flexural behavior of the C/C–ZrC composites. In general, some components with specific shapes are ineluctable in practical applications so as to meet the aerodynamic design to reduce drag. A more accurate, valid, and realistic evaluation of the ablation properties of C_f /UHTCMC is imperative in extreme environments in combination with the realizable testing conditions constructed by lab-scale methods and the shape design of the composites [244].

In summary, the ablation property of C_f /UHTCMC is first regulated by the rapid chemical reaction of carbon and ceramic with oxygen on the surface, then governed by the oxygen diffusion rate through the protective layer. This section summarizes the latest research progress of C_f /UHTCMC in multiple matrix modification, structure and property regulation, oxidation ablation mechanism, RE elements modification, etc., aiming to provide reference to further promote the research and development of C_f /UHTCMC. To date, there is no unified standard for the oxidation ablation test conditions and sample specifications of C_f /UHTCMC, which makes it difficult to compare the oxidation ablation properties reported in different literatures, and cannot provide guidance for the optimization

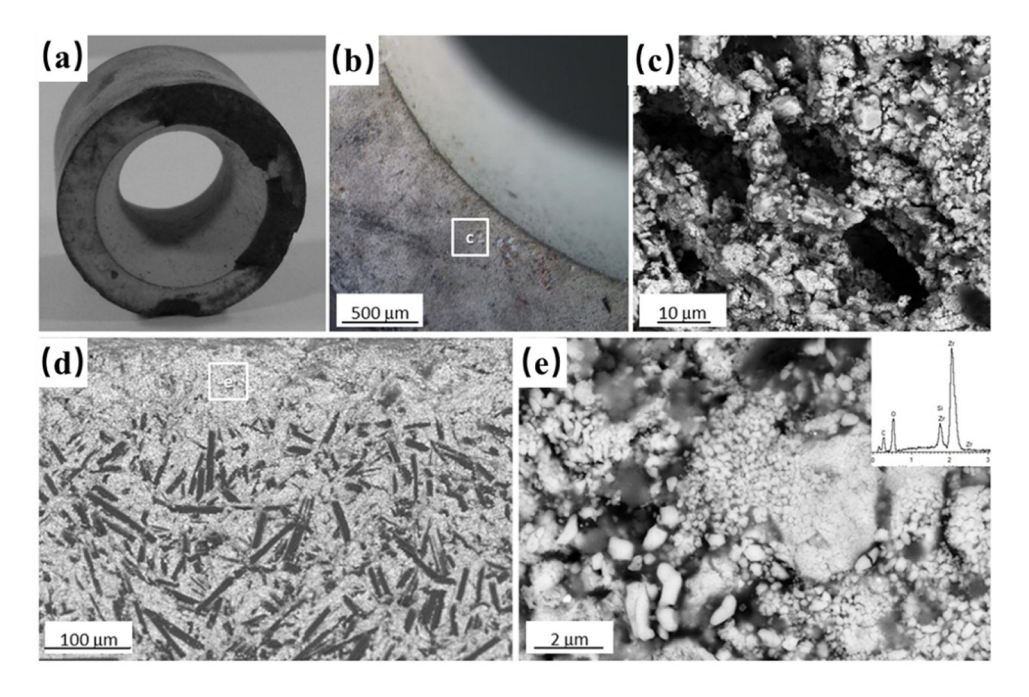


Figure 23: (a) Macroscopic image of the nozzle after the HVOF test; (b) Optical microscopy image of the front part of the nozzle; (c) SEM image of the boxed area in (b); (d) cross section of the oxidized layer; (e) microstructure detail of the oxidized layer in (d) with the corresponding EDS spectrum inset [242].

and improvement of C_f/UHTCMC performance. Therefore, there is also a need to establish a unified ablation evaluation standard. Moreover, the volume content and distribution pattern of each constituent of UHTCs matrix, heat flux density, oxygen partial pressure, *etc.*, are the decisive factors for the ablation behavior of C_f/UHTCMC, whereas there is limited information available on relatively systematic and indepth quantitative research reports.

4 Elevated temperature mechanical properties of C_f/UHTCMC

Understanding the elevated temperature mechanical properties of $C_f/UHTCMC$ is crucial to comprehend their performance in force/heat/oxygen extreme environment. Although many results on the mechanical properties of $C_f/UHTCMC$ at room temperature have been reported to date, which mainly reflects the influence of different preparation process on the mechanical properties, Vinci *et al.* [245] investigated the mechanical behavior of $C_f/ZrC-SiC$ and $C_f/TaC-SiC$ composites at elevated temperature in Ar atmosphere, as shown in Figure 24(a) and (b). Compared to room temperature, the flexural strengths of both composites at 1,500°C are substantially enhanced (approximately

450 MPa), which was attributed to the relaxation of residual stresses accumulated during HP. At 1,800°C, the flexural strengths of both composites began to decrease, but were still greater than the room temperature values. At 2,100°C, both C_f/ZrC-SiC and C_f/TaC-SiC composites experienced significant plastic deformation, with flexural strengths of 440 MPa and 368 MPa, respectively. The micromorphology after testing at 1,500–2,100°C revealed that no grain growth or fiber degradation was observed, so it can be concluded that most of the plastic deformation was caused by grain boundary sliding (Figure 24(c)). Jia et al. [246] reported the in situ tensile properties and flexural properties of C/C-ZrC-SiC-ZrB2 composites at 1,500-1,800°C. The flexural test indicated that the C/C-ZrC-SiC-ZrB2 composites exhibited brittle fracture characteristics at ambient temperature, while the flexural strength decreased at elevated temperatures, showing a pseudo-ductile fracture behavior. Zoli et al. [247] found that the flexural strength of homogeneously distributed unidirectional carbon fibers reinforced ZrB2-SiC-Si3N4 composites increased from 360 MPa at room temperature to 550 MPa at 1,500°C, and up to 420 MPa after thermal shock of 1,175°C, which was owing to the trade-off between the residual stress release and the formation of new cracks. Ding et al. [248,249] discussed the role of interphase (PyC and PyC/ SiC) between fiber and matrix in mechanical properties and microstructure evolution of 3D C_f/SiBCN composites at elevated temperatures in detail. According to Figure 25, the

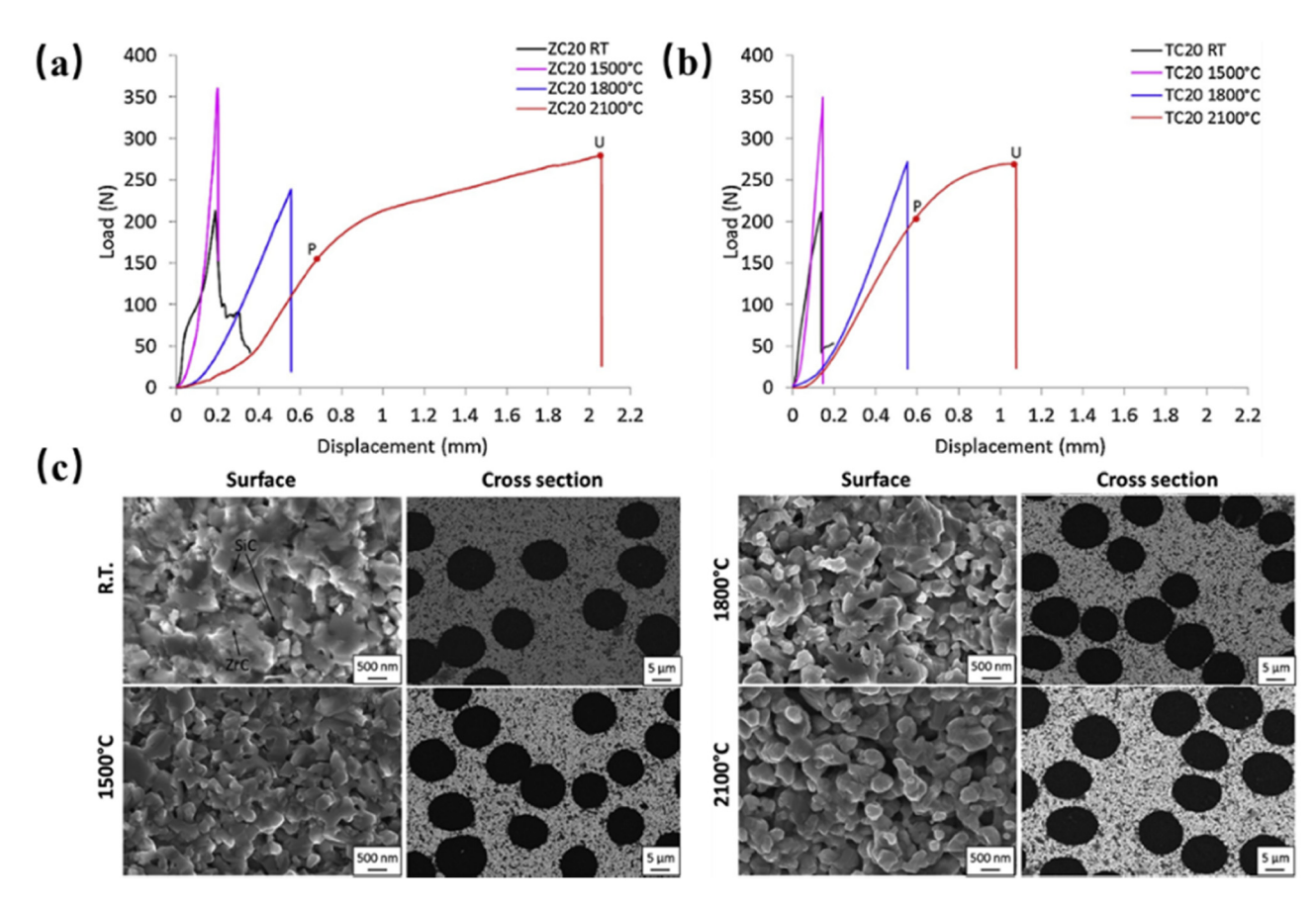


Figure 24: Load–displacement curves at room temperature, 1,500, 1,800, and 2,100°C for (a) C_t/ZrC–SiC and (b) C_t/TaC–SiC composites, (c) microstructure of C_t/ZrC–SiC composite after mechanical testing at room temperature, 1,500, 1,800, and 2,100°C [245].

fiber with PyC/SiC coating, which can effectively retard the carbothermal reduction reaction (mainly by 2C + 2Si - N \rightarrow 2SiC + N₂ \uparrow , partly by 2C + Si - O \rightarrow SiC + CO \uparrow) at elevated temperatures, enhanced the load transfer between the fiber and the matrix, thus flexural strength (330 \pm 7 MPa) of the 3D C_f/SiBCN composites was maintained well at 1,600°C. The significance of interphase on the mechanical properties of C_f/UHTCMC has also been emphasized elsewhere [250].

Under the simultaneous action of mechanical and thermal load, the UHTCs phase undergoing dislocation slip, grain deflection, etc., exhibits plastic deformation characteristics, therefore the high temperature mechanical properties better reflect the mechanical characteristics of $C_f/UHTCMC$. At higher temperatures, some of the gas-phase products are generated and escape from the interior of the material, the mechanical behavior of $C_f/UHTCMC$ will be more complicated. However, in the existing literature, the microscopic mechanism of plastic deformation of UHTCs is not clear well. The slip of dislocations along $\langle 110 \rangle \{111\}$ has long been recognized as the dominant microscopic mechanism for plastic deformation of TaC [251,252]; however, it has been

postulated that Ta diffusion is the main creep mechanism [253]. The pivotal reason why there are few high temperature mechanical studies of C_f/UHTCMC is the difficulty of testing at elevated temperatures. Gangireddy et al. [254,255] proposed a non-contact means of thermo-mechanical testing, where electrical current is utilized to heat the sample and a Lorentz force is applied to the sample through the application of a magnetic field. Using this method, he ascertained the activation energies, dislocation behavior, and deflection behavior of TaC and HfC above 2,000°C [256]. No reports have been found to date on the long-time service properties of C_f/UHTCMC subjected to cyclic (fatigue) and constant (creep) loading. This is likely to be primarily due to much of the current research focuses on applications that require only a short service life, usually seconds to a few minutes [257]. In conclusion, the high temperature mechanical behavior of C_f/UHTCMC is quite sensitive to the testing conditions, and there is no consensus so far on the high temperature mechanical mechanism of C_f/UHTCMC and the mechanism of the high temperature plastic deformation of the UHTCs phase, so further studies are still needed.

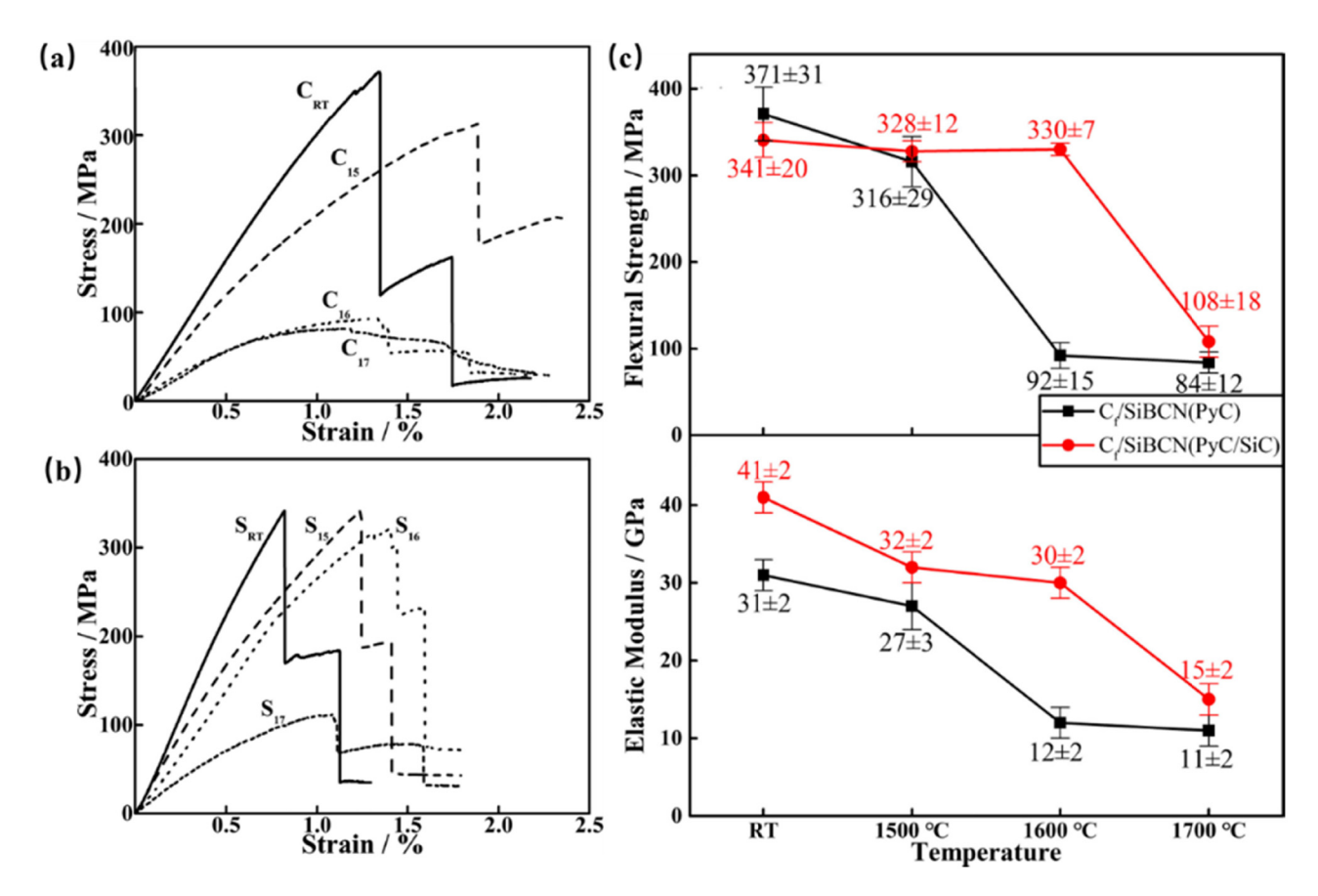


Figure 25: Flexural stress–strain curves of the composites tested at room temperature, 1500, 1600 and 1700 °C. (a) C_f/SiBCN (PyC), (b) C_f/SiBCN (PyC/SiC); (c) Summary of flexural strength and elastic modulus of the composites [248].

5 Summary and outlook

As thermal protection materials with great potential for hypersonic vehicles, $C_f/UHTCMC$ have been the focus of research on high temperature structural materials in extreme environmental conditions in recent years. This study presents the state of the art on $C_f/UHTCMC$ in terms of preparation processes, matrix modification, structure and property regulation, oxidation ablation mechanism, and high temperature mechanical properties. The aim is to enhance understanding of the critical scientific issues related to the structural transformation and property mechanisms of $C_f/UHTCMC$.

The physical and chemical properties of C_f/UHTCMC is highly reliant upon both the processing method and process conditions at the fabricator's disposal. The processing approaches of C_f/UHTCMC mainly include PIP, CVI, RMI, SI, HP, SPS, among others. Although the PIP method can better solve the problem of inhomogeneous UHTC phase distribution, the difficulty in synthesizing UHTC precursors and high price restrict its development. Moreover, the lower ceramic yield of UHTC precursors leads to the larger

porosity of C_f/UHTCMC, which is another important factor limiting the wide application of PIP method. For C_f/UHTCMC components serving in high temperature oxidation environments, high densification (i.e., low porosities) are essential to ensure composites performance. The RMI method has the unique advantages of short cycle and rapid densification, which is a more economical and efficient preparation approach for C_f/UHTCMC compared with other preparation approaches such as PIP and CVI. In the RMI process, the pore structure of the permeated preform has a decisive influence on the melt seepage, in situ reaction as well as the morphology and structure of UHTCs phase. Therefore, it is of great significance to adjust and modify the pore structure of the permeated preform based on the principle of pore regulation for eliminating residual metals and improving the ablation resistance. The CVI process is very useful in that it enables to produce the desired interphase and partial UHTC matrix at low fabrication temperatures that do not cause the fiber degradation. Due to the intrinsically long preparation cycle, almost no C_f/UHTCMC prepared totally by CVI have been reported. The SI method has the characteristics of easy control of UHTC composition and content, simple equipment

and process, low cost, and fewer defects. However, the agglomeration of UHTC particles is expected to block the pores of the preform outer layer, resulting in difficulties in continuous densification and is not suitable for components with complex geometry. HP and SPS are the most common routes for sintering $C_f/UHTCMC$, which reduces processing time and allows for high densification. Nevertheless, the high temperature and pressure generated are pernicious to the carbon fiber and interphase. Overall, to achieve the targeted properties of $C_f/UHTCMC$, including microstructural characterization, mechanical, oxidation, and ablation properties, a combination of two or more preparation approaches is imperative.

The ablation resistance of C_f/UHTCMC can be obviously improved by compositional design, resulting in an immiscible multicomponent oxide protective layer. The oxygen consumption by carbide/boride during oxidation, the stability of the oxide protective layer, the viscosity of the multicomponent glass phase, the dense oxygen diffusion barrier as well as the heat absorbed by the melting or evaporation of the oxide layer are considered responsible for the observed improvement in ablation resistance of the C_f/UHTCMC. Optimizing the type and quantity of transition metal and RE elements in the oxide protective layer formed in C_f/UHTCMC is conducive to obtaining superior oxidation and ablation properties for extreme temperature applications. While the incorporation of multicomponent UHTCs phases, HECs and RE elements probably enhance the ablation resistance, there is also a need to supervise the type and amount of transition metal and RE elements so as to balance the physical, mechanical, and thermal properties of the composites to best suit practical applications. It is worth noting that the C_f/UHTCMC exhibit anisotropic mechanical and ablation behavior due to the different braided structure of carbon fiber preforms. Therefore, a suitable preform structure should be adopted according to the dimension of C_f/ UHTCMC component, mechanical load, thermal load, and operating conditions for the specific application.

Considering the advantages and disadvantages of various ablation testing methods, it is essential to establish a rapid and low-cost assessment method for large $C_f/UHTCMC$ with complex geometry under real or near-real service environment conditions. Moreover, the uniform oxidation ablation assessment standard can provide a more accurate direction for $C_f/UHTCMC$ to achieve performance optimization and long-term service at elevated temperature.

 C_{1} /UHTCMC as structural component for ultra-high temperature extreme environment applications, the existing research reports on their elevated temperature mechanical properties are still scarce. Although it has been confirmed that the UHTCs phase undergo dislocation slip, grain

deflection, and plastic deformation at elevated temperature, the influence of dislocation slip mechanism, atomic diffusion mechanism, and external conditions on the plastic deformation of $C_f/UHTCMC$ still need to be further investigated.

Most of the research works remain on improving the fabrication process and composition; however, there is limited information available on the structural design and regulation of $C_f/UHTCMC$. According to the required properties with respect to its intended operability window, targeted multiscale structural design and regulation can help to maximize the performance of $C_f/UHTCMC$. Meanwhile, advanced characterization techniques for $C_f/UHTCMC$ with atomic scale resolution capabilities will be further explored to gain insight into the mechanical and ablation behavior of $C_f/UHTCMC$. Create hybrid processes or develop new processes to avoid fiber and interphase degradation while obtaining the desired combination of properties.

C_f/UHTCMC is a rapidly developing and growing new composite with extremely bright prospect as thermal structures and anti-ablation components of hypersonic vehicles and rockets, especially in sharp noses, leading edges, and engine components, as a result of their superior thermal shock, oxidation ablation resistance and damage tolerance. They can be further explored in various technical fields, such as simulation studies and life prediction of ablation process, new fiber/matrix interphase design, ablation and mechanical behavior under the coupling of force, heat, and oxygen, multiscale structural design and regulation in order to optimize oxidation ablation properties and prolong the service life as well as thermal protection system design. Simulation modelling, based on the accumulation of a large amount of product inspection data, creates mapping relationships between matrix, fiber, interphase, microstructure, processing, and properties, thus reducing the manufacturing and inspection costs. This offers considerable economic benefits in terms of improving the utilization efficiency of resources and energy.

Acknowledgments: This work was supported by the Development of fiber reinforced ceramic matrix composites resistant to extreme high temperature (No. 2023JBGS12-01).

Funding information: This work was supported by the Development of fiber reinforced ceramic matrix composites resistant to extreme high temperature (No. 2023[BGS12-01).

Author contributions: All authors have accepted responsibility for the entire content of this manuscript and approved its submission.

Conflict of interest: The authors state no conflict of interest.

Data availability statement: The datasets generated during and/or analysed during the current study are available from the corresponding author on reasonable request.

References

- [1] Bertin, J. J. and R. M. Cummings. Fifty years of hypersonics: where we've been, where we're going. Progress in Aerospace Sciences, Vol. 39, No. 6, 2003, pp. 511-536.
- [2] Sziroczak, D. and H. Smith. A review of design issues specific to hypersonic flight vehicles. Progress in Aerospace Sciences, Vol. 84, 2016, pp. 1-28.
- [3] Stollery, J. L. Hypersonic flight. Nature, Vol. 240, No. 5377, 1972, pp. 133-135.
- [4] Padture, N. P. Advanced structural ceramics in aerospace propulsion. Nature Materials, Vol. 15, No. 8, 2016, pp. 804-809.
- [5] Opeka, M. M., I. G. Talmy, and J. A. Zaykoski. Oxidation-based materials selection for 2000°C + hypersonic aerosurfaces: Theoretical considerations and historical experience. Journal of Materials Science, Vol. 39, No. 19, 2004, pp. 5887-5904.
- [6] Moses, P. L., V. L. Rausch, L. T. Nguyen, and J. R. Hill. NASA hypersonic flight demonstrators - overview, status, and future plans. Acta Astronautica, Vol. 55, No. 3, 2004, pp. 619-630.
- [7] Binner, J. and T. S. R. C. Murthy. Structural and thermostructural ceramics. Encyclopedia of Materials: Technical Ceramics and Glasses, In: M. Pomeroy, (Ed.), Elsevier, Oxford, 2021, pp. 3-24.
- [8] Voland, R. T., L. D. Huebner, and C. R. McClinton. X-43A Hypersonic vehicle technology development. Acta Astronautica, Vol. 59, No. 1, 2006, pp. 181-191.
- [9] Zhang, S., X. Li, J. Zuo, J. Qin, K. Cheng, Y. Feng, et al. Research progress on active thermal protection for hypersonic vehicles. Progress in Aerospace Sciences, Vol. 119, 2020, id. 100646.
- Le, V. T., N. S. Ha, and N. S. Goo. Advanced sandwich structures for thermal protection systems in hypersonic vehicles: A review. Composites Part B: Engineering, Vol. 226, 2021, id. 109301.
- Yang, Y., J. Yang, and D. Fang. Research progress on thermal protection materials and structures of hypersonic vehicles. Applied Mathematics and Mechanics, Vol. 29, No. 1, 2008, pp. 51-60.
- [12] Kane, K. A., B. A. Pint, D. Mitchell, and J. A. Haynes. Oxidation of ultrahigh temperature ceramics: kinetics, mechanisms, and applications. Journal of the European Ceramic Society, Vol. 41, No. 13, 2021, pp. 6130-6150.
- [13] Levine, S. R., E. J. Opila, M. C. Halbig, J. D. Kiser, M. Singh, and J. A. Salem. Evaluation of ultra-high temperature ceramics for aeropropulsion use. Journal of the European Ceramic Society, Vol. 22, No. 14, 2002, pp. 2757-2767.
- [14] Savino, R., L. Criscuolo, G. D. Di Martino, and S. Mungiguerra. Aero-thermo-chemical characterization of ultra-high-temperature ceramics for aerospace applications. Journal of the European Ceramic Society, Vol. 38, No. 8, 2018, pp. 2937-2953.
- Glass, D. E. Hypersonic materials and structures, NASA Langley Research Center Hampton Publishing, VA, United States, 2016.

- Squire, T. H. and J. Marschall. Material property requirements for analysis and design of UHTC components in hypersonic applications. Journal of the European Ceramic Society, Vol. 30, No. 11, 2010, pp. 2239-2251.
- [17] Yang, X., Y. Gui, W. Tang, Y. Du, D. Wei, G. Xiao, et al. Surface chemical effects on hypersonic nonequilibrium aeroheating in dissociated carbon-oxygen mixture. Journal of Spacecraft and Rockets, Vol. 55, No. 3, 2018, pp. 687-697.
- [18] Yang, Y., B. P. Bewlay, Y. A. S.-L. Chen, and Chang. Application of phase diagram calculations to development of new ultra-high temperature structural materials. Transactions of Nonferrous Metals Society, Vol. 17, No. 6, 2007, pp. 1396-1404.
- Sonber, J. K., T. S. R. C. Murthy, S. Majumdar, and V. Kain. Processing of ZrB₂- and HfB₂-based ultra-high temperature ceramic materials: a review. Materials Performance and Characterization, Vol. 10, No. 2, 2021, pp. 89-121.
- Opeka, M. M., I. G. Talmy, E. J. Wuchina, J. A. Zaykoski, and S. J. Causey. Mechanical, thermal, and oxidation properties of refractory hafnium and zirconium compounds. Journal of the European Ceramic Society, Vol. 19, No. 13-14, 1999, pp. 2405-2414.
- [21] Ni, D., Y. Cheng, J. Zhang, J.-X. Liu, J. Zou, B. Chen, et al. Advances in ultra-high temperature ceramics, composites, and coatings. Journal of Advanced Ceramics, Vol. 11, 2022, pp. 1-56.
- [22] Nisar, A., R. Hassan, A. Agarwal, and K. Balani. Ultra-high temperature ceramics: Aspiration to overcome challenges in thermal protection systems. Ceramics International, Vol. 48, No. 7, 2022, pp. 8852-8881.
- Ferro, D., J. V. Rau, V. Rossi Albertini, A. Generosi, R. Teghil, and [23] S. M. Barinov. Pulsed laser deposited hard TiC, ZrC, HfC and TaC films on titanium: Hardness and an energy-dispersive X-ray diffraction study. Surface and Coatings Technology, Vol. 202, No. 8, 2008, pp. 1455-1461.
- [24] Savino, R., M. De Stefano Fumo, L. Silvestroni, and D. Sciti. Arc-jet testing on HfB2 and HfC-based ultra-high temperature ceramic materials. Journal of the European Ceramic Society, Vol. 28, No. 9, 2008, pp. 1899-1907.
- [25] Binner, J., M. Porter, B. Baker, J. Zou, V. Venkatachalam, V. R. Diaz, et al. Selection, processing, properties and applications of ultrahigh temperature ceramic matrix composites, UHTCMCs - a review. International Materials Reviews, Vol. 65, No. 7, 2020. pp. 389-444.
- Tang, S. and C. Hu. Design, preparation and properties of carbon [26] fiber reinforced ultra-high temperature ceramic composites for aerospace applications: a review. Journal of Materials Science & Technology, Vol. 33, No. 2, 2017, pp. 117-130.
- [27] Fitzer, E. The future of carbon-carbon composites. Carbon, Vol. 25, No. 2, 1987, pp. 163-190.
- [28] Saccone, G., R. Gardi, D. Alfano, A. Ferrigno, and A. Del Vecchio. Laboratory, on-ground and in-flight investigation of ultra high temperature ceramic composite materials. Aerospace Science and Technology, Vol. 58, 2016, pp. 490-497.
- [29] Baklanova, N. I., T. M. Zima, A. I. Boronin, S. V. Kosheev, A. T. Titov, and N. V. Isaeva. Protective ceramic multilayer coatings for carbon fibers. Surface and Coatings Technology, Vol. 201, No. 6, 2006, pp. 2313-2319.
- [30] Rueschhoff, L. M., C. M. Carney, Z. D. Apostolov, and M. K. Cinibulk. Processing of fiber-reinforced ultra-high temperature ceramic composites: A review. International Journal of Ceramic Engineering & Science, Vol. 2, No. 1, 2020, pp. 22-37.

- [31] Newcomb, B. A. Processing, structure, and properties of carbon fibers. Composites - Part A: Applied Science and Manufacturing, Vol. 91, 2016, pp. 262-282.
- [32] Ruland, W. Carbon fibers. Advanced Materials, Vol. 2, No. 11, 1990, pp. 528-536.
- Yang, F., X. Zhang, J. Han, and S. Du. Mechanical properties of short carbon fiber reinforced ZrB2-SiC ceramic matrix composites. Materials Letters, Vol. 62, No. 17-18, 2008, pp. 2925-2927.
- [34] Foong, L. K., M. A. Mu'azu, and Z. Lyu. Effect of SiC whisker on densification and mechanical properties of hot-pressed TiC-based composites. Ceramics International, Vol. 46, No. 17, 2020, pp. 27734-27741.
- Sha, J., J. Li, S. Wang, Y. Wang, Z. Zhang, and J. Dai. Toughening effect of short carbon fibers in the ZrB₂–ZrSi₂ ceramic composites. Materials & Design, Vol. 75, 2015, pp. 160-165.
- Feng, T., M. Tong, S. Yao, H. Li, H. Lin, S. Wen, et al. Ablation behaviour and mechanical property of the B-modified SiC/ HfC-SiC composites in cyclic ablation environment. Corrosion Science, Vol. 174, 2020, id. 108829.
- [37] Zeng, Y., D. Wang, X. Xiong, X. Zhang, P. J. Withers, W. Sun, et al. Ablation-resistant carbide Zr0.8Ti0.2C0.74B0.26 for oxidizing environments up to 3,000°C. Nature Communications, Vol. 8, No. 1, 2017, id. 15836.
- [38] Pienti, L., D. Sciti, L. Silvestroni, A. Cecere, and R. Savino. Ablation tests on HfC- and TaC-based ceramics for aeropropulsive applications. Journal of the European Ceramic Society, Vol. 35, No. 5, 2015, pp. 1401-1411.
- [39] Liu, L., B. Li, W. Feng, C. Tang, J. Zhang, X. Yao, et al. Effect of loading spectrum with different single pulsing time on the cyclic ablation of C/C-SiC-ZrB₂-ZrC composites in plasma. Corrosion Science, Vol. 192, 2021, id. 109817.
- Zhao, Z., K. Li, and W. Li. Ablation behavior of ZrC-SiC-ZrB2 and ZrC-SiC inhibited carbon/carbon composites components under ultrahigh temperature conditions. Corrosion Science, Vol. 189, 2021, id. 109598.
- [41] Ai, J. P., S. S. Luo, W. K. Li, S. W. Wang, and G. H. Zhou. Mechanical properties and microstructure of 2.5D C_f/ZrO₂ composites prepared by precursor infiltration and pyrolysis. Key Engineering Materials, Vol. 697, 2016, pp. 639-643.
- Li, Q., S. Dong, Z. Wang, P. He, and H. Zhou. Fabrication and properties of 3-D C_f/SiC-ZrC composites, using ZrC precursor and polycarbosilane. Journal of the American Ceramic Society, Vol. 95, No. 4, 2012, pp. 1216-1219.
- Tan, W., K. Li, H. Li, J. Zhang, C. Ni, A. Cao, et al. Ablation behavior and mechanism of C/C-HfC-SiC composites. Vacuum, Vol. 116, 2015, pp. 124-129.
- [44] Lee, S. H., M. Weinmann, and F. Aldinger. Fabrication of fiberreinforced ceramic composites by the modified slurry infiltration technique. Journal of the American Ceramic Society, Vol. 90, No. 8, 2010, pp. 2657-2660.
- Paul, A., S. Venugopal, J. G. P. Binner, B. Vaidhyanathan, A. C. J. [45] Heaton, and P. M. Brown. UHTC-carbon fibre composites: Preparation, oxyacetylene torch testing and characterisation. Journal of the European Ceramic Society, Vol. 33, No. 2, 2013,
- [46] Tang, S., J. Deng, S. Wang, W. Liu, and K. Yang. Ablation behaviors of ultra-high temperature ceramic composites. Materials Science & Engineering, A: Structural Materials: Properties, Microstructure and Processing, Vol. 465, No. 1, 2007, pp. 1-7.

- [47] Singh, M. and D. R. Behrendt. Reactive melt infiltration of siliconmolybdenum alloys into microporous carbon preforms. Materials Science & Engineering, A: Structural Materials: Properties, Microstructure and Processing, Vol. 194, No. 2, 1995, pp. 193-200.
- [48] Einset, E. O. Analysis of reactive melt infiltration in the processing of ceramics and ceramic composites. Chemical Engineering Science, Vol. 53, No. 5, 1998, pp. 1027-1039.
- [49] Zou, L., N. Wali, J.-M. Yang, and N. P. Bansal. Microstructural development of a C_f/ZrC composite manufactured by reactive melt infiltration. Journal of the European Ceramic Society, Vol. 30, No. 6, 2010, pp. 1527-1535.
- [50] Delhaes, P. Chemical vapor deposition and infiltration processes of carbon materials. Carbon, Vol. 40, No. 5, 2002, pp. 641-657.
- [51] Lackey, W. I. Review, status, and future of the chemical vapor infiltration process for fabrication of fiber-reinforced ceramic composites. A Collection of Papers Presented at the 13th Annual Conference on Composites and Advanced Ceramic Materials: Ceramic Engineering and Science Proceedings, 1989, pp. 577-584.
- Wang, Y., Q. Liu, J. Liu, L. Zhang, and L. Cheng. Deposition mechanism for chemical vapor deposition of zirconium carbide coatings. Journal of the American Ceramic Society, Vol. 91, No. 4, 2010, pp. 1249-1252.
- [53] Kakroudi, M. G., M. D. Alvari, M. S. Asl, N. P. Vafa, and T. Rabizadeh. Hot pressing and oxidation behavior of ZrB₂-SiC-TaC composites. Ceramics International, Vol. 46, No. 3, 2020, pp. 3725-3730.
- [54] Kannan, R. and L. Rangaraj. Properties of C_f/SiC-ZrB₂-Ta_xC_v composite produced by reactive hot pressing and polymer impregnation pyrolysis (RHP/PIP). Journal of the European Ceramic Society, Vol. 39, No. 7, 2019, pp. 2257-2265.
- [55] Tang, C., A. Dang, T. Li, T. Zhao, H. Li, and S. Jiao. Influence of fiber content on C/C-SiC brake materials fabricated by compression molding and hot sintering. Tribology International, Vol. 136, 2019, pp. 404-411.
- [56] Nasiri, Z., M. Mashhadi, and A. Abdollahi. Effect of short carbon fiber addition on pressureless densification and mechanical properties of ZrB₂-SiC-C_{sf} nanocomposite. *International Journal of* Refractory Metals and Hard Materials, Vol. 51, 2015, pp. 216-223.
- [57] Zhou, Z., C. Tao, H. Liao, W. Mao, X. Fan, L. Zhang, et al. Pressureless sintering and ablation behavior of PyC-C_{sf}/ ZrB₂-SiC-ZrC ceramics doped with B₄C. Journal of the European Ceramic Society, Vol. 43, No. 3, 2023, pp. 748-759.
- [58] Li, Z., P. Xiao, and X. Xiong. Preparation and properties of C/C-SiC brake composites fabricated by warm compacted-in situ reaction. International Journal of Minerals, Metallurgy and Materials, Vol. 17, No. 4, 2010, pp. 500-505.
- [59] Xiao, P., Z. Li, Z. Zhu, and X. Xiong. Preparation, properties and application of C/C-SiC composites fabricated by warm compacted-in situ reaction. Journal of Materials Science and Technology, Vol. 26, No. 3, 2010, pp. 283-288.
- [60] Li, C., K. Li, H. Li, Y. Zhang, H. Ouyang, D. Yao, et al. Microstructure and ablation resistance of carbon/carbon composites with a zirconium carbide rich surface layer. Corrosion Science, Vol. 85, 2014, pp. 160-166.
- [61] Yin, X., X. Zhang, H. Liu, Q. Fu, and H. Li. Novel structural design strategies in ceramic-modified C/C composites. Accounts of Materials Research, Vol. 4, No. 12, 2023, pp. 1095-1107.
- [62] Jiang, Y., D. Ni, Q. Ding, B. Chen, X. Chen, Y. Kan, et al. Synthesis and characterization of nano-crystalized HfC based on an

- aqueous solution-derived precursor. RSC Advances, Vol. 8, No. 69, 2018, pp. 39284-39290.
- [63] Yao, J., B. Liang, C. Hu, S. Pang, R. Zhao, S. Tang, et al. Pitch resin addition induced evolution of composition, microstructure and mechanical property of C/C-SiC-ZrC composites. Journal of the European Ceramic Society, Vol. 42, No. 14, 2022, pp. 6412-6424.
- Jiao, X., Q. Tan, Q. He, M. Qing, Y. Wang, and X. Yin. Cyclic ablation [64] behavior of mullite-modified C/C-HfC-SiC composites under an oxyacetylene flame at about 2400 °C. Journal of the European Ceramic Society, Vol. 43, No. 10, 2023, pp. 4309-4321.
- Cai, T., D. Liu, W. Qiu, W. Han, and T. Zhao. Polymer precursorderived HfC-SiC ultrahigh-temperature ceramic nanocomposites. Journal of the American Ceramic Society, Vol. 101, No. 1, 2018, pp. 20-24.
- [66] Zhao, X., Y. Wang, L. Duan, L. Luo, and Y. Lu. Improved ablation resistance of C/SiC-ZrB₂ composites via polymer precursor impregnation and pyrolysis. Ceramics International, Vol. 43, No. 15, 2017, pp. 12480-12489.
- [67] Sun, Y., L. Ye, Y. Zhang, F. Chen, W. Han, W. Qiu, et al. Synthesis of high entropy carbide ceramics via polymer precursor route. Ceramics International, Vol. 48, No. 11, 2022, pp. 15939-15945.
- [68] Cai, F., D. Ni, B. Chen, L. Ye, Y. Sun, J. Lu, et al. Fabrication and properties of C_f/(Ti_{0.2}Zr_{0.2}Hf_{0.2}Nb_{0.2}Ta_{0.2})C-SiC high-entropy ceramic matrix composites via precursor infiltration and pyrolysis. Journal of the European Ceramic Society, Vol. 41, No. 12, 2021, pp. 5863-5871.
- [69] Cai, F., D. Ni, W. Bao, B. Chen, J. Lu, X. Zou, et al. Ablation behavior and mechanisms of Cf/(Ti0.2Zr0.2Hf0.2Nb0.2Ta0.2)C-SiC highentropy ceramic matrix composites. Composites Part B: Engineering, Vol. 243, 2022, id. 110177.
- Ziegler, G., I. Richter, and D. Suttor. Fiber-reinforced composites with polymer-derived matrix: processing, matrix formation and properties. Composites Part A: Applied Science and Manufacturing, Vol. 30, No. 4, 1999, pp. 411-417.
- [71] Parthasarathy, T. A., C. P. Przybyla, R. S. Hay, and M. K. Cinibulk. Modeling environmental degradation of SiC-based fibers. Journal of the American Ceramic Society, Vol. 99, No. 5, 2016, pp. 1725–1734.
- [72] King, D., Z. Apostolov, T. Key, C. Carney, and M. Cinibulk. Novel processing approach to polymer-derived ceramic matrix composites. International Journal of Applied Ceramic Technology, Vol. 15, No. 2, 2018, pp. 399-408.
- Yan, C., R. Liu, C. Zhang, Y. Cao, and X. Long. Mechanical behaviour and microstructure of C_f/ZrC, C_f/SiC and C_f/ZrC - SiC composites. Advances in Applied Ceramics, Vol. 115, No. 7, 2016, pp. 391-395.
- [74] Hu, P., D. Zhang, S. Dong, Q. Qu, and X. Zhang. A novel vibrationassisted slurry impregnation to fabricate C_f/ZrB₂-SiC composite with enhanced mechanical properties. Journal of the European Ceramic Society, Vol. 39, No. 4, 2019, pp. 798-805.
- Chen, J., Y. Wang, L. Cheng, and L. Zhang. Thermal diffusivity of [75] three-dimensional needled C/SiC-TaC composites. Ceramics International, Vol. 37, No. 8, 2011, pp. 3095-3099.
- [76] Baker, B., V. Rubio, P. Ramanujam, J. Binner, A. Hussain, T. Ackerman, et al. Development of a slurry injection technique for continuous fibre ultra-high temperature ceramic matrix composites. Journal of the European Ceramic Society, Vol. 39, No. 14, 2019, pp. 3927-3937.
- [77] Rubio, V., J. Binner, S. Cousinet, G. Le Page, T. Ackerman, A. Hussain, et al. Materials characterisation and mechanical

- properties of Cf-UHTC powder composites. Journal of the European Ceramic Society, Vol. 39, No. 4, 2019, pp. 813-824.
- [78] Tammana, S. R. C. M., M. Duan, J. Zou, J. Wade, V. Venkatachalam, B. Baker, et al. Ablation behaviour of Cf-ZrC-SiC with and without rare earth metal oxide dopants. Open Ceramics, Vol. 10, 2022, id. 100270.
- Zhang, D., J. Feng, P. Hu, L. Xun, M. Liu, S. Dong, et al. Enhanced mechanical properties and thermal shock resistance of C_f/ ZrB₂-SiC composite via an efficient slurry injection combined with vibration-assisted vacuum infiltration. Journal of the European Ceramic Society, Vol. 40, No. 15, 2020, pp. 5059-5066.
- [80] Chen, B.-W., D.-W. Ni, C.-J. Liao, Y.-L. Jiang, J. Lu, Y.-S. Ding, et al. Chemical reactions and thermal stress induced microstructure evolution in 2D-C_f/ZrB₂-SiC composites. Journal of Materials Science & Technology, Vol. 83, 2021, pp. 75-82.
- [81] Sciti, D., L. Zoli, T. Reimer, A. Vinci, and P. Galizia. A systematic approach for horizontal and vertical scale up of sintered ultrahigh temperature ceramic matrix composites for aerospace advances and perspectives. Composites Part B: Engineering, Vol. 234, 2022, id. 109709.
- [82] Chen, S.a, C. Zhang, Y. Zhang, and H. Hu. Influence of pyrocarbon amount in C/C preform on the microstructure and properties of C/ZrC composites prepared via reactive melt infiltration. Materials & Design, Vol. 58, 2014, pp. 570-576.
- [83] Zou, L., N. Wali, J. M. Yang, N. P. Bansal, and Y. Dong. Microstructural characterization of a C_f/ZrC composite manufactured by reactive melt infiltration. International Journal of Applied Ceramic Technology, Vol. 8, No. 2, 2011, pp. 329-341.
- [84] Luo, L., Y. Wang, L. Duan, L. Liu, and G. Wang. Ablation behavior of C/SiC-HfC composites in the plasma wind tunnel. Journal of the European Ceramic Society, Vol. 36, No. 15, 2016, pp. 3801-3807.
- [85] Wang, Y., X. Zhu, L. Zhang, and L. Cheng. Reaction kinetics and ablation properties of C/C-ZrC composites fabricated by reactive melt infiltration. Ceramics International, Vol. 37, No. 4, 2011, pp. 1277-1283.
- Wang, Y., X. Zhu, L. Zhang, and L. Cheng. C/C-SiC-ZrC composites [86] fabricated by reactive melt infiltration with Si_{0.87}Zr_{0.13} alloy. Ceramics International, Vol. 38, No. 5, 2012, pp. 4337–4343.
- Zeng, Y., D. Wang, X. Xiong, S. Gao, Z. Chen, W. Sun, et al. Ultra-[87] high-temperature ablation behavior of SiC-ZrC-TiC modified carbon/carbon composites fabricated via reactive melt infiltration. Journal of the European Ceramic Society, Vol. 40, No. 3, 2020,
- [88] Zeng, Y., X. Xiong, D. Wang, L. Wu, Z. Chen, W. Sun, et al. High temperature corrosion of carbon/carbon composites in Zr-Ti melts during liquid metal infiltration. Corrosion Science, Vol. 98, 2015, pp. 98-106.
- Chen, X., Q. Feng, H. Zhou, S. Dong, J. Wang, Y. Cao, et al. Ablation [89] behavior of three-dimensional C_f/SiC-ZrC-ZrB₂ composites prepared by a joint process of sol-gel and reactive melt infiltration. Corrosion Science, Vol. 134, 2018, pp. 49-56.
- [90] Chen, X., D. Ni, Y. Kan, Y. Jiang, H. Zhou, Z. Wang, et al. Reaction mechanism and microstructure development of ZrSi2 melt-infiltrated C_f/SiC-ZrC-ZrB₂ composites: The influence of preform pore structures. Journal of Materiomics, Vol. 4, No. 3, 2018, pp. 266-275.
- [91] Chen, X., Q. Feng, L. Gao, X. Zhang, S. Dong, J. Wang, et al. Interphase degradation of three-dimensional C_f/SiC-ZrC-ZrB₂ composites fabricated via reactive melt infiltration. Journal of the American Ceramic Society, Vol. 100, No. 10, 2017, pp. 4816-4826.
- [92] Guo, W., J. Hu, W. Fang, Y. Ye, S. Zhang, and S. Bai. A novel strategy for rapid fabrication of continuous carbon fiber

- reinforced (TiZrHfNbTa)C high-entropy ceramic composites: Highentropy alloy in-situ reactive melt infiltration. Journal of the European Ceramic Society, Vol. 43, No. 6, 2023, pp. 2295-2305.
- [93] Tong, Y., S. Bai, Q. H. Qin, Y. Ye, and H. Zhang. Reaction mechanism and microstructure development of Zr-Si alloyed melt-infiltrated ZrC-modified C/C composite. Journal of the American Ceramic Society, Vol. 98, No. 7, 2015, pp. 2065-2073.
- Vinci, A., L. Zoli, P. Galizia, M. Kütemever, D. Koch, M. Frieß, et al. [94] Reactive melt infiltration of carbon fibre reinforced ZrB2/B composites with Zr₂Cu. Composites Part A: Applied Science and Manufacturing, Vol. 137, 2020, id. 105973.
- [95] Kütemeyer, M., L. Schomer, T. Helmreich, S. Rosiwal, and D. Koch. Fabrication of ultra high temperature ceramic matrix composites using a reactive melt infiltration process. Journal of the European Ceramic Society, Vol. 36, No. 15, 2016, pp. 3647-3655.
- [96] Xu, Y., W. Sun, C. Miao, Y. Shen, H. Chen, Y. Liu, et al. Ablation properties of C/C-UHTCs and their preparation by reactive infiltration of K₂MeF₆ (Me = Zr, Ti) molten salt. Journal of the European Ceramic Society, Vol. 41, No. 11, 2021, pp. 5405-5416.
- [97] Xu, Y., W. Sun, X. Xiong, F. Liu, and C. Miao. Chloride salt assisted reactive molten infiltration method for Cf-UHTCs and their unique microstructure. Ceramics International, Vol. 46, No. 5, 2020, pp. 6424-6435.
- [98] Chen, X., Q. Feng, Y. Kan, D. Ni, H. Zhou, L. Gao, et al. Effects of preform pore structure on infiltration kinetics and microstructure evolution of RMI-derived C_f/ZrC-ZrB₂-SiC composite. Journal of the European Ceramic Society, Vol. 40, No. 7, 2020, pp. 2683-2690.
- [99] Zhong, Q., X. Zhang, S. Dong, J. Yang, J. Hu, L. Gao, et al. Reactive melt infiltrated C_f/SiC composites with robust matrix derived from novel engineered pyrolytic carbon structure. Ceramics International, Vol. 43, No. 7, 2017, pp. 5832-5836.
- Guo, P., J. Li, S. Pang, C. Hu, S. Tang, and H.-M. Cheng. Ultralight carbon fiber felt reinforced monolithic carbon aerogel composites with excellent thermal insulation performance. Carbon, Vol. 183, 2021, pp. 525-529.
- Li, J., P. Guo, C. Hu, S. Pang, J. Ma, R. Zhao, et al. Fabrication of large aerogel-like carbon/carbon composites with excellent loadbearing capacity and thermal-insulating performance at 1800°C. ACS Nano, Vol. 16, No. 4, 2022, pp. 6565-6577.
- [102] Zhao, R., S. Pang, C. Hu, J. Li, B. Liang, S. Tang, et al. Fabrication of C/SiC composites by siliconizing carbon fiber reinforced nanoporous carbon matrix preforms and their properties. Journal of the European Ceramic Society, Vol. 43, No. 2, 2023, pp. 273–282.
- [103] Appiah, K. A., Z. L. Wang, and W. J. Lackey. Characterization of interfaces in C fiber-reinforced laminated C-SiC matrix composites. Carbon, Vol. 38, No. 6, 2000, pp. 831-838.
- [104] Vignoles, G. L. 8 Chemical vapor deposition/infiltration processes for ceramic composites. Advances in Composites Manufacturing and Process Design, In: P. Boisse, (Ed.), Woodhead Publishing, Pessac, France, 2015, pp. 147-176.
- Sayir, A. Carbon fiber reinforced hafnium carbide composite. Journal of Materials Science, Vol. 39, No. 19, 2004, pp. 5995-6003.
- Chen, Z.-k, X. Xiong, B.-y Huang, G.-d Li, F. Zheng, P. Xiao, et al. Phase composition and morphology of TaC coating on carbon fibers by chemical vapor infiltration. Thin Solid Films, Vol. 516, No. 23, 2008, pp. 8248-8254.
- Deck, C. P., H. E. Khalifa, B. Sammuli, and C. A. Back. Modeling forced flow chemical vapor infiltration fabrication of SiC-SiC composites for advanced nuclear reactors. Science and Technology of Nuclear Installations, Vol. 2013, 2013, id. 127676.

- [108] Hu, C., W. Hong, X. Xu, S. Tang, S. Du, and H.-M. Cheng. Sandwichstructured C/C-SiC composites fabricated by electromagneticcoupling chemical vapor infiltration. Scientific Reports, Vol. 7, No. 1, 2017, id. 13120.
- [109] Hu, C., R. Zhao, S. Ali, Y. Wang, S. Pang, J. Li, et al. Deposition kinetics and mechanism of pyrocarbon for electromagnetic-coupling chemical vapor infiltration process. Journal of Materials Science & Technology, Vol. 101, 2022, pp. 118-127.
- [110] He, Q., H. Li, C. Wang, S. Chen, and J. Lu. Densification behavior and ablation property of C/C-ZrC composites prepared by chemical liquid vapor deposition process at temperatures from 800 to 1100 °C. Ceramics International, Vol. 44, No. 7, 2018, pp.
- [111] Lu, I., O. He, Y. Wang, H. Li, and O. Fu, Preparation of co-deposited C/C-ZrC composites by CLVD process and its properties. Journal of Alloys and Compounds, Vol. 686, 2016, pp. 823-830.
- [112] He, Q., J. Lu, Y. Wang, and C. Wang. Effects of joint processes of CLVD and PIP on the microstructure and mechanical properties of C/C-ZrC composites. Ceramics International, Vol. 42, No. 15, 2016, pp. 17429-17435.
- Li, Q., S. Dong, Z. Wang, J. Hu, B. Wu, H. Zhou, et al. Fabrication of [113] a ZrC-SiC matrix for ceramic matrix composites via in-situ reaction and its application. Ceramics International, Vol. 39, No. 1, 2013, pp. 877-881.
- [114] Shen, X.-T., K.-Z. Li, H.-J. Li, Q.-G. Fu, S.-P. Li, and F. Deng. The effect of zirconium carbide on ablation of carbon/carbon composites under an oxyacetylene flame. Corrosion Science, Vol. 53, No. 1, 2011, pp. 105-112.
- [115] Li, C., K. Li, H. Ouyang, J. Huang, H. Li, Y. Zhang, et al. Effect of ZrO₂ morphology on the ablation resistance of carbon/carbon composites containing ZrC prepared by the carbothermal reduction reaction. Corrosion Science, Vol. 102, 2016, pp. 405-412.
- [116] Chen, X., S. Dong, Y. Kan, H. Zhou, J. Hu, and D. Wang. 3D C_f/SiC-ZrC-ZrB₂ composites fabricated via sol-gel process combined with reactive melt infiltration. Journal of the European Ceramic Society, Vol. 36, No. 15, 2016, pp. 3607-3613.
- Zeng, C., K. Tong, M. Zhang, Q. Huang, Z. Su, C. Yang, et al. The effect of sol-gel process on the microstructure and particle size of ZrC-SiC composite powders. Ceramics International, Vol. 46, No. 4, 2020, pp. 5244-5251.
- [118] ZhongLiu, W., X. Peng, L. Zhuan, H. Wen, L. Heng, Y. XiaoYu, et al. Microstructure and oxidation behavior of sol-gel mullite coating on SiC-coated carbon/carbon composites. Journal of the European Ceramic Society, Vol. 35, No. 14, 2015, pp. 3789-3796.
- Ni, Y., R. Luo, and H. Luo. Fabrication and mechanical properties of 3-D C_f/C-SiC-TiC composites prepared by RMI. Journal of Alloys and Compounds, Vol. 798, 2019, pp. 784-789.
- [120] Xin, Y., H. Qizhong, S. Zhean, C. Xin, X. Liang, Z. Ping, et al. Ablative property and mechanism of C/C-ZrB₂-ZrC-SiC composites reinforced by SiC networks under plasma flame. Corrosion Science, Vol. 107, 2016, pp. 9-20.
- [121] He, Q., H. Li, Q. Tan, J. Lu, and Y. Wang. Influence of carbon preform density on the microstructure and ablation resistance of CLVD-C/C-ZrC-SiC composites. Corrosion Science, Vol. 190, 2021,
- [122] Shen, X.-T., L. Liu, W. Li, and K.-Z. Li. Ablation behaviour of C/ C-ZrC composites in a solid rocket motor environment. Ceramics International, Vol. 41, No. 9, Part B, 2015, pp. 11793-11803.
- [123] Zeng, C., M. Zhang, H. He, X. Wang, K. Tong, Y. Wang, et al. The effect of carbon source addition order during sol-gel process on

- the properties of C/C-ZrC-SiC composites. Ceramics International, Vol. 47, No. 24, 2021, pp. 35366-35377.
- [124] Tang, S., J. Deng, S. Wang, and W. Liu. Fabrication and characterization of an ultra-high-temperature carbon fiber-reinforced ZrB₂-SiC matrix composite. *Journal of the American Ceramic Society*, Vol. 90, No. 10, 2007, pp. 3320-3322.
- [125] Sciti, D., A. N. Murri, V. Medri, and L. Zoli. Continuous C fibre composites with a porous ZrB2 matrix. Materials & Design, Vol. 85, 2015, pp. 127-134.
- [126] Sciti, D. and L. Silvestroni. Processing, sintering and oxidation behavior of SiC fibers reinforced ZrB2 composites. Journal of the European Ceramic Society, Vol. 32, No. 9, 2012, pp. 1933-1940.
- Cheng, Y., C. Liu, P. Hu, B. Sun, P. Hu, C. Ma, et al. Using PyC coated short chopped carbon fiber to tackle the dilemma between toughness and strength of ZrC-SiC. Ceramics International, Vol. 45, No. 1, 2019, pp. 503-509.
- [128] Zoli, L., A. Vinci, P. Galizia, C. F. Gutièrrez-Gonzalez, S. Rivera, and D. Sciti. Is spark plasma sintering suitable for the densification of continuous carbon fibre - UHTCMCs? Journal of the European Ceramic Society, Vol. 40, No. 7, 2020, pp. 2597-2603.
- [129] Sciti, D., L. Zoli, A. Vinci, L. Silvestroni, S. Mungiguerra, and P. Galizia. Effect of PAN-based and pitch-based carbon fibres on microstructure and properties of continuous C_f/ZrB₂-SiC UHTCMCs. Journal of the European Ceramic Society, Vol. 41, No. 5, 2021, pp. 3045-3050.
- [130] Xing, H., B. Zou, X. Wang, Y. Hu, C. Huang, and K. Xue. Fabrication and characterization of SiC whiskers toughened Al₂O₃ paste for stereolithography 3D printing applications. Journal of Alloys and Compounds, Vol. 828, 2020, id. 154347.
- [131] Yang, J., R. Yu, X. Li, Y. He, L. Wang, W. Huang, et al. Silicon carbide whiskers reinforced SiOC ceramics through digital light processing 3D printing technology. Ceramics International, Vol. 47, No. 13, 2021, pp. 18314-18322.
- [132] Sun, C., J. Xiang, M. Xu, Y. He, Z. Tong, and X. Cui. 3D extrusion free forming of geopolymer composites: Materials modification and processing optimization. Journal of Cleaner Production, Vol. 258, 2020, id. 120986.
- Lv, X., F. Ye, L. Cheng, and L. Zhang. 3D printing "wire-on-sphere" hierarchical SiC nanowires/SiC whiskers foam for efficient hightemperature electromagnetic wave absorption. Journal of Materials Science & Technology, Vol. 109, 2022, pp. 94-104.
- [134] Peng, E., D. Zhang, and J. Ding. Ceramic robocasting: recent achievements, potential, and future developments. Advanced Materials, Vol. 30, No. 47, 2018, id. 1802404.
- [135] Chong, L., S. Ramakrishna, and S. Singh. A review of digital manufacturing-based hybrid additive manufacturing processes. International Journal of Advanced Manufacturing Technology, Vol. 95, No. 5, 2018, pp. 2281-2300.
- [136] Sun, J., D. Ye, J. Zou, X. Chen, Y. Wang, J. Yuan, et al. A review on additive manufacturing of ceramic matrix composites. Journal of Materials Science & Technology, Vol. 138, 2023, pp. 1-16.
- [137] Wang, W., L. Zhang, X. Dong, J. Wu, Q. Zhou, S. Li, et al. Additive manufacturing of fiber reinforced ceramic matrix composites: Advances, challenges, and prospects. Ceramics International, Vol. 48, No. 14, 2022, pp. 19542-19556.
- [138] Mei, H., Y. Yan, L. Feng, K. G. Dassios, H. Zhang, and L. Cheng. First printing of continuous fibers into ceramics. Journal of the American Ceramic Society, Vol. 102, No. 6, 2018, pp. 3244-3255.
- Zhang, H., Y. Yang, K. Hu, B. Liu, M. Liu, and Z. Huang. Stereolithography-based additive manufacturing of lightweight

- and high-strength C_f/SiC ceramics. Additive Manufacturing, Vol. 34, 2020, id. 101199.
- [140] Tang, J., H. Chang, X. Guo, M. Liu, Y. Wei, Z. Huang, et al. Preparation of carbon fiber-reinforced SiC ceramics by stereolithography and secondary silicon infiltration. Ceramics International, Vol. 48, No. 17, 2022, pp. 25159-25167.
- Wang, W., X. Bai, L. Zhang, S. Jing, C. Shen, and R. He. Additive manufacturing of C_{sf}/SiC composites with high fiber content by direct ink writing and liquid silicon infiltration. Ceramics International, Vol. 48, No. 3, 2022, pp. 3895-3903.
- [142] Fu, H., W. Zhu, Z. Xu, P. Chen, C. Yan, K. Zhou, et al. Effect of silicon addition on the microstructure, mechanical and thermal properties of C_f/SiC composite prepared via selective laser sintering. *Journal of Allovs and Compounds*, Vol. 792, 2019, pp. 1045–1053.
- [143] Tammana, S. R. C. M., V. Venkatachalam, J. Zou, M. Porter, and J. Binner. Oxidation studies of SiC-coated 2.5D carbon fibre preforms. Open Ceramics, Vol. 15, 2023, id. 100385.
- [144] Liu, Y., Y. Cheng, D. Ma, N. Hu, W. Han, D. Liu, et al. Continuous carbon fiber reinforced ZrB2-SiC composites fabricated by direct ink writing combined with low-temperature hot-pressing. Journal of the European Ceramic Society, Vol. 42, No. 9, 2022, pp. 3699-3707.
- Lu, J., D. Ni, C. Liao, H. Zhou, Y. Jiang, B. Chen, et al. Fabrication [145] and microstructure evolution of Csf/ZrB2-SiC composites via direct ink writing and reactive melt infiltration. Journal of Advanced Ceramics, Vol. 10, 2021, pp. 1371-1380.
- [146] Eakins, E., D. D. Jayaseelan, and W. E. Lee. Toward oxidationresistant ZrB2-SiC ultra high temperature ceramics. Metallurgical and Materials Transactions A: Physical Metallurgy and Materials Science, Vol. 42, No. 4, 2011, pp. 878-887.
- [147] Vogel, W. Historical development of glass chemistry. Glass Chemistry, In: W. Vogel, (Ed.), Springer Berlin Heidelberg, Berlin,
- [148] Shimada, S., M. Inagaki, and M. Suzuki. Microstructural observation of the ZrC/ZrO2 interface formed by oxidation of ZrC. Journal of Materials Research, Vol. 11, No. 10, 1996, pp. 2594-2597.
- [149] Bargeron, C. B., R. C. Benson, A. N. Jette, and T. E. Phillips. Oxidation of hafnium carbide in the temperature range 1400-2060°C. Journal of the American Ceramic Society, Vol. 76, No. 4, 2005, pp. 1040-1046.
- [150] Chang, Y., W. Sun, X. Xiong, Z. Chen, Y. Wang, Z. Hao, et al. Microstructure and ablation behaviors of a novel gradient C/C-ZrC-SiC composite fabricated by an improved reactive melt infiltration. Ceramics International, Vol. 42, No. 15, 2016, pp. 16906-16915.
- [151] Wang, S., H. Li, M. Ren, Y. Zuo, M. Yang, J. Zhang, et al. Microstructure and ablation mechanism of C/C-ZrC-SiC composites in a plasma flame. Ceramics International, Vol. 43, No. 14, 2017, pp. 10661-10667.
- [152] Liu, Y., Z. Xia, L. Ma, P. Yang, B. Chen, Y. Feng, et al. Microstructure and ablation mechanism of C/C-ZrC-SiC composite in the solid scramjet plumes environment. Materials Characterization, Vol. 198, 2023, id. 112754.
- Jin, X., X. Fan, C. Lu, and T. Wang. Advances in oxidation and [153] ablation resistance of high and ultra-high temperature ceramics modified or coated carbon/carbon composites. Journal of the European Ceramic Society, Vol. 38, No. 1, 2018, pp. 1-28.
- Zhao, D., C. Zhang, H. Hu, and Y. Zhang. Ablation behavior and mechanism of 3D C/ZrC composite in oxyacetylene torch environment. Composites Science and Technology, Vol. 71, No. 11, 2011, pp. 1392-1396.

- [155] Xue, L., Z.-a Su, X. Yang, D. Huang, T. Yin, C. Liu, et al. Microstructure and ablation behavior of C/C-HfC composites prepared by precursor infiltration and pyrolysis. *Corrosion Science*, Vol. 94, 2015, pp. 165–170.
- [156] Yao, J., S. Pang, C. Hu, J. Li, S. Tang, and H.-M. Cheng. Mechanical, oxidation and ablation properties of C/(C-SiC)_{CVI}-(ZrC-SiC)_{PIP} composites. *Corrosion Science*, Vol. 162, 2020, id. 108200.
- [157] Tang, Z., M. Yi, Q. Xiang, Y. Du, and K. Peng. Mechanical and ablation properties of a C/C-HfB₂-SiC composite prepared by high-solid-loading slurry impregnation combined with precursor infiltration and pyrolysis. *Journal of the European Ceramic Society*, Vol. 41, No. 13, 2021, pp. 6160–6170.
- [158] Kou, S., S. Fan, X. Ma, Y. Ma, C. Luan, J. Ma, et al. Ablation performance of C/HfC–SiC composites with in-situ HfSi₂/HfC/SiC multi-phase coatings under 3000°C oxyacetylene torch. *Corrosion Science*, Vol. 200, 2022, id. 110218.
- [159] Lu, J., K. Hao, L. Liu, H. Li, K. Li, J. Qu, et al. Ablation resistance of SiC-HfC-ZrC multiphase modified carbon/carbon composites. *Corrosion Science*, Vol. 103, 2016, pp. 1–9.
- [160] Li, Q., S. Dong, Z. Wang, and G. Shi. Fabrication and properties of 3-D C_f/ZrB₂–ZrC–SiC composites via polymer infiltration and pyrolysis. *Ceramics International*, Vol. 39, No. 5, 2013, pp. 5937–5941.
- [161] Kannan, R. and L. Rangaraj. Processing and characterization of C_r/ ZrB₂-SiC-ZrC composites produced at moderate pressure and temperature. *Ceramics International*, Vol. 43, No. 2, 2017, pp. 2625–2631.
- [162] Shojaie-Bahaabad, M. and A. Hasani-Arefi. Ablation properties of ZrC-SiC-HfB₂ ceramic with different amount of carbon fiber under an oxyacetylene flame. *Materials Research Express*, Vol. 7, No. 2, 2020, id. 025604.
- [163] Arai, Y., M. Saito, A. Samizo, R. Inoue, K. Nishio, and Y. Kogo. Hotcorrosion of refractory high-entropy ceramic matrix composites synthesized by alloy melt-infiltration. *Ceramics International*, Vol. 47, No. 22, 2021, pp. 31740–31748.
- [164] Silvestroni, L., S. Failla, I. Neshpor, and O. Grigoriev. Method to improve the oxidation resistance of ZrB₂-based ceramics for reusable space systems. *Journal of the European Ceramic Society*, Vol. 38, No. 6, 2018, pp. 2467–2476.
- [165] Chen, S.a, H. Hu, Y. Zhang, C. Zhang, and Q. Wang. Effects of high-temperature annealing on the microstructure and properties of C/SiC–ZrB₂ composites. *Materials & Design*, Vol. 53, 2014, pp. 791–796.
- [166] Yan, C., R. Liu, Y. Cao, C. Zhang, and D. Zhang. Ablation behavior and mechanism of C/ZrC, C/ZrC–SiC and C/SiC composites fabricated by polymer infiltration and pyrolysis process. *Corrosion Science*, Vol. 86, 2014, pp. 131–141.
- [167] Poerschke, D. L., M. D. Novak, N. Abdul-Jabbar, S. Krämer, and C. G. Levi. Selective active oxidation in hafnium boride-silicon carbide composites above 2000°C. *Journal of the European Ceramic Society*, Vol. 36, No. 15, 2016, pp. 3697–3707.
- [168] Chen, S.a, C. Zhang, Y. Zhang, D. Zhao, H. Hu, and Z. Zhang. Mechanism of ablation of 3D C/ZrC–SiC composite under an oxyacetylene flame. *Corrosion Science*, Vol. 68, 2013, pp. 168–175.
- [169] Tong, M., Q. Fu, L. Zhou, T. Feng, H. Li, T. Li, et al. Ablation behavior of a novel HfC–SiC gradient coating fabricated by a facile one-step chemical vapor co-deposition. *Journal of the European Ceramic Society*, Vol. 38, No. 13, 2018, pp. 4346–4355.
- [170] Xie, J., K. Li, H. Li, Q. Fu, and L. Guo. Ablation behavior and mechanism of C/C–ZrC–SiC composites under an oxyacetylene

- torch at 3000°C. *Ceramics International*, Vol. 39, No. 4, 2013, pp. 4171–4178.
- [171] Zhang, J.-P., J.-L. Qu, and Q.-G. Fu. Ablation behavior of noseshaped HfB₂-SiC modified carbon/carbon composites exposed to oxyacetylene torch. *Corrosion Science*, Vol. 151, 2019, pp. 87–96.
- [172] Wang, P., H. Li, R. Yuan, J.a Kong, T. Li, and Y. Zhang. A CrSi₂-HfB₂-SiC coating providing oxidation and ablation protection over 1973 K for SiC coated C/C composites. *Corrosion Science*, Vol. 167, 2020, id. 108536.
- [173] Tang, S., J. Deng, S. Wang, and W. Liu. Comparison of thermal and ablation behaviors of C/SiC composites and C/ZrB₂–SiC composites. *Corrosion Science*, Vol. 51, No. 1, 2009, pp. 54–61.
- [174] Zhang, X., P. Hu, J. Han, and S. Meng. Ablation behavior of ZrB₂–SiC ultra high temperature ceramics under simulated atmospheric re-entry conditions. *Composites Science and Technology*, Vol. 68, No. 7, 2008, pp. 1718–1726.
- [175] Makurunje, P., F. Monteverde, and I. Sigalas. Self-generating oxidation protective high-temperature glass-ceramic coatings for C_f/C-SiC-TiC-TaC UHTC matrix composites. *Journal of the European Ceramic Society*, Vol. 37, No. 10, 2017, pp. 3227–3239.
- [176] Castle, E., T. Csanádi, S. Grasso, J. Dusza, and M. Reece. Processing and properties of high-entropy ultra-high temperature carbides. *Scientific Reports*, Vol. 8, No. 1, 2018, id. 8609.
- [177] Xiang, H., Y. Xing, F.-Z. Dai, H. Wang, L. Su, L. Miao, et al. High-entropy ceramics: Present status, challenges, and a look forward. Journal of Advanced Ceramics, Vol. 10, No. 3, 2021, pp. 385–441.
- [178] Oses, C., C. Toher, and S. Curtarolo. High-entropy ceramics. Nature Reviews Materials, Vol. 5, No. 4, 2020, pp. 295–309.
- [179] Dusza, J., T. Csanádi, D. Medveď, R. Sedlák, M. Vojtko, M. Ivor, et al. Nanoindentation and tribology of a (Hf-Ta-Zr-Nb-Ti)C highentropy carbide. *Journal of the European Ceramic Society*, Vol. 41, No. 11, 2021, pp. 5417–5426.
- [180] Feng, L., W. T. Chen, W. G. Fahrenholtz, and G. E. Hilmas. Strength of single-phase high-entropy carbide ceramics up to 2300 °C. *Journal of the American Ceramic Society*, Vol. 104, No. 1, 2021, pp. 419–427.
- [181] Zhang, R. Z. and M. J. Reece. Review of high entropy ceramics: design, synthesis, structure and properties. *Journal of Materials Chemistry A: Materials for Energy and Sustainability*, Vol. 7, No. 39, 2019, pp. 22148–22162.
- [182] Zhang, L., W. Wang, N. Zhou, X. Dong, F. Yuan, and R. He. Low temperature fabrication of C_f/BN_i/(Ti_{0.2}Zr_{0.2}Hf_{0.2}Nb_{0.2}Ta_{0.2})C–SiC_m high entropy ceramic matrix composite by slurry coating and laminating combined with precursor infiltration and pyrolysis. *Journal of the European Ceramic Society*, Vol. 42, No. 7, 2022, pp. 3099–3106.
- [183] Wang, Y. C., D. Yu, J. Yin, B. H. Zhang, H. F. Zhang, X. J. Liu, et al. Ablation behavior of (Hf-Ta-Zr-Nb-Ti)C high-entropy carbide and (Hf-Ta-Zr-Nb-Ti)C-xSiC composites. *Journal of the American Ceramic Society*, Vol. 105, No. 10, 2022, pp. 6395–6406.
- [184] Guo, W., J. Hu, Y. Ye, and S. Bai. Ablation behavior of (TiZrHfNbTa) C high-entropy ceramics with the addition of SiC secondary under an oxyacetylene flame. *Ceramics International*, Vol. 48, No. 9, 2022, pp. 12790–12799.
- [185] Li, Q., H. Zhou, S. Dong, Z. Wang, J. Yang, B. Wu, et al. Fabrication and comparison of 3D C_f/ZrC–SiC composites using ZrC particles/ polycarbosilane and ZrC precursor/polycarbosilane. *Ceramics International*, Vol. 38, No. 6, 2012, pp. 5271–5275.
- [186] Jia, Y., X. Yao, J. Sun, and H. Li. Effect of ZrC particle size on the ablation resistance of C/C-ZrC-SiC composites. *Materials & Design*, Vol. 129, 2017, pp. 15–25.

- [187] Wu, X., Z. Su, Q. Huang, K. Tong, X. Xie, and C. Zeng. Effect of ZrC particle distribution on the ablation resistance of C/C-SiC-ZrC composites fabricated using precursor infiltration pyrolysis. Ceramics International, Vol. 46, No. 10, Part B, 2020, pp. 16062-16067.
- [188] Xie, J., K. Li, G. Sun, and H. Li. Effects of precursor concentration on the microstructure and properties of ZrC modified C/C composites prepared by precursor infiltration and pyrolysis. Ceramics International, Vol. 43, No. 17, 2017, pp. 14642-14651.
- [189] Zhou, H., J. Yang, G. Le, D. Ni, H. Wang, and S. Dong. Effect of ZrC amount and distribution on the thermomechanical properties of C_f/SiC-ZrC composites. International Journal of Applied Ceramic Technology, Vol. 16, No. 4, 2019, pp. 1321-1328.
- [190] He, Q., H. Li, C. Wang, T. Li, and J. Lu. Microstructure and ablation property of gradient ZrC-SiC modified C/C composites prepared by chemical liquid vapor deposition. Ceramics International, Vol. 45, No. 10, 2019, pp. 13283-13296.
- [191] Feng, B., H. Li, Y. Zhang, L. Liu, and M. Yan. Effect of SiC/ZrC ratio on the mechanical and ablation properties of C/C-SiC-ZrC composites. Corrosion Science, Vol. 82, 2014, pp. 27-35.
- [192] Yan, C., R. Liu, C. Zhang, and Y. Cao. Ablation and mechanical properties of 3D braided C/ZrC-SiC composites with various SiC/ZrC ratios. Ceramics International, Vol. 42, No. 16, 2016, pp. 19019-19026.
- [193] Karlsdottir, S. N. and J. W. Halloran. Oxidation of ZrB2-SiC: influence of SiC content on solid and liquid oxide phase formation. Journal of the American Ceramic Society, Vol. 92, No. 2, 2009, pp. 481-486.
- [194] Ouyang, H., Y. Zhang, C. Li, G. Li, J. Huang, and H. Li. Effects of ZrC/ SiC ratios on mechanical and ablation behavior of C/C–ZrC–SiC composites prepared by carbothermal reaction of hydrothermal co-deposited oxides. Corrosion Science, Vol. 163, 2020, id. 108239.
- [195] Yan, C., R. Liu, C. Zhang, Y. Cao, and Y. Wang. Effects of SiC/HfC ratios on the ablation and mechanical properties of 3D C_f/HfC-SiC composites. Journal of the European Ceramic Society, Vol. 37, No. 6, 2017, pp. 2343-2351.
- Ma, Y., Q. Li, S. Dong, Z. Wang, G. Shi, H. Zhou, et al. Microstructures and ablation properties of 3D 4-directional C_f/ZrC-SiC composite in a plasma wind tunnel environment. Ceramics International, Vol. 40, No. 7, Part B, 2014, pp. 11387-11392.
- [197] Xie, J., K. Li, G. Sun, H. Li, X. Su, Y. Han, et al. Effects of surface structure unit of 2D needled carbon fiber preform on the microstructure and ablation properties of C/C-ZrC-SiC composites. Ceramics International, Vol. 45, No. 9, 2019, pp. 11912-11919.
- [198] Yan, C., R. Liu, Y. Cao, C. Zhang, and D. Zhang. Preparation and properties of 3D needle-punched C/ZrC-SiC composites by polymer infiltration and pyrolysis process. Ceramics International, Vol. 40, No. 7, Part B, 2014, pp. 10961-10970.
- [199] Yang, X.-H., K.-Z. Li, and L.-T. Bai. Effects of preform structures on the mechanical and ablation properties of C/ZrC-SiC composites. International Journal of Applied Ceramic Technology, Vol. 17, No. 4, 2020, pp. 1582-1600.
- [200] Inoue, R., Y. Arai, Y. Kubota, K. Goto, and Y. Kogo. Development of short-and continuous carbon fiber-reinforced ZrB2-SiC-ZrC matrix composites for thermal protection systems. Ceramics International, Vol. 44, No. 13, 2018, pp. 15859-15867.
- [201] Liu, Y., Z. Chen, J. Zhu, Y. Jiang, B. Li, F., et al. Comparison of 3D four-directional and five-directional braided SiO_{2f}/SiO₂ composites with respect to mechanical properties and fracture behavior.

- Materials Science & Engineering, A: Structural Materials: Properties, Microstructure and Processing, Vol. 558, 2012, pp. 170-174.
- [202] Zhu, T. and Z. Wang. Research and application prospect of short carbon fiber reinforced ceramic composites. Journal of the European Ceramic Society, Vol. 43, No. 15, 2023, pp. 6699-6717.
- [203] Xue, L., Z. Chen, J. Liao, Q. Xiao, and Y. Li. Compressive strength and damage mechanisms of 3D needle-punched C_f/SiC-Al composites. Journal of Alloys and Compounds, Vol. 853, 2021, id. 156934.
- Chen, T., J. Liao, G. Liu, F. Zhang, and Q. Gong. Effects of needle-punched felt structure on the mechanical properties of carbon/carbon composites. Carbon, Vol. 41, No. 5, 2003, pp. 993-999.
- [205] Ding, J., S. Wen, L. Fu, T. Feng, H. Lin, M. Tong, et al. Effect of carbon fiber preform structures on the mechanical properties of C_f@PyC/SiC composites. Journal of Alloys and Compounds, Vol. 930, 2023, id. 167400.
- [206] Zhao, Z., K. Li, W. Li, and L. Zhang. Cyclic ablation behavior of C/C-ZrC-SiC-ZrB₂ composites under oxyacetylene torch with two heat fluxes at the temperatures above 2000°C. Corrosion Science, Vol. 181, 2021, id. 109202.
- Lamouroux, F., R. Naslain, and J.-M. Jouin. Kinetics and mechanisms of oxidation of 2D woven C/SiC composites: II, theoretical approach. Journal of the American Ceramic Society, Vol. 77, No. 8, 1994, pp. 2058-2068.
- [208] Liu, J., L. Zhang, F. Hu, J. Yang, L. Cheng, and Y. Wang. Polymerderived yttrium silicate coatings on 2D C/SiC composites. Journal of the European Ceramic Society, Vol. 33, No. 2, 2013, pp. 433-439.
- [209] Rezaie, A., W. G. Fahrenholtz, and G. E. Hilmas. Evolution of structure during the oxidation of zirconium diboride-silicon carbide in air up to 1500°C. Journal of the European Ceramic Society, Vol. 27, No. 6, 2007, pp. 2495-2501.
- Rama Rao, G. A. and V. Venugopal. Kinetics and mechanism of the oxidation of ZrC. Journal of Alloys and Compounds, Vol. 206, No. 2, 1994, pp. 237-242.
- [211] Shimada, S. and T. Ishil. Oxidation kinetics of zirconium carbide at relatively low temperatures. Journal of the American Ceramic Society, Vol. 73, No. 10, 1990, pp. 2804–2808.
- Edamoto, K., T. Nagayama, K. Ozawa, and S. Otani. Angle-resolved [212] and resonant photoemission study of the ZrO-like film on ZrC (100). Surface Science, Vol. 601, No. 21, 2007, pp. 5077-5082.
- Murthy, T. S. R. C., L. Reeman, J. Zou, V. Venkatachalam, B. Baker, [213] M. Wang, et al. Role of rare earth oxide particles on the oxidation behaviour of silicon carbide coated 2.5D carbon fibre preforms. Open Ceramics, Vol. 2, 2020, id. 100018.
- [214] Zacate, M. O., L. Minervini, D. J. Bradfield, R. W. Grimes, and K. E. Sickafus. Defect cluster formation in M2O3-doped cubic ZrO2. Solid State Ionics, Vol. 128, No. 1, 2000, pp. 243-254.
- Liu, H., X. Yang, C. Fang, A. Shi, L. Chen, and Q. Huang. Ablation [215] resistance and mechanism of SiC-LaB₆ and SiC-LaB₆-ZrB₂ ceramics under plasma flame. Ceramics International, Vol. 46, No. 10, Part B, 2020, pp. 16249-16256.
- Zhang, X.-h, P. Hu, J.-c Han, L. Xu, and S.-h Meng. The addition of [216] lanthanum hexaboride to zirconium diboride for improved oxidation resistance. Scripta Materialia, Vol. 57, No. 11, 2007, pp. 1036-1039.
- [217] Zapata-Solvas, E., D. D. Jayaseelan, P. M. Brown, and W. E. Lee. Thermal properties of La₂O₃-doped ZrB₂- and HfB₂-based ultrahigh temperature ceramics. Journal of the European Ceramic Society, Vol. 33, No. 15, 2013, pp. 3467-3472.

- [218] Zapata-Solvas, E., D. D. Jayaseelan, P. M. Brown, and W. E. Lee. Effect of La₂O₃ addition on long-term oxidation kinetics of ZrB₂-SiC and HfB₂-SiC ultra-high temperature ceramics. Journal of the European Ceramic Society, Vol. 34, No. 15, 2014, pp. 3535-3548.
- Zhang, X., Q. He, M. Qing, J. Feng, Z. Liu, Y. Wang, et al. Ablation behavior of La₂O₃ modified C/C-ZrC composites fabricated by precursor infiltration and pyrolysis. Ceramics International, Vol. 49, No. 9, Part A, 2023, pp. 14335-14345.
- [220] Segall, M. D., C. J. Pickard, R. Shah, and M. C. Payne. Population analysis in plane wave electronic structure calculations. Molecular Physics, Vol. 89, No. 2, 1996, pp. 571-577.
- [221] Xie, W., Q. Fu, C. Cheng, and N. Yan. Experimental and theoretical study on the effect of different rare-earth oxides on the hightemperature stability of SiO₂ glass at 1973K. Ceramics International, Vol. 46, No. 15, 2020, pp. 24371-24378.
- [222] Xie, W., Q. Fu, C. Cheng, P. Wang, J. Li, and N. Yan. Effect of Lu₂O₃ addition on the oxidation behavior of SiC-ZrB₂ composite coating at 1500°C: Experimental and theoretical study. Corrosion Science, Vol. 192, 2021, id. 109803.
- [223] Uhlmann, D. R. and N. J. Kreidl. Glass: science and technology. Viscosity and Relaxation, Vol. 3, 1986.
- Murthy, V. S. R., G. S. Murty, G. Banuprakash, and S. Das. [224] Rheological behaviour of borosilicate composites with metallic and non-metallic dispersions. Journal of the European Ceramic Society, Vol. 20, No. 11, 2000, pp. 1717-1728.
- [225] Jia, Y., H. Li, X. Yao, J. Sun, and Z. Zhao. Long-time ablation protection of carbon/carbon composites with different-La₂O₃-content modified ZrC coating. Journal of the European Ceramic Society, Vol. 38, No. 4, 2018, pp. 1046-1058.
- [226] Pan, X., Y. Niu, T. Liu, X. Zhong, C. Li, M. Shi, et al. Ablation resistance and mechanism of ZrC-SiC-Yb2O3 ternary composite coatings fabricated by vacuum plasma spray. Journal of the European Ceramic Society, Vol. 39, No. 13, 2019, pp. 3604-3612.
- [227] Pan, X., C. Li, Y. Niu, X. Zhong, L. Huang, Y. Zeng, et al. Effect of Yb₂O₃ addition on oxidation/ablation behaviors of ZrB₂-MoSi₂ composite coating under different environment. Corrosion Science, Vol. 175, 2020, id. 108882.
- [228] Chen, M., H. Li, X. Yao, G. Kou, Y. Jia, and C. Zhang. High temperature oxidation resistance of La₂O₃-modified ZrB₂-SiC coating for SiC-coated carbon/carbon composites. Journal of Alloys and Compounds, Vol. 765, 2018, pp. 37-45.
- [229] Luo, L., J. Liu, L. Duan, and Y. Wang. Multiple ablation resistance of La₂O₃/Y₂O₃-doped C/SiC-ZrC composites. Ceramics International, Vol. 41, No. 10, Part A, 2015, pp. 12878-12886.
- [230] Lin, H., Y. Liu, W. Liang, Q. Miao, S. Zhou, J. Sun, et al. Effect of the Y₂O₃ amount on the oxidation behavior of ZrB₂-SiC-based coatings for carbon/carbon composites. Journal of the European Ceramic Society, Vol. 42, No. 12, 2022, pp. 4770-4782.
- Ma, H., Q. Miao, W. Liang, Y. Liu, H. Lin, H. Ma, et al. High temperature oxidation resistance of Y₂O₃ modified ZrB₂-SiC coating for carbon/carbon composites. Ceramics International, Vol. 47, No. 5, 2021, pp. 6728-6735.
- [232] Vinci, A., L. Zoli, P. Galizia, and D. Sciti. Influence of Y₂O₃ addition on the mechanical and oxidation behaviour of carbon fibre reinforced ZrB₂/SiC composites. Journal of the European Ceramic Society, Vol. 40, No. 15, 2020, pp. 5067-5075.
- [233] Shen, X., X. Wang, Z. Shi, C. Li, J. Huang, and K. Li. Effect of yttrium carbide on ablation behavior of zirconium carbide modified

- carbon/carbon composites. Corrosion Science, Vol. 170, 2020, id. 108675.
- [234] Fang, C., X. Yang, K. He, L. Chen, G. Zeng, A. Shi, et al. Microstructure and ablation properties of La₂O₃ modified C/C-SiC composites prepared via precursor infiltration pyrolysis. Journal of the European Ceramic Society, Vol. 39, No. 4, 2019, pp. 762-772.
- [235] Fang, C., B. Huang, X. Yang, K. He, L. Chen, A. Shi, et al. Effects of LaB₆ on the microstructures and ablation properties of 3D C/ C-SiC-ZrB₂-LaB₆ composites. Journal of the European Ceramic Society, Vol. 40, No. 8, 2020, pp. 2781-2790.
- [236] Fang, C., X. Yang, L. Chai, Z. Zhang, Y. Weng, L. Zheng, et al. Modifying effects of in-situ grown LaB₆ on composition, microstructure and ablation property of C/C-SiC-ZrC composites. Corrosion Science, Vol. 209, 2022, id. 110672.
- [237] Parthasarathy, T. A., R. A. Rapp, M. Opeka, and R. J. Kerans. A model for the oxidation of ZrB2, HfB2 and TiB2. Acta Materialia, Vol. 55, No. 17, 2007, pp. 5999-6010.
- [238] Zhu, S., G. Zhang, Y. Bao, D. Sun, Q. Zhang, X. Meng, et al. Progress in preparation and ablation resistance of ultra-hightemperature ceramics modified C/C composites for extreme environment. Reviews on Advanced Materials Science, Vol. 62, No. 1, 2023, id. 20220276.
- Liu, Y., Q. Fu, Y. Guan, B. Wang, and Q. Shen. Ablation behavior of [239] sharp-shape C/C-SiC-ZrB₂ composites under oxyacetylene flame. Journal of Alloys and Compounds, Vol. 713, 2017, pp. 19-27.
- Stollery, J. L. Hypersonic viscous interaction on curved surfaces. Journal of Fluid Mechanics, Vol. 43, No. 3, 1970, pp. 497-511.
- [241] Duan, L., L. Luo, L. Liu, and Y. Wang. Ablation of C/SiC-HfC composite prepared by precursor infiltration and pyrolysis in plasma wind tunnel. Journal of Advanced Ceramics, Vol. 9, No. 3, 2020, pp. 393-402.
- Sciti, D., L. Zoli, L. Silvestroni, A. Cecere, G. Di Martino, and R. Savino. Design, fabrication and high velocity oxy-fuel torch tests of a C_f-ZrB₂-fiber nozzle to evaluate its potential in rocket motors. Materials & Design, Vol. 109, 2016, pp. 709-717.
- [243] Liu, T., Q. Fu, B. Liu, and J. Zhang. Effect of temperature gradient on the ablation and flexural behavior of C/C-ZrC composites. Corrosion Science, Vol. 191, 2021, id. 109736.
- [244] Miller-Oana, M., P. Neff, M. Valdez, A. Powell, M. Packard, L. S. Walker, et al. Oxidation Behavior of aerospace materials in high enthalpy flows using an oxyacetylene torch facility. Journal of the American Ceramic Society, Vol. 98, No. 4, 2015, pp. 1300-1307.
- [245] Vinci, A., L. Zoli, D. Sciti, J. Watts, G. E. Hilmas, and W. G. Fahrenholtz. Mechanical behaviour of carbon fibre reinforced TaC/SiC and ZrC/SiC composites up to 2100°C. Journal of the *European Ceramic Society*, Vol. 39, No. 4, 2019, pp. 780–787.
- Jia, Y., S.a Chen, Y. Li, S. Wang, and H. Hu. High-temperature [246] mechanical properties and microstructure of C/C-ZrC-SiC-ZrB₂ composites prepared by a joint process of precursor infiltration and pyrolysis and slurry infiltration. Journal of Alloys and Compounds, Vol. 811, 2019, id. 151953.
- Zoli, L., A. Vinci, P. Galizia, C. Melandri, and D. Sciti. On the thermal [247] shock resistance and mechanical properties of novel unidirectional UHTCMCs for extreme environments. Scientific Reports, Vol. 8, No. 1, 2018, id. 9148.
- [248] Ding, Q., D. Ni, Z. Wang, Y. Kan, P. He, X. Zhang, et al. Effect of interphase on mechanical properties and microstructures of 3D C_f/SiBCN composites at elevated temperatures. Journal of the American Ceramic Society, Vol. 102, No. 6, 2019, pp. 3630-3640.

- [249] Ding, Q., D. Ni, Z. Wang, H. Wang, H. Zhou, Y. Kan, et al. Mechanical properties and microstructure evolution of 3D C_f/ SiBCN composites at elevated temperatures. Journal of the American Ceramic Society, Vol. 101, No. 10, 2018, pp. 4699-4707.
- [250] Wang, Z., S. Dong, X. Zhang, H. Zhou, D. Wu, Q. Zhou, et al. Fabrication and properties of Cf/SiC-ZrC composites. Journal of the American Ceramic Society, Vol. 91, No. 10, 2008, pp. 3434–3436.
- [251] Rowcliffe, D. J. and W. J. Warren. Structure and properties of tantalum carbide crystals. Journal of Materials Science, Vol. 5, No. 4, 1970, pp. 345-350.
- [252] Rowcliffe, D. J. and G. E. Hollox. Plastic flow and fracture of tantalum carbide and hafnium carbide at low temperatures. Journal of Materials Science, Vol. 6, No. 10, 1971, pp. 1261–1269.
- [253] Johansen, H. and J. Cleary. The ductile-brittle transition in tantalum carbide. Journal of the Electrochemical Society, Vol. 113, 1966, p. 378.

- [254] Gangireddy, S., J. W. Halloran, and Z. N. Wing. Non-contact mechanical property measurements at ultrahigh temperatures. Journal of the European Ceramic Society, Vol. 30, No. 11, 2010, pp. 2183-2189.
- [255] Gangireddy, S., J. W. Halloran, and Z. N. Wing. Flexural creep of zirconium diboride-silicon carbide up to 2200°C in minutes with non-contact electromagnetic testing. Journal of the European Ceramic Society, Vol. 33, No. 15, 2013, pp. 2901-2908.
- Smith, C. J., M. A. Ross, N. De Leon, C. R. Weinberger, and G. B. [256] Thompson. Ultra-high temperature deformation in TaC and HfC. Journal of the European Ceramic Society, Vol. 38, No. 16, 2018, pp. 5319-5332.
- [257] Tandon, R., H. P. Dumm, E. L. Corral, R. E. Loehman, and P. G. Kotula. Ultra high temperature ceramics for hypersonic vehicle applications, Albuquerque, NM, and Livermore, United States, 2006.